

**ANALYSIS AND DESIGN OF SHEAR WALL-TRANSFER BEAM
STRUCTURE**

ONG JIUN DAR

Universiti Teknologi Malaysia

UNIVERSITI TEKNOLOGI MALAYSIA

BORANG PENGESAHAN STATUS TESIS**JUDUL: ANALYSIS AND DESIGN OF SHEAR WALL-TRANSFER BEAM STRUCTURE****SESI PENGAJIAN: 2006/2007**Saya _____ **ONG JIUN DAR**
(HURUF BESAR)

mengaku membenarkan tesis (PSM/~~Sarjana/Doktor Falsafah~~)* ini disimpan di Perpustakaan Universiti Teknologi Malaysia dengan syarat-syarat kegunaan seperti berikut:

1. Tesis adalah hakmilik Universiti Teknologi Malaysia.
2. Perpustakaan Universiti Teknologi Malaysia dibenarkan membuat salinan untuk tujuan pengajian sahaja.
3. Perpustakaan dibenarkan membuat salinan tesis ini sebagai bahan pertukaran antara institusi pengajian tinggi.
4. **Sila tandakan (✓)

SULIT

(Mengandungi maklumat yang berdarjah keselamatan atau kepentingan Malaysia seperti yang termaktub di dalam AKTA RAHSIA RASMI 1972)

TERHAD

(Mengandungi maklumat TERHAD yang telah ditentukan oleh organisasi/badan di mana penyelidikan dijalankan)

TIDAK TERHAD

Disahkan oleh

(TANDATANGAN PENULIS)_____
(TANDATANGAN PENYELIA)

Alamat Tetap:

L28-201, JALAN PANDAN 4,
PANDAN JAYA,
55100 KUALA LUMPUR

IR AZHAR AHMAD

Nama Penyelia

Tarikh: 18 APRIL 2007

Tarikh: 18 APRIL 2007

CATATAN: * Potong yang tidak berkenaan.

** Jika tesis ini SULIT atau TERHAD, sila lampirkan surat daripada pihak berkuasa/organisasi berkenaan dengan menyatakan sekali sebab dan tempoh tesis ini perlu dikelaskan sebagai SULIT atau TERHAD.

†Tesis dimaksudkan sebagai tesis bagi Ijazah Doktor Falsafah dan Sarjana secara penyelidikan, atau disertasi bagi pengajian secara kerja kursus dan penyelidikan, atau Laporan Projek Sarjana Muda (PSM).

“I/~~we~~* hereby declare that I/~~we~~* have read this thesis and in my/~~our~~* opinion this thesis is sufficient in terms of scope and quality for the award of the degree of Bachelor/~~Master/~~ Engineering Doctorate/~~Doctor of Philosophy~~ of Civil Engineering

Signature :
Name of Supervisor : IR AZHAR AHMAD
Date : 18 APRIL 2007

- *Delete as necessary*

**ANALYSIS AND DESIGN OF SHEAR WALL-TRANSFER BEAM
STRUCTURE**

ONG JIUN DAR

A project report submitted in partial fulfilment of the requirements for the award of
the degree of Bachelor of Civil Engineering

Faculty of Civil Engineering
University Technology Malaysia

APRIL 2007

I declare that this thesis entitled “*Analysis and Design of Shear Wall-Transfer Beam Structure*” is the result of my own research except as cited in the references. The thesis has not been accepted for any degree and is not concurrently submitted in candidature of any other degree.

Signature :

Name : ONG JIUN DAR

Date : 18 APRIL 2007

This thesis is dedicated to my beloved mother and father

ACKNOWLEDGEMENT

First of all, a sincere appreciation goes to my supervisor, Ir Azhar Ahmad for his amazing energy, talent and belief in this thesis. Thank you for offering me enormous and professional advice, encouragement, guidance and suggestion towards the success of this thesis.

I would also like to express my gratitude to Perpustakaan Sultanah Zanariah of UTM for the assistance in supplying the relevant literatures.

My fellow postgraduate students should also be recognised for their support. My sincere appreciation also extends to all my colleagues and others who have provided assistance at various occasions. Their views and tips are useful indeed. Unfortunately, it is not possible to list all of them in this limited space. I am grateful to all my family members.

ABSTRACT

Shear wall configuration in tall buildings makes access difficult to public lobby areas at lower levels of these buildings. The large openings are generally achieved by use of large transfer beams to collect loadings from the upper shear walls and then distribute them to the widely spaced columns that support the transfer girders. The current practice in designing the transfer beam–shear wall systems does not generally consider the significant interaction of the transfer beam and the upper shear walls, thus leading to an unreasonable design for the internal forces of structural members and the corresponding steel reinforcement detailing. The objective of this project is to analyse the stress behaviour of shear wall and transfer beam due to the interaction effect and then design the transfer beam based on the stress parameters obtained from the finite element analysis. The 2D finite element analysis is carried out with the aid of LUSAS 13.5 software. With the aid of the software, a 22-storey highrise structure's model, constituted of shear wall, the supporting transfer beam and columns, is created. In this project, two analysis is carried out on the model. Firstly, the model is subjected to superimposed vertical loads only and analysed to verify the obtained stress behaviour against that of the previously-established result. The results obtained in this projects resemble that of the previous established research carried out by J.S Kuang and Shubin LI (2001). The analysis result shows that the interaction effect affects the distribution of shear stress, vertical stress and horizontal bending stress in the shear wall within a height equals the actual span of transfer beam, measured from to surface of the transfer beam. In the second case, the structure is subjected to both lateral wind load and superimposed vertical loads to observe the difference in stress behaviour. The analysis produces a series of related results such as bending moment and shear stress subsequently used for the design of transfer beam. Based on the data obtained in the second case, the transfer beam's reinforcement is designed according to the CIRIA Guide 2:1977.

ABSTRAK

Susunan dinding ricih di bangunan tinggi biasanya menyulitkan penyediaan laluan di ruang lobi tingkat bawah bangunan. Untuk mengatasi masalah ini, “transfer beam” disediakan untuk menyokong dinding ricih di bahagian atasnya sedangkan ia pula disokong oleh tiang di bahagian bawah rasuk, demi menyediakan bukaan di bahagian lobi. Kebanyakan rekabentuk struktur sebegini masa kini masih belum mengambil kira kesan interaksi antara “transfer beam” dan dinding ricih dalam analisis dan ini menghasilkan rekabentuk dan analisis daya dalaman yang tidak tepat. Objective projek ini adalah untuk menganalisis taburan tegasan dinding ricih dan “transfer beam” natijah daripada kesan interaksi antara kedua-dua struktur tersebut dan seterusnya merekabentuk “transfer beam” tersebut berdasarkan parameter tegasan yang diperoleh daripada analisis unsur terhingga. Analisis 2D tersebut dijalankan dengan menggunakan perincian LUSAS 13.5. Dengan bantuannya, sebuah model unsur terhingga bangunan 22 tingkat yang terdiri daripada dinding ricih disokong oleh “transfer beam” dan tiang di bahagian bawah dibina. Dalam projek ini, dua kes analisis dijalankan ke atas model tersebut. Mula-mula, model itu cuma dikenakan beban keaanan pugak lalu dianalisis untuk membandingkan dan mengesahkan ketepatan taburan tegasan yang diperoleh daripada analisis projek ini dengan yang diperoleh daripada hasil kajian pengkaji terdahulu. Daripada kajian projek ini, adalah didapati hasil analisis yang diperoleh adalah mirip dengan hasil kajian J.S Kuang and Shubin LI (2001). Keputusannya menunjukkan bahawa kesan interaksi mempengaruhi taburan tegasan ricih, ufuk dan pugak dinding ricih dalam lingkungan tinggi dari permukaan atas rasuk yang menyamai panjang sebenar “transfer beam”. Dalam kes kedua, struktur itu dikenakan daya ufuk angin dan daya keaanan pugak lalu perbezaan taburan tegasan kedua-dua kes dicerap. Momen lentur dan daya ricih yang diperoleh daripada kes ini digunakan untuk merkabentuk “transfer beam” tersebut berpandukan “CIRIAGuide2:1977”.

CONTENT

CHAPTER	TOPIC	PAGE
	TITLE	i
	DECLARATION	ii
	DEDICATION	iii
	ACKNOWLEDGEMENTS	iv
	ABSTRACT	v
	ABSTRAK	vi
	TABLE OF CONTENTS	vii
	LIST OF TABLES	xi
	LIST OF FIGURES	xiii
	LIST OF SYMBOLS	xv
	LIST OF APPENDICES	xvi
1	INTRODUCTION	1
	1.1 Introduction	1
	1.2 Problem Statement	2
	1.3 Objective	3
	1.4 Research Scopes	4
2	LITERATURE REVIEW	5
	2.1 Finite Element Modelling of Transfer Beam – Shear Wall System Using Finite Element Code SAP 2000	5
	2.1.1 Structural Behaviour - Vertical Stress in Wall	7
	2.1.2 Structural Behaviour - Horizontal Stress in Wall	8

2.1.3	Structural Behaviour - Shear Stress in Wall	9
2.1.4	Structural Behaviour – Bending Moment in Beam	9
2.1.5	Interaction-based Design Table	11
2.1.6	Interaction-Based Design Formulas for Transfer Beams Based on Box Foundation Analogy	12
2.2	Analysis of Transfer Beam – Shear Wall System Using Non-Finite Element Method	13
2.2.1	Governing Equation	14
2.2.2	Axial Force of Walls	16
2.2.3	Moment of Walls	17
2.2.4	Top Deflection of Walls	18
2.2.5	Shear Stress of Walls	18
2.3	Behaviour of Deep Beam	18
2.3.1	Elastic Analysis	19
2.3.2	Flexural Failure	20
2.3.3	Shear Failure	20
2.3.4	Bearing Capacity	21
2.3.5	Deformation and Deflection	21
2.4	Struts and Ties Models for Transfer Beam	22
2.4.1	Strut-and-Tie Models for Deep Beams	22
2.4.2	Suitable Strut-and-Tie Layouts	23
2.4.3	Behaviour of Shear Wall	23
2.5	Finite Element Analysis of Shear Wall-Transfer Beam Structure	26
2.5.1	Introduction to Finite Element	27
2.5.2	Basic Finite Element Equations	27
2.5.3	Formulation of Standard 2D Isoparametric Elements	30
3	METHODOLOGY	32
3.1	Introduction	32
3.2	LUSAS Finite Element System	33

3.2.1	Selecting Geometry of Shear Wall-Transfer Beam Finite Element Model	34
3.2.2	Defining Attribute of Shear Wall-Transfer Beam Finite Element Model	34
3.2.2.1	Mesh	34
3.2.2.2	Element Selection	34
3.2.2.3	Defining the Geometric Properties	35
3.2.2.4	Defining Material Properties	35
3.2.2.5	Defining Support Condition	36
3.2.2.6	Loading Assignment	36
3.2.3	Model Analysis and Results Processing	36
3.3	Design Procedures of Transfer Beam Based on Ciria Guide 2 and CP 110	37
3.3.1	Geometry	37
3.3.2	Force Computation	39
3.3.3	Ultimate Limit State	39
3.3.3.1	Strength in Bending	39
3.3.3.2	Shear Capacity	40
3.3.3.3	Bearing Capacity at Supports	41
3.3.4	Serviceability Limit State	42
3.3.4.1	Deflection	42
3.3.4.2	Crack Width	42
4	ANALYSIS AND RESULTS	43
4.1	Introduction	43
4.2	Geometry of Transfer Beam	46
4.3	Analysis of Shear Wall-Transfer Beam Structure Using LUSAS 13.5	46
4.3.1	Case 1: Analysis of Shear Wall-Transfer Beam Structure Subjected to Vertical Loads Only	47
4.3.1.1	Deformation of Shear Wall – Transfer Beam Structure	47
4.3.1.2	Vertical Stress in Shear Wall	48

4.3.1.3	Horizontal Stress in Shear Wall	52
4.3.1.4	Shear Stress in Shear Wall and Transfer Beam	55
4.3.1.5	Mean Shear Stress along Transfer Beam	58
4.3.1.6	Bending Moment along Transfer Beam	60
4.3.2	Case 2: Analysis of Shear Wall-Transfer Beam Structure Subjected to Vertical Loads and Wind Load	62
4.3.2.1	Deformation of Shear Wall – Transfer Beam Structure	62
4.3.2.2	Vertical Stress in Shear Wall	63
4.3.2.3	Horizontal Stress in Shear Wall	67
4.3.2.4	Shear Stress in Shear Wall and Transfer Beam	70
4.3.2.5	Mean Shear Stress along Transfer Beam	73
4.3.2.6	Bending Moment along Transfer Beam	75
4.4	Design of Transfer Beam Using Analysis Result of Case 2	76
5	CONCLUSION AND RECOMMENDATION	78
5.1	Conclusion	78
5.1.1	Case 1: Analysis of Shear Wall-Transfer Beam Structure subjected to Vertical Loads Only	78
5.1.2	Case 2: Analysis of Shear Wall-Transfer Beam Structure Subjected to Vertical Loads and Wind Load.	79
5.1.3	Design of Reinforcement for Transfer Beam	80
5.2	Recommendations	81
	REFERENCES	83
	APPENDICES	85-94

LIST OF TABLES

TABLE NO.	TITLE	PAGE
4.1	Vertical stress of shear wall at Section A-A (Y = 6m)	50
4.2	Vertical stress of shear wall at Section B-B (Y = 9m)	50
4.3	Vertical stress of shear wall at Section C-C (Y = 14m)	50
4.4	Vertical stress of shear wall at Section D-D (Y = 45m)	50
4.5	Horizontal stress of shear wall at Section A-A (X = 2m)	53
4.6	Horizontal stress of shear wall at Section B-B (X = 4m)	53
4.7	Horizontal stress of shear wall at Section C-C (X = 5m)	53
4.8	Shear stress of transfer beam at Section A-A (Y = 4m)	56
4.9	Shear stress of shear wall at Section B-B (Y = 6m)	56
4.10	Shear stress of shear wall at Section C-C (Y = 14m)	56
4.11	Shear stress of shear wall at Section D-D (Y = 45m)	56
4.12	Shear stress and shear force along transfer beam	59
4.13	Bending stress and bending moment along clear span of transfer beam	61
4.14	Vertical stress of shear wall at Section A-A (Y = 6m)	65
4.15	Vertical stress of shear wall at Section B-B (Y = 9m)	65
4.16	Vertical stress of shear wall at Section D-D (Y = 14m)	65
4.17	Vertical stress of shear wall at Section D-D (Y = 45m)	65
4.18	Horizontal stress of shear wall at Section A-A (X = 2m)	69
4.19	Horizontal stress of shear wall at Section B-B (X = 4m)	69
4.20	Horizontal stress of shear wall at Section C-C (X = 5m)	69
4.21	Shear stress of shear wall at Section A-A (Y = 4m)	71
4.22	Shear stress of shear wall at Section B-B (Y = 6m)	71
4.23	Shear stress of shear wall at Section C-C (Y = 14m)	71

4.24	Shear stress of shear wall at Section D-D ($Y = 45\text{m}$)	71
4.25	Shear stress and shear force along transfer beam	74
4.26	Bending stress and bending moment along clear span of transfer beam	75

LIST OF FIGURES

FIGURE NO.	TITLE	PAGE
2.1	Finite element model	6
2.2	Typical transfer beam–shear wall system	6
2.3	Distribution of vertical stress in shear wall	7
2.4	Distribution of horizontal stress in the wall–beam system	8
2.5	Distribution of shear stress in the system	9
2.6	Variation of bending moment in the beam along the span	10
2.7	Variation of bending moment at mid-span against different depth–span ratios for different support stiffness	10
2.8	Equivalent portal frame model	11
2.9	Box foundation analogy: a) Transfer beam–shear wall system; and b) box foundation and upper structure	13
2.10	Coupled shear wall–continuous transfer girder system	15
2.11	(a) continuum model; (b) forces in continuum	16
2.12	Bending moment modification coefficients for varying values of R	17
2.13	Stress at midplane of the beam under top load	19
2.14	Typical deep beam failures in flexure	20
2.15	Stress trajectories of single span transfer beam supporting a uniform load	24
2.16	Cracking control – Strut-and-tie models	25
2.17	Finite element model of box-shaped shear wall	25
2.18	Example illustrating the use of plane stress elements subject to in plane loading	30
3.1	Plane stress (QPM8) surface elements	35
3.2	Results processing	37

3.3	Basic dimension of deep beam	38
3.4	Bands of reinforcement for hogging moment	40
4.1	The views of the shear wall-transfer beam structure with dimension.	44
4.2	(a) Partial view and (b) full view of the shear wall-transfer beam structure's finite element model with meshing	45
4.3	The exaggerated deformation of shear wall-transfer beam structure at the interaction zone of shear wall, transfer beam and columns	49
4.4	Result of analysis of vertical stress in shear wall	52
4.5	Result of analysis of horizontal stress in shear wall	55
4.6	Result of analysis of shear stress in shear wall and transfer beam	57
4.7	Shear force distribution along the transfer beam.	59
4.8	Bending moment distribution along the clear span of transfer beam.	62
4.9	Exaggerated deformation of the shear wall-transfer beam structure under vertical imposed loads and lateral wind load	64
4.10	Result of analysis of vertical stress in shear wall	66
4.11	Result of analysis of horizontal stress in shear wall	69
4.12	Result of analysis of shear stress in shear wall and transfer beam	72
4.13	Shear force distribution along the transfer beam	74
4.14	Bending moment distribution along the clear span of transfer beam.	76
4.15.	Detailing of transfer beam in longitudinal and cross section view (not to scale).	77

LIST OF SYMBOLS

A_s	=	Area of main sagging or hogging steel
A_{sv}	=	Area of shear links
b	=	Thickness of beam
c_1, c_2	=	Support width
d	=	Distance from the effective top of beam to the centroid of the steel
f_{cu}	=	Characteristic compressive strength of concrete cubes
f_y	=	Characteristic tensile strength of steel reinforcement
F_{bt}	=	Tensile force in the bar
G_k	=	Dead load
h	=	Height of beam
h_a	=	Effective height of beam
k_s	=	Shear stress modifying factor
l_o	=	Clear span
l	=	Effective span
M	=	Design moment at ultimate limit state
Q_k	=	Live load
s_v	=	Spacing of shear links
v_c	=	Ultimate concrete shear stress
x_e	=	Effective clear span
Z	=	Lever arm at which the reinforcement acts
ϕ	=	Bar diameter

LIST OF APPENDICES

APPENDIX	TITLE	PAGE
A	Internal forces of the transfer beam-shear wall system subjected to uniformly distributed load by J.S Kuang and Shubin Li (2001)	85
B	Minimum Reinforcement in Deep Beam and Maximum Bar Spacing	88
C	Calcualtion of Lateral Wind Load on Shear Wall as per BS 6399 Loading for Buildings): Part 2 (Wind Loads): 1997	89
D	Calculation of vertical load transferred from slab to shear Wall	90
E	Design of Transfer Beam as per CIRIA Guide 2 1977 (Section 2 – Simple Rules for the Analysis of Deep Beams)	91

CHAPTER 1

INTRODUCTION

1.1 Introduction

Generally, shear wall can be defined as structural vertical member that is able to resist combinations of shear, moment and axial load induced by lateral wind load and gravity load transferred to the wall from other structural members. It also provides lateral bracing to the structure. On the other hand, transfer beam is a structure, normally deep and large, used to transfer loading from shear wall/columns of the upper structure to the lower framed structure. It can be classified as deep beam provided its span/depth ratio is less than 2.5.

The use of shear wall structure has gained popularity in high-rise building construction, especially in the construction of service apartment or office/commercial tower. It has been proven that this system provides efficient structural systems for multi-storey buildings in the range of 30-35 storeys (Marsono and Subedi, 2000). To add credit to it, it is well-known that the use of reinforced concrete shear wall has become one of the most efficient methods of ensuring the lateral stability of tall building (Marsono and Subedi, 2000). In the past 30 years of the recorded service history of tall buildings containing shear wall elements, none has collapsed during strong wind and earthquake events (Fintel, 1995).

In tall buildings, shear wall configuration, however, generally makes access difficult to the public lobby area at the base such as the car park area. In view of this,

large openings at the ground floor level are required. This can be achieved by the use of large transfer beams to collect loadings from the upper shear walls and then distribute them to the widely spaced columns that support the shear walls (Stafford Smith and Coull, 1991). This arrangement divides the whole tower into two portions – one with shear wall units at the upper part of the tower and the other with the conventional framed structure at the lower part (normally serves as car park podium).

1.2 Problem Statement

Due to the significance of transfer beam–shear wall system in high rise building construction, the stresses behaviour at the interaction zone between the shear wall and transfer beam has drawn interest from various researchers. These stresses behaviour is so critical that improper analysis could lead to uneconomic design or even erroneous design and consequently the failure of the whole structure.

In current practice, the design of a transfer beam–shear wall system is still based largely on the experience of designers and simplification of the structure, where the beam is modelled as an equivalent grid structure (Computers and Structures, 1998). As a result, interaction of the transfer beam and the supported shear walls cannot appropriately be included in the analysis. This may lead to unreasonable design for the internal forces of structural components and corresponding steel reinforcement details.

The complexity in the use of transfer beams arises from the interaction between the beam system and the upper structural walls. The interaction has been shown to cause a significant effect on stress redistributions both in the transfer beam and in the shear walls within an interactive zone (Kuang and Zhang, 2003). The current practice of design for a transfer beam-shear wall system in tall buildings, however, does not generally include the interaction effect of the transfer beam and the supported shear walls in terms of the structural behaviour of the system.

The use of ordinary beam or deep beam theories to model the behaviour for the analysis of transfer beam is not appropriate due to the beam-wall interaction. Lateral load, namely the wind load exerted on the shear wall also induces additional stresses on the transfer beam as the shear wall transfer the vertical stress and moment straight to the transfer beam.

1.3 Objective

The major objective of this project is to study the stress distribution in the shear wall-transfer beam structure due to the wall-beam interaction effect, with the aid of LUSAS 13.5 finite element software. In order to carry out the analysis, a typical shear wall-transfer beam finite element model is created using the finite element software. Stress parameters such as vertical stress, horizontal stress, shear stress and bending moment are derived from the analysis to explain the behaviour of the transfer beam and shear wall due to the interaction effect.

The shear wall-transfer beam structure is to be analysed in two cases. In the first case, the structure is subjected to vertical loads only. Analysis is carried out with the aim of comparing the structure's stress distribution with the results obtained by J.S Kuang and Shubin LI (2001) using finite element code SAP 2000 in their previous research.

In the second case, the structure is subjected to vertical loads and wind load. The analysis procedures are repeated for this case in order to examine the stress behaviour of the structure due to the additional lateral wind load. Based on the analysis, shear force and bending moment in beam yielded will be utilized to design for the reinforcement of the transfer beam.

1.4 Research Scopes

The scopes of research that needs to be carried out are as follows:

1. Select a case study comprising in plane shear wall supported by a transfer beam to study the stress behaviour of the shear wall-transfer beam structure.
2. Create a 2D, linear elastic finite element model which consists of a strip of in-plane shear wall supported by a transfer beam. The whole structure is to be subjected to both wind load and vertical dead load and live load.
3. From the structure model developed, analyze the shear wall-transfer beam structure using finite element method with the aid of Lusas 13.5 software. The analysis is aimed at investigating the interaction effects between the transfer beam and the shear wall. The interaction effects will well explain structural behaviour such as:
 - a) Vertical stress in wall
 - b) Horizontal stress in wall
 - c) Shear stress in wall
 - d) Bending moment in beam
- 4 Compare the structural behaviours of the shear wall-transfer beam structure using finite element method (with the aid of Lusas 13.5 software) with those yielded from analysis carried out by J.S Kuang and Shubin LI (2001) using finite element code SAP 2000 (Computers and Structures, 1997).
- 5 Design for the reinforcement of the transfer beam as per Ciria Guide 2: 1977 and BS8110 based on the results of analysis in case 2.

CHAPTER 2

LITERATURE REVIEW

2.1 Finite Element Modelling of Transfer Beam – Shear Wall System Using Finite Element Code SAP 2000

In a case study carried out by J.S Kuang and Shubin LI (2001) aimed at investigating the interaction effects between the transfer beam and the shear wall, a finite element model has been developed to analyze the system (Figure 2.1). Four-node square plane-stress elements are used to analyze the transfer beam, support columns and wall. Computations are performed by employing the finite element code SAP2000 (Computers and Structures, 1997) to generate the stresses of the structure.

In order to investigate the interaction effects between the transfer beam and the shear wall on the structural behaviour of the system, the height of the shear wall H is taken to be larger than twice the total span of the transfer beam L . The breadth of the beam is twice the thickness of the shear wall (Figure 2.2). Figure 2.1 shows the finite element model for the system.

2.1.1 Structural Behaviour - Vertical Stress in Wall

The investigation carried out by J.S Kuang and Shubin LI (2001) shows that vertical loads are generally transferred to the beam system through the compression arch as shown in Figure 2.3.

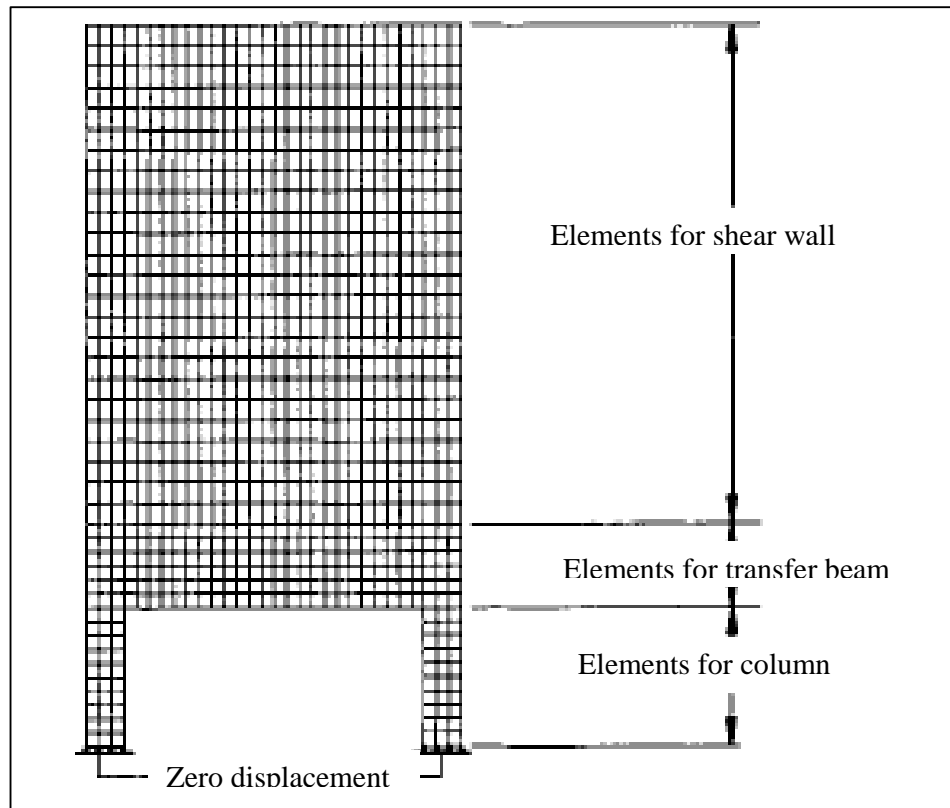


Figure 2.1 Finite element model

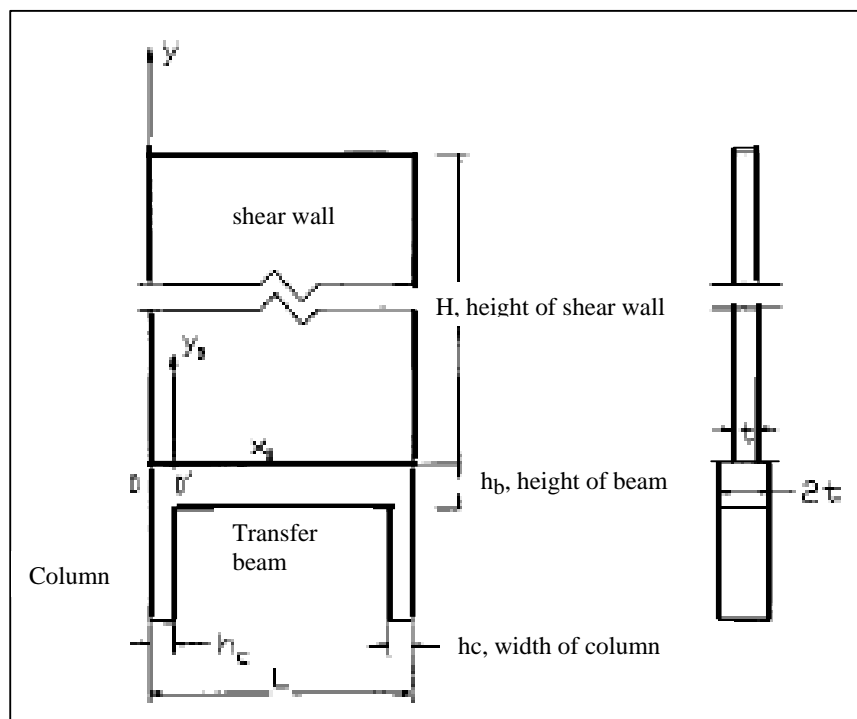


Figure 2.2 Typical transfer beam-shear wall system

Figure 2.3 shows the distribution of the vertical stress over the height of the wall, when the wall is subjected to a uniformly distributed vertical load w per unit length. It can be seen that although the wall is subjected to uniformly distributed loading, the distribution of the vertical stress in the lower part of the shear wall becomes non-uniform. The vertical loading is transferred towards the support columns through the compression arch. The arching effect is due to the interaction of the transfer beam and shear wall.

It can also be seen from Figure 2.3 that, beyond a height approximately equal to the total span of the transfer beam L from the wall-beam surface, the interaction of the transfer beam and the shear wall has little effect on the distribution of the vertical stress, which tends to be uniform. It can be seen that the vertical stresses of the wall are redistributed within the height L . The stress redistribution reaches its most significant at the level of the wall-beam interface.

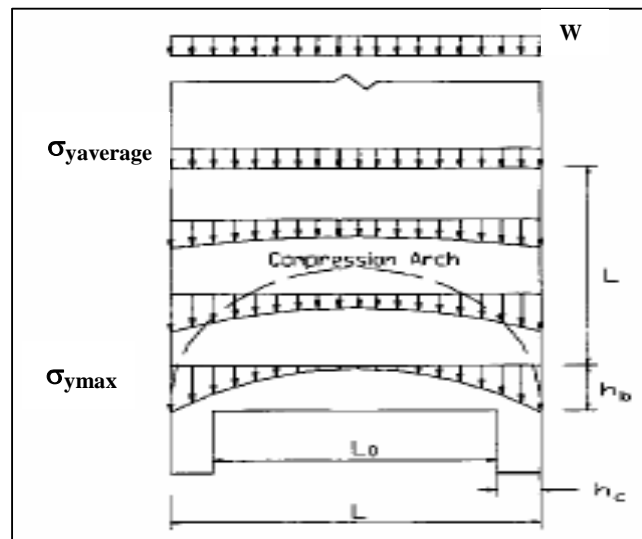


Figure 2.3 Distribution of vertical stress in shear wall

2.1.2 Structural Behaviour - Horizontal Stress in Wall

The distribution of the horizontal stress σ_x is shown in Figure 2.4. J.S Kuang and Shubin LI (2001) prove that the shear wall is almost in compression in the

horizontal direction though it is subjected to vertical loading. The intensity of the horizontal stress varies along the vertical direction; the value of σ_x is small at the wall-beam interface and almost equal to zero beyond a height equal to L (total span of the transfer beam) from the wall-beam interface.

When the depth of the beam is relatively small, the transfer beam is in full tension along the span owing to the interaction between the wall and the beam, as shown in Figure 2.4(a). When the depth of the beam is large enough, compression stress may appear in the upper part of the beam, but the compression zone is relatively small. It is obvious from Figure 2.4 that the transfer beam does not behave as an ordinary beam in bending or a deep beam, but is in full tension or flexural-tension along the span due to the interaction between the wall and beam. Therefore, unlike an ordinary beam or a deep beam, a transfer beam supporting in-plane loaded shear walls should generally be considered as a flexural-tensile member.

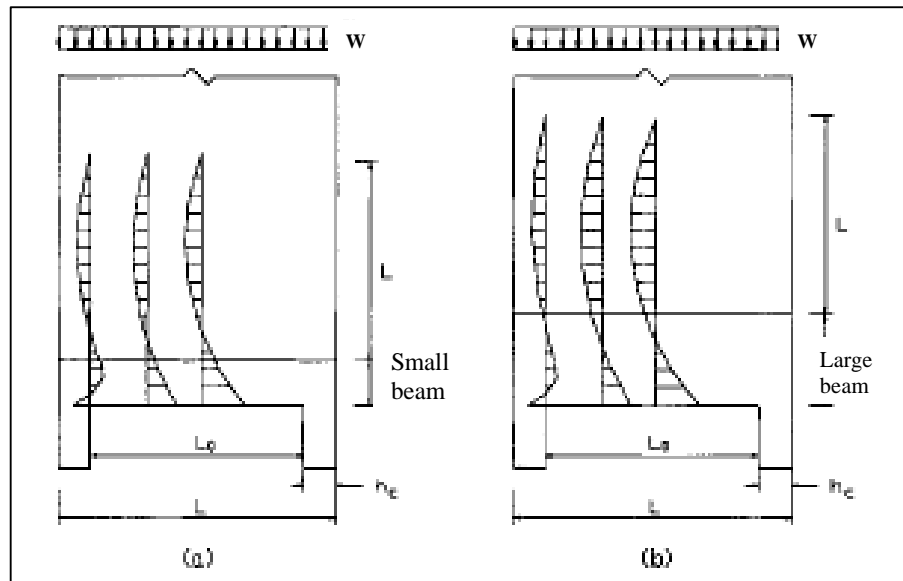


Figure 2.4 Distribution of horizontal stress in the wall-beam system

2.1.3 Structural Behaviour - Shear Stress in Wall

The distribution of shear stress in the wall-beam system is shown in Figure 2.5. J.S Kuang and Shubin LI (2001) find out that the shear stress is dominated in the lower part of the shear wall, and the maximum intensity of shear stress is reached at the wall-beam interface. Figure 2.5 also shows that the intensity of the shear stress is equal to zero beyond a height equal to L above the wall-beam interface. It indicates that in the higher parts of the shear wall the interaction effect does not affect the shear stress distribution in the wall.

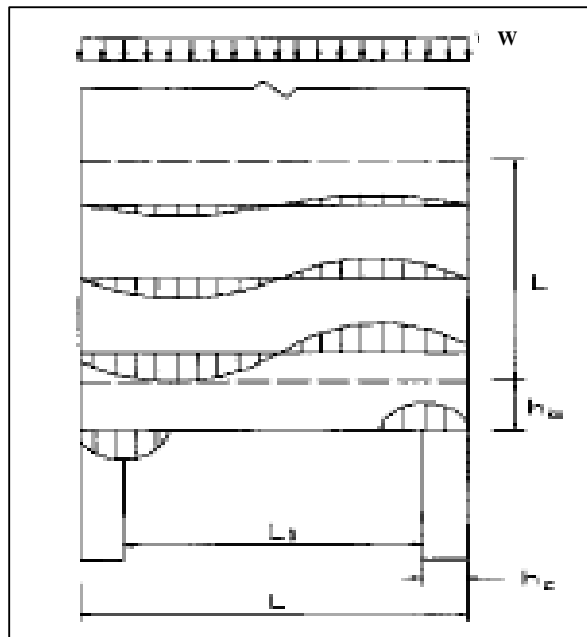


Figure 2.5 Distribution of shear stress in the system

2.1.4 Structural Behaviour – Bending Moment in Beam

The distribution of bending moments in the transfer beam along the span is shown in Figure 2.6. J.S Kuang and Shubin LI (2001) find out that the maximum bending moment occurs at the mid-span of the beam and decreases towards the support columns. Two contraflexural points are observed in the figure, which indicate that negative moments occur close to the ends of the beam.

Figure 2.7 shows the bending moments at mid-span against different depth–span ratios for different support stiffness hc/L . It is seen that as the depth of the transfer beam increases, the bending moment increases when the value of the support stiffness is fixed.

From Figure 2.7 it can also be seen that the bending moment of the beam decreases as the stiffness of the support columns increases. If the stiffness of the support columns is large enough, the columns can effectively restrain the displacement of the beam. Then the transfer beam behaves as a fixed beam, and the contraflexural points of the bending moment are normally located about $0.1L - 0.2L$ from the supports of the beam. If the stiffness of the support columns is relatively small, the beam will behave as a simply supported beam.

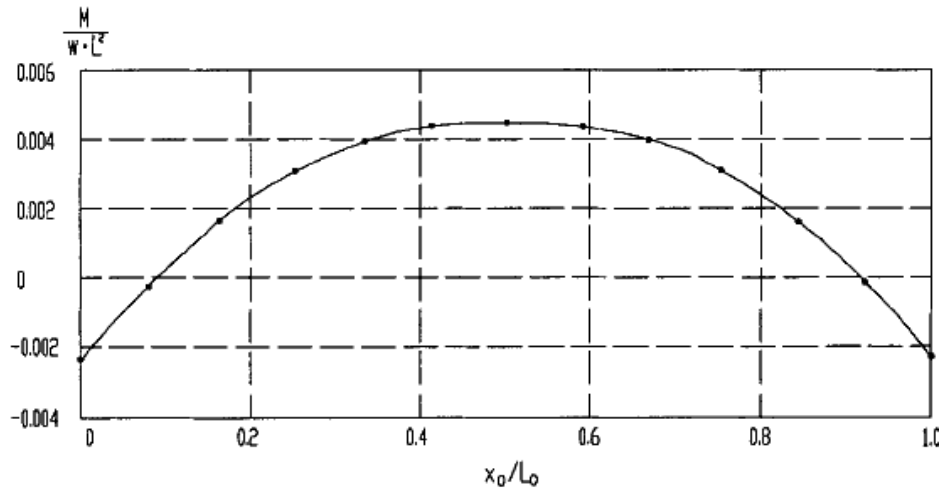


Figure 2.6 Variation of bending moment in the beam along the span

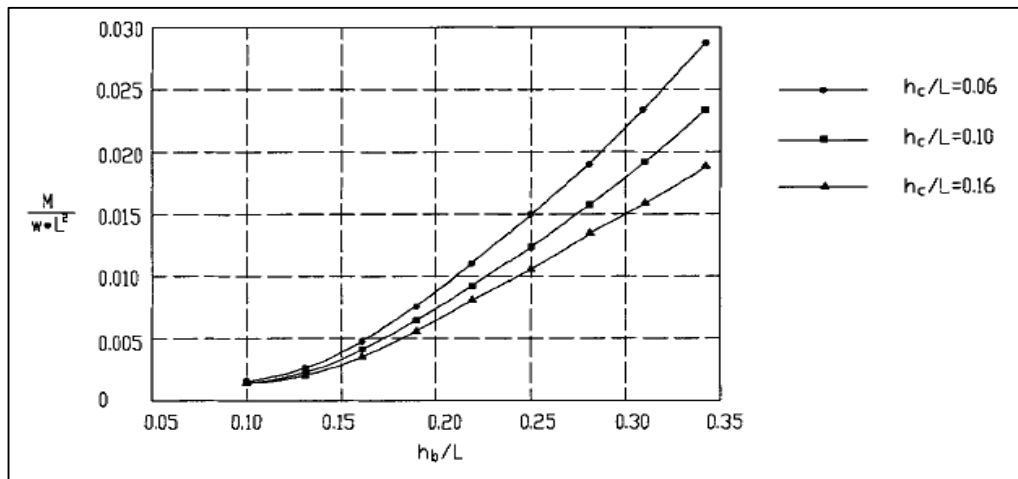


Figure 2.7 Variation of bending moment at mid-span against different depth–span ratios for different support stiffness

2.1.5 Interaction-based Design Table

Based on the finite element analysis of the interaction behaviour of the transfer beam–shear wall system, J.S Kuang and Shubin LI (2001) has developed a set of interaction-based design tables for determining the internal forces of the transfer beam supporting in-plane loaded shear walls. The design tables are presented based on an equivalent portal frame model shown in Figure 2.8. It can be seen from the figure that unlike an ordinary portal frame an axial force T has been introduced in the transfer beam owing to the interaction between the beam and the shear wall. Moreover, the bending moments M_2 and M_3 are not equal. This is because the shear wall takes some part of the bending moment from the transfer beam.

Interaction-based design tables are presented in Tables A1 to A6 in Appendix A for design of the transfer beam–shear wall system subjected to uniformly distributed loading. The widths of the transfer beam are double and triple the thickness of the shear wall, e.g. $b = 2t$ and $b = 3t$, respectively, which are the common cases in design practice. The coefficients of internal forces in the tables are calculated corresponding to two important design parameters: span/depth ratio of the transfer beam L/h_b and relative flexural stiffness of support columns hc/L . By using these tables, the maximum vertical stress in the shear wall σ_y and bending moments in the beam and support columns M_1 , M_2 , M_3 and M_4 are conveniently determined.

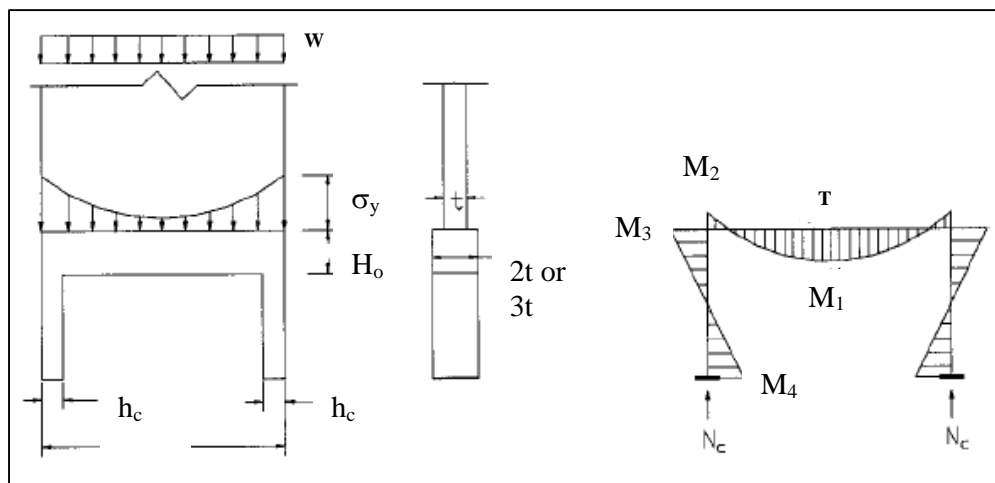


Figure 2.8 Equivalent portal frame model

2.1.6 Interaction-Based Design Formulas for Transfer Beams Based on Box Foundation Analogy

J.S Kuang and Shubin LI (2005) has, in their latest studies, presented a series of simplified formulas used for determining the maximum bending moment in the transfer beam based on the box foundation analogy, which could be utilized to check the result of finite element analysis on the shear wall-transfer beam structure.

The structural response of the beam-wall system can be studied by considering the transfer beam and the shear wall replaced by a box foundation and the upper structure, respectively. Fig. 2.9b shows a box foundation where the vertical loading is transferred from the upper structure to the basement through structural walls. The total moment caused by a uniformly distributed load could be distributed to the upper structure and the box foundation according to the stiffness ratio of the upper structure and the box foundation. Thus, the moment taken by the box foundation, M_b , can be written as

$$M_b = M_o \frac{E_b I_b}{E_w I_w + E_b I_b}$$

where $E_b I_b$ and $E_w I_w$ =flexural stiffnesses of the basement and the upper structures, respectively; $I_w = 1/12tH_e^3$, $H_e = [0.47+0.08 \log (E_b I_b/E_c I_c)]L$ and M_o =total moment caused by applied loading, given by

$$M_o = \frac{1}{8} w L_e^2$$

where

$$L_e = L_o, \quad \text{when } \frac{E_b I_b}{E_c I_c} \geq 10$$

$$L_e = \left(0.9 + 0.1 \cdot \log \frac{E_b I_b}{E_c I_c} \right) L_o, \quad \text{when } 0.1 < \frac{E_b I_b}{E_c I_c} < 10$$

$$L_e = 0.8 L_o, \quad \text{when } \frac{E_b I_b}{E_c I_c} \leq 0.1$$

It can be seen from the equations that, if the flexural stiffness of the transfer beam is much larger than that of the support columns, the beam behaves as a simply supported one, whereas, when the flexural stiffness of support columns is much larger than that of the transfer beam, the beam can be analyzed as a fixed-end one. Further, it has been proven that the results of the proposed design formulas agree very well with those of the finite element analysis.

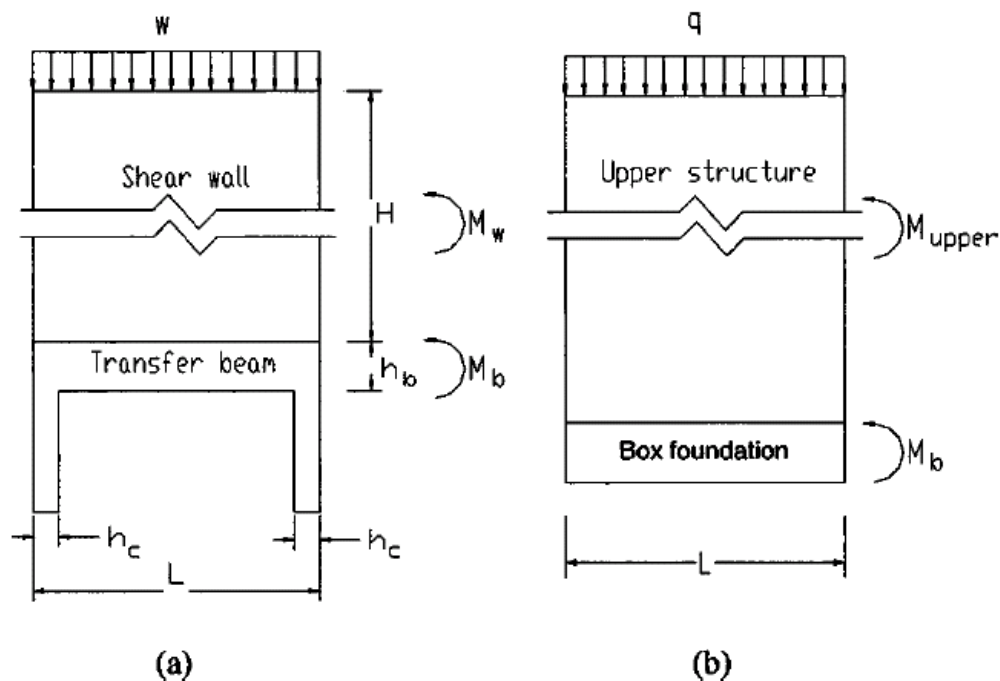


Figure 2.9 Box foundation analogy: a) Transfer beam–shear wall system; and b) box foundation and upper structure

2.2 Analysis of Transfer Beam – Shear Wall System Using Non-Finite Element Method

Kuang and Atanda (1998) has presented an approximate method to obtain rapid solution for the walls and girder in the analysis for a continuous coupled shear wall–transfer girder system subjected to uniformly distributed lateral loading. The upper coupled shear wall structure will be analyzed with the continuum technique assuming a rigid girder support. The forces at the interface will subsequently be imposed on the transfer girder system to obtain its internal forces. The object of the

method is to facilitate the practical design of such systems and serves as a guide in checking the results of sophisticated techniques.

2.2.1 Governing Equation

In the analysis carried out by Kuang and Atanda (1998), a coupled shear wall on continuous transfer beam system as shown in Figure 2.9 is considered. By employing the continuous medium approach of analysis, the system can be represented by a continuum structure as shown in Figure 2.10(a). Introducing a cut along the line of contraflexure of the lamina, a shear flow q per unit length will be released along the cut as shown in Figure 2.10(b). The axial force in the walls is given by,

where N is the axial force in the continuum.

$$N = - \int_0^x q dx$$

For no relative vertical displacement at the ends of the cut lamina, the vertical compatibility condition is,

$$\delta_1 + \delta_2 + \delta_3 + \delta_4 = 0$$

For a rigid support in which $\delta_4 = 0$, Kuang & Atanda (1997) shows that the governing differential equation can be written in terms of the axial force and the deflection along the height, respectively as

$$\frac{d^2 N}{dx^2} - \alpha^2 N = -\gamma M_e$$

$$\frac{d^4 y}{dx^4} - \alpha^2 \frac{d^2 y}{dx^2} = \frac{d^2 M_e}{dx^2 EI} - \alpha^2 (1 - \beta) \frac{M_e}{EI}$$

where M_e is the external moment. The parameters in the equations are defined as:

$$\alpha = \left(\frac{\gamma L}{\beta} \right)^{1/2}$$

$$\beta = \left(1 + \frac{AI}{A_1 A_2 L^2} \right)^{-1}$$

$$\gamma = \left(\frac{12LI_b}{b^3 h I} \right)$$

in which $A = A_1 + A_2$ and $I = I_1 + I_2$.

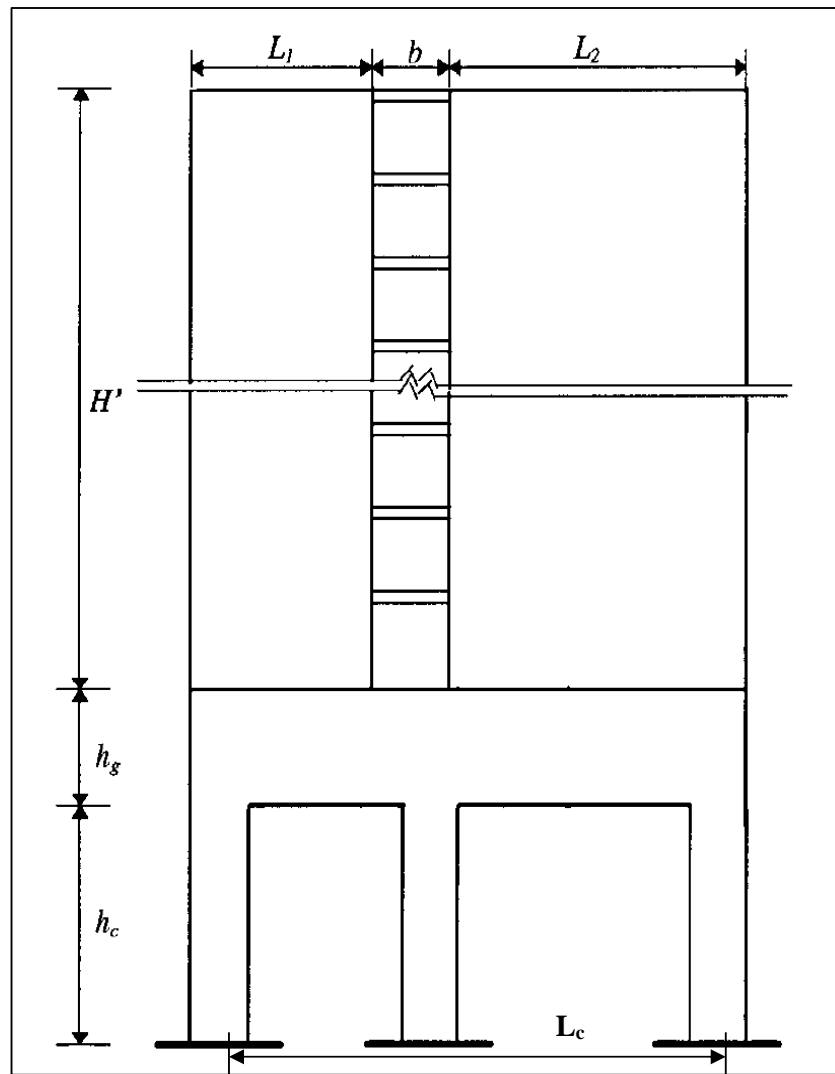


Figure 2.10 Coupled shear wall-continuous transfer girder system

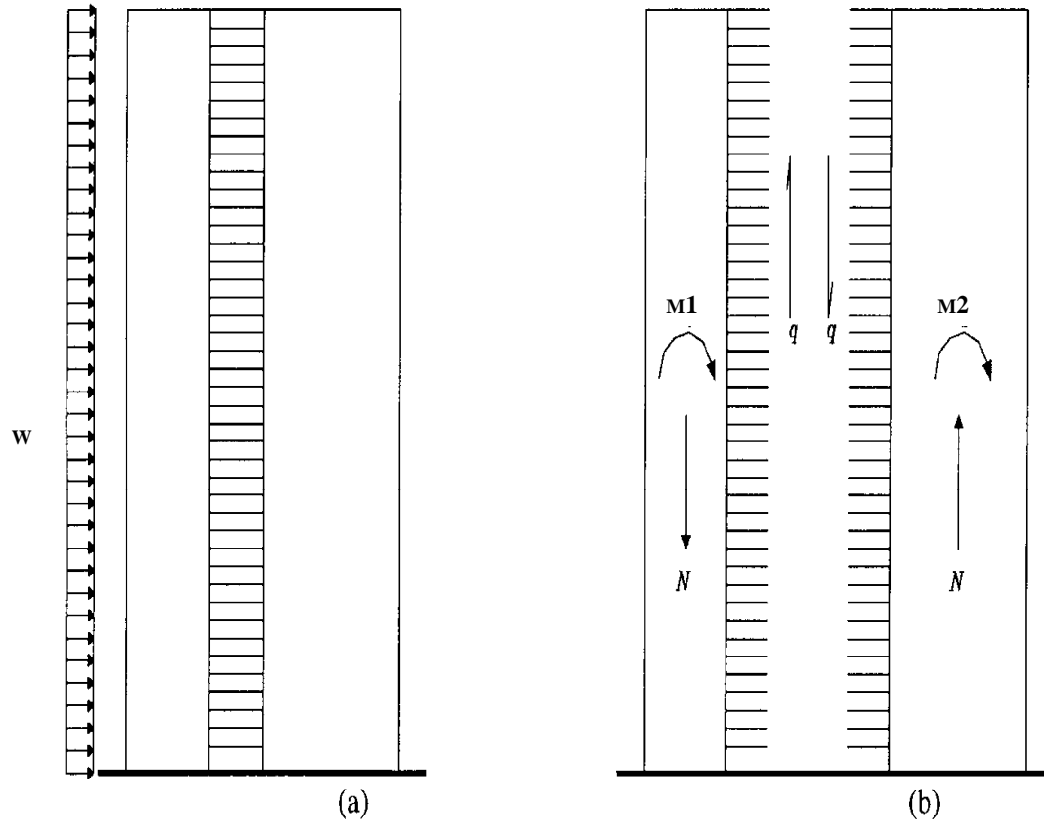


Figure 2.11 (a) continuum model; (b) forces in continuum

2.2.2 Axial Force of Walls

As the coupling beams get stiffer, the axial forces of the walls increase towards the base. This effect is significant only within height $\cong 2.5 Lc$ from the girder. Kuang and Atanda (1998) define the axial force at any distance x from the baseline for the continuum as

$$N = \frac{u\gamma}{\alpha^4} \left(1 - \frac{\cosh \alpha x + \alpha H \sinh \alpha(H-x)}{\cosh \alpha H} + \frac{\alpha^2(H-x)^2}{2} \right)$$

2.2.3 Moment of Walls

The stiffness of transfer would significantly affect the moment induced on the shear wall. The wall moment decreases with increasing stiffness of the coupling beam. This effect is insignificant after height $\cong 2.5 L_c$ from the girder. Kuang and Atanda (1998) express the moment at any point along the height of the walls as

$$M^* = \left[\frac{uH^2}{2} \left(1 - \frac{x}{H} \right)^2 - N^*L \right] c_3$$

where c_3 can be valuated from Figure 2.11.

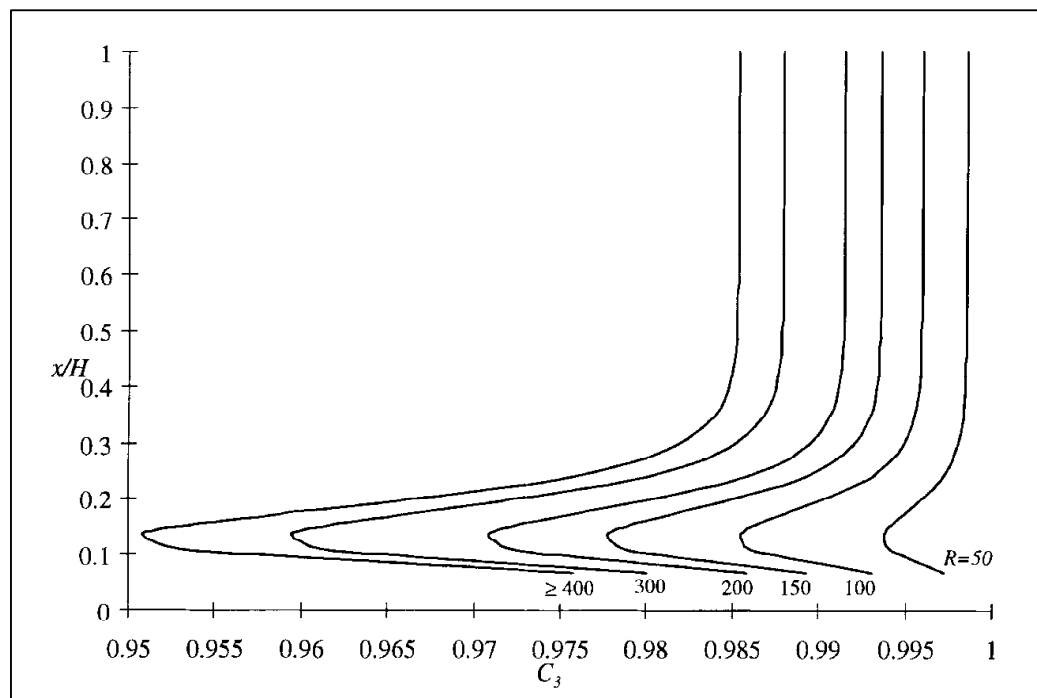


Figure 2.12 Bending moment modification coefficients for varying values of R

In this case, R is relative stiffness of wall and transfer girder and is given by:

$$R = \frac{t(L_w^3 - b^3)E_w L_a^2}{b_g h_g^3 E_g L_w^2}$$

where E_w is modulus of elasticity of walls, E_g modulus of elasticity of transfer beam

2.2.4 Top Deflection of Walls

Top deflection of shear wall depends a lot on the stiffness of its support, namely columns and transfer beam. Greater stiffness of the supports could help reduce the deflection. In comparison, the stiffness of transfer beam has greater effects on the shear wall's top deflection.

Kuang and Atanda (1998) explained that the axial forces developed in the walls are induced by shears from the double curvature bending of the coupling beam while resisting the free bending of the wall. The coupling beams thus cause a proportion of the applied moment to be resisted by axial forces. It then follows that the stiffer the connecting beams the more resistance they can offer to the walls' free bending, and hence the smaller the proportion of the external moment the walls need to resist. This will consequently result in a decrease in the value of the top deflection.

2.2.5 Shear Stress of Walls

The shears in the coupling beams increase with the stiffness of the beams. The increase in the stiffness of the transfer girder reduces the shear in the coupling beam up to within height $\cong 2.5 L_c$, beyond which there is no effect. (Kuang & Atanda, 1998)

2.3 Behaviour of Deep Beam

Transfer beam can be approximated to deep beam in terms of its geometry (provided that span/depth ratio less than 2.5) and structure behaviour. There are various methods available in analyzing the behaviour of deep beam in terms of linear elastic analysis such as finite element and experimental photo elasticity. These procedures assume an isotropic materials complying with Hooke's Law.

2.3.1 Elastic Analysis

In deep beam, plane sections across the beam do not remain plane (Arup, 1977). It is shown in Figure 2.12 that there is high peak of tensile stress at midplane of the beam and that the area of compressive stress is increased for a deep beam under uniformly distributed load. The geometry of deep beams is such that the flow of stress can spread a significant distance along the beam. It is thus noted that the shear transfer of the loads to the supports takes place in the lower half of the beam. It is also noted from the figure that the principal tensile stress is almost horizontal near the support under UDL.

Experimental work has shown that the stresses conform to elastic behaviour before cracking occurs. The presence of cracking due to excessive loading, however, disrupts the elastic-linear behaviour of the beam. The extending bending cracks tend to increase increase the lever arm and decrease the area of compressive zone, especially at mid span of the beam (Arup et al, 1977). The deviation from the elastic-linear behaviour becomes greater with the increase in the size and number of cracks. Leonhardt (1970) has shown that the crack can be controlled and that the beam could maintain a closer elastic behaviour through closer reinforcement alignment.

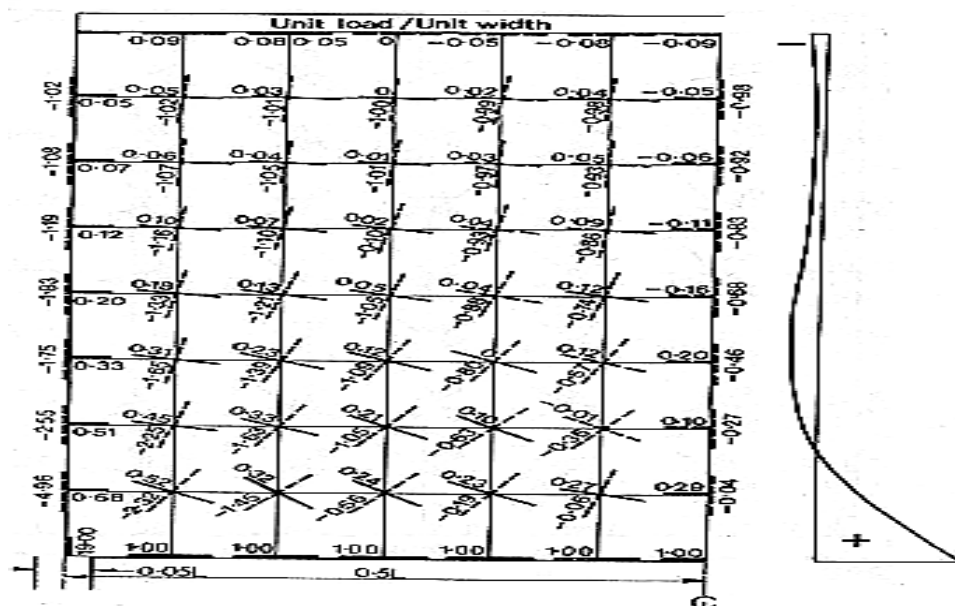


Figure 2.13 Stress at midplane of the beam under top load

2.3.2 Flexural Failure

Flexural failures may be recognized by the inelastic yielding and the final fracture of the bending reinforcement (Arup et al, 1977). Vertical cracks propagate from the soffit and rise with increasing load to almost the full effective height of the beam as shown in Figure 2.13. Failure usually occurs due to breakage of the reinforcement rather than crushing of the concrete.

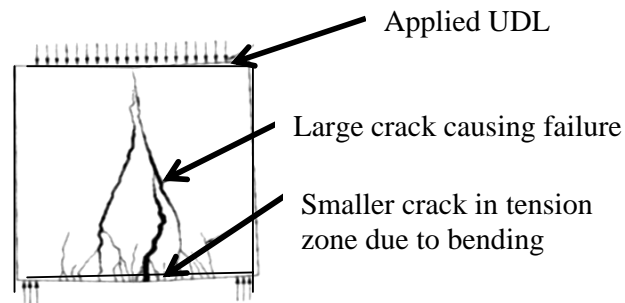


Figure 2.14 Typical deep beam failures in flexure

2.3.3 Shear Failure

Due to their geometric proportions, the capacity of reinforced concrete deep beams is governed mainly by shear strength. There are two distinct mechanisms which provide shear resistance in deep beam. The first is compressive strength brought into action by top loads, and the second is the tensile capacity of the web reinforcement which is brought into action by bottom and indirect loads.

The behaviour of deep beam in bending is not affected by the type and location of the load (Arup et al, 1977). But the failure in shear is typified by the widening of a series of diagonal cracks and the crushing of the concrete between them and is notably dependant upon the location and distribution of the applied loads.

Consider behaviour after cracking has occurred in a deep beam with reinforcement. Since the cracks run parallel to the direction of the strut, it might be

supposed that the ultimate capacity is simply that of the sum of their compressive strength, which would not be significantly diminished by the degree of cracking (Arup et al, 1977).

In the shear area of a deep beam, the concrete struts between diagonal cracks split progressively, becoming eccentrically loaded but restrained against in-plane bending by web reinforcement (Arup et al, 1977). Leonhardt (1970) has suggested that the shear capacity of deep beams cannot be improved by the addition of web reinforcement but Kong (1972) has demonstrated that improvement is possible to as little as 30%. The reinforcement is best provided normal to the direction of cracks and is most effective close to the beam soffit (Kong, 1972). The most effective arrangement of web reinforcement depends on the angle of inclination of the shear crack or the ratio of shear span to the effective height. When the ratio is less than 0.3, horizontal bars are more effective than vertical (Kong, 1972).

2.3.4 Bearing Capacity

High compressive stress may occur over supports and under concentrated loads. At the support, the typical elastic stress distribution maybe represented by a stress block in which the design stress is limited to $0.4f_{cu}$ (Arup et al, 1977). Leonhardt (1970) has, however, suggested that at intermediate supports in a continuous beam system, design bearing stress at $0.67f_{cu}$ would be acceptable because of the biaxial state of stress.

2.3.5 Deformation and Deflection

Deformation of deep beams under service load is not usually significant (Arup et al, 1977). The mathematical model used in computing the deformation includes time dependant effects of creep and shrinkage, and the stiffening effect of the concrete surrounding the steel tie of the deep beam arch.

2.4 Struts and Ties Models for Transfer Beam

ACI section 10.7.7 defines a beam which is loaded on one face and supported on the opposite face so that compression struts can develop between the loads and the supports, and having clear span equal or less than four times the overall member height, as a deep beam. Typically, deep beams occur as transfer beam (Rogowsky and Macgregor, 1986). In this research, the transfer beam is loaded on the top face by distributed load from shear wall and supported on the bottom face by columns.

2.4.1 Strut-and-Tie Models for Deep Beams

A strut-and-tie model for a deep beam/transfer beam consists of compressive struts and tensile ties, and joints referred to as nodes. The concrete around the nodes is called a nodal zone. The nodal zones transfer the forces from struts to ties and to the reactions (Schlaich and Weischede, 1982). The struts represent concrete compressive stress fields (Schlaich and Weischede, 1991) and the ties represent concrete tensile stress fields.

The model of uncracked, elastic, single-span transfer beam supporting a strip of shear wall has the stress trajectories as shown in Figure 2.14a. The distributions of horizontal stresses on vertical sections at midspan and quarter point are plotted in Figure 2.14b. The distribution shown is similar to that of J.S Kuang and Shubin LI (2001), as illustrated in Figure 2.4. The stress trajectories can be represented by the simple truss as in Figure 2.14c or the slightly more complex truss in Figure 2.14d (Rogowsky and Macgregor, 1986). The crack pattern is as show in Figure 2.14e.

The strut-and-tie model must be in equilibrium with the loads. There must be an early laid out load path. This load path can be determined by observation or finite element analysis (Adebar and Zhou, 1993). From an elastic stress analysis, it is possible to derive the stress trajectories for a transfer beam loaded with distributed shear wall load. Principal compression stresses act parallel to the dashed lines, which

are known as compressive stress trajectories. Principal tensile stresses act parallel to the solid lines, which are called tensile stress trajectories (Adebar and Zhou, 1993). The compressive struts should roughly follow the direction of the compressive stress trajectories, with a tolerance $\pm 15^\circ$. For a tie, there is less restriction on the conformance of ties with the tensile stress trajectories. However, they should be in the general direction of the tension stress trajectories (Adebar and Zhou, 1993). The layout of the strut-and-tie model of a transfer beam loaded with shear wall on top of it can hence be illustrated as Figure 2.14d.

2.4.2 Suitable Strut-and-Tie Layouts

The axis of a strut representing the compression zone in a deep flexural member such as a transfer beam should be located about $a/2$ from the compression face of the beam, where a is the depth of the rectangular stress block. Likewise, the axis of a tensile tie should be about $a/2$ from the tensile face of the beam (Adebar and Zhou, 1993). Angle between the strut and attached ties at a node should be about 45° and never less than 25° as specified in ACI section A.2.5. Besides that, it is recommended that the strut to be at a slope of 2:1 relative to the axis of the applied load used as shown in Figure 2.15 (Adebar and Zhou, 1993).

2.4.3 Behaviour of Shear Wall

In general, most shear wall supports the loads transferred from floor slab which also acts as lateral restraint to the lateral wind load. Since the thickness of the shear wall is relatively small compared to its width and height, it is reasonable to model the structure as a quasi-three-dimensional structure which is composed of plane elements ignoring their out-of-plane bending and shear stiffness. Thus a complex three-dimensional reinforced concrete shear wall-slab structure with non-linearity of the materials is represented by assembling iso-parametric plane elements with four nodes for wall panels (Ioue, Yang and Shibata, 1997).

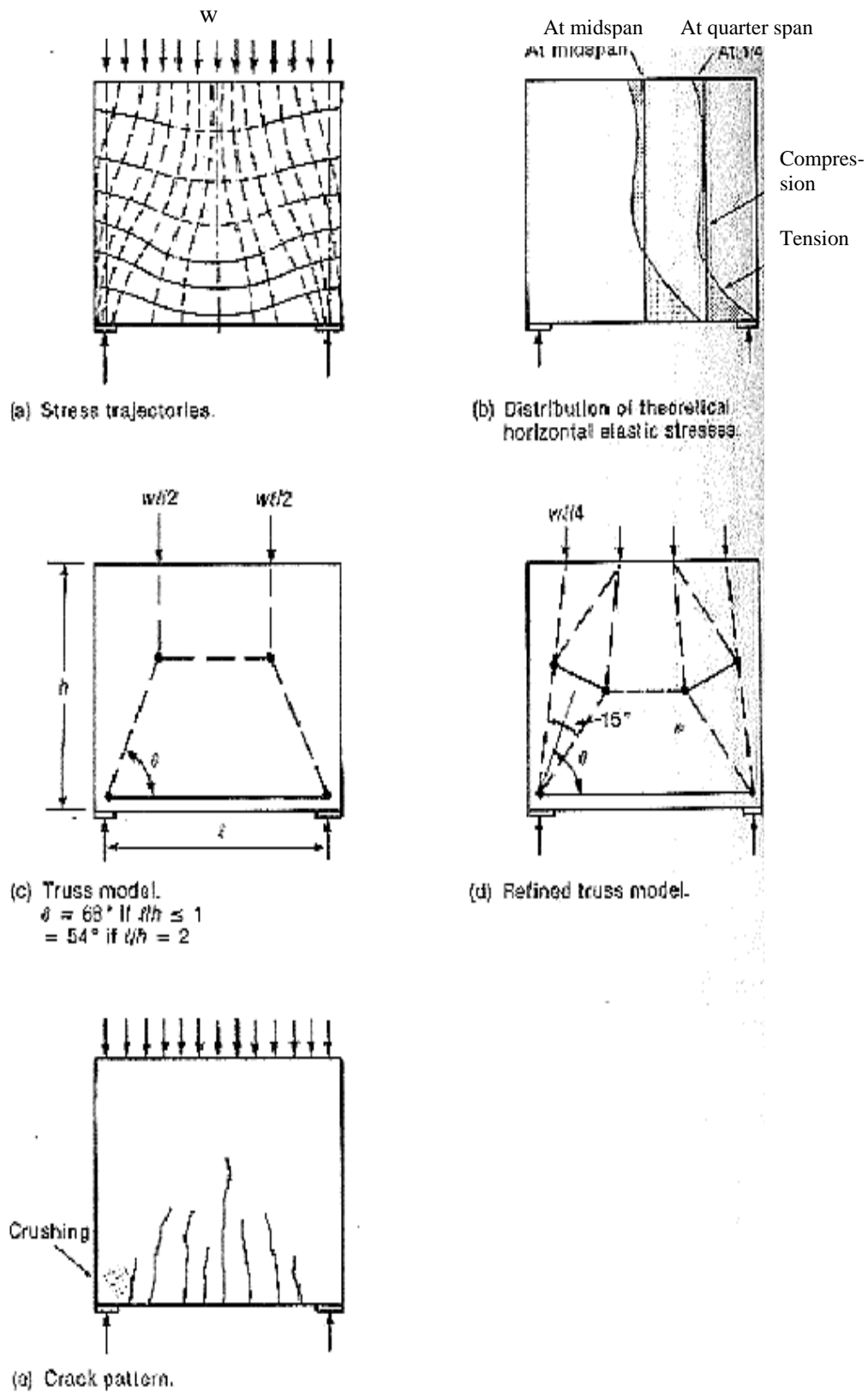


Figure 2.15 Stress trajectories of single span transfer beam supporting a uniform load

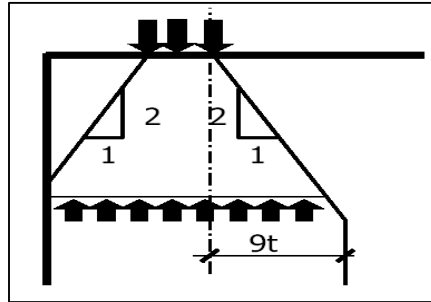


Figure 2.16 Cracking control – Strut-and-tie models

For slab subjected to vertical load only, the slab is modelled by plane elements in which the thickness of the slab elements need to be defined as geometric properties. The stiffness of these elements is increased to represent the solid condition of the slab. By clamping the element nodes along the lower boundary of the shear wall, a description of foundation fixity representing the transfer beam is provided (Kotsovos and Pavlovic, 1995). An example of the model is shown in (Figure 2.16)

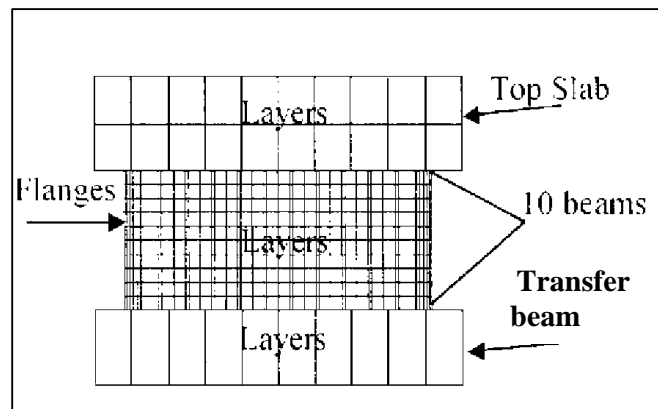


Figure 2.17 Finite element model of box-shaped shear wall

In order to define the model's loading condition, the model is loaded with uniformly distributed edge pressure and traction along the upper boundary of the wall. Constant pressure simulates the applied constant vertical load, while edge traction simulates the incremental applied horizontal load (Kotsovos and Pavlovic, 1995).

In order to verify the accuracy of 2D finite element modeling Lefas, Kotsovos and Ambraseys (1990) had carried out an experiment comprising 13 samples of structural walls covering a considerable range of parameters such as height-to-width ratio h/l , concrete strength, reinforcement detailing, and levels of axial load. In the experiments, the walls are considered to represent the critical storey element of a structural wall system with a rectangular cross section. In all cases, the walls are monolithically connected to an upper and lower beam which acts as slab/beam sustaining load and transfer beam serving as rigid foundation, respectively.

The results obtained from the experiment show that the analytical model has yielded realistic predictions of the ultimate horizontal load sustained by the wall in spite of the fact that the plane stress analysis employed in the analytical modeling ignores triaxial stress conditions that develop within the shear wall at their ultimate limit state. The analytical predictions using finite element analysis should, however, be considered to represent lower-bound values of the failure load as the supposed triaxial stress conditions normally lead to relatively higher strength values (Kotsovos and Pavlovic, 1995).

A comparison of typical load-deflection curves both experimentally and analytically (finite element analysis) as obtained from the experiments conducted by Lefas and Kotsovos (1987) indicates that the plane stress analysis cannot yield a very accurate prediction of the ductile deformation at the ultimate limit state. This is mainly because the ductile behaviour of under-reinforced concrete sections is associated with triaxial conditions rather than uniaxial stress-strain considered in 2D analysis.

2.5 Finite Element Analysis of Shear Wall-Transfer Beam Structure

Finite element has become a widely recognized tool in structural analysis, including the analysis of shear wall-transfer beam structure. Normal practice in the analysis of shear wall-transfer beam structure is such that the structure is treated as a two-dimensional problem, and that two-dimensional stress analysis methods should be used in order to obtain a realistic stress distribution in the structure.

2.5.1 Introduction to Finite Element

Finite element analysis is a mean of evaluating the response of a complex shape to any external loading, by dividing the complex shape up into lots of smaller simpler shapes. The shape of each finite element is defined by the coordinates of its nodes. The manner in which the Finite Element Model will react is given by the degrees of freedom, which are expressed at the nodes.

Since we can express the response of a single Finite Element to a known stimulus, we can build up a model for the whole structure by assembling all of the simple expressions into a set of simultaneous equations with the degrees of freedom at each node as the unknowns. These are then solved using a matrix solution technique (Finite Element Analysis Ltd, 2003).

LUSAS is one of the application programs applicable in the market normally used by specialist in creating numerical model in order to investigate the stresses behaviour of a structure. It is an associative feature-based modeller. The model geometry is entered in terms of features which are discretised into finite elements in order to perform the analysis. Increasing the discretisation of the features will usually result in an increase in accuracy of the solution, but with a corresponding increase in solution time and disk space required.

2.5.2 Basic Finite Element Equations

For linear problems, when a structure is loaded work is stored in the form of recoverable strain energy i.e. energy that would be recovered if the system was unloaded. This relates to the area under the stress/strain graph the strain energy is given by Zienkiewicz (1977) as

$$U = \int_V \underline{\epsilon}^T \underline{\sigma} dv$$

, where $\underline{\epsilon}$ and $\underline{\sigma}$ are the total strains and stresses.

The governing equations of equilibrium may be formed by utilizing the principle of virtual work. This states that, for any small, virtual displacements δu imposed on the body, the total internal work must equal the total external work for equilibrium to be maintained (Finite Element Analysis Ltd, 2001), i.e.

$$\int_V \delta \underline{\underline{\varepsilon}}^T \underline{\underline{\sigma}} \, dv = \int_V \delta \underline{u}^T \underline{f} \, dv + \int_S \delta \underline{u}^T \underline{t} \, ds + \sum \delta \underline{u}^T \underline{F}$$

, where $\delta \underline{u}$ is the virtual displacements corresponding to the virtual displacements, δu .
 \underline{t} - Surface forces, \underline{f} - body force, \underline{F} - concentrated loads

In finite element analysis, the body is approximated as an assemblage of discrete elements interconnected at nodal points. The displacements within any element are then interpolated from the displacements at the nodal points corresponding to that element (Finite Element Analysis Ltd, 2001), i.e. for element e

$$\underline{u}^{(e)} = \underline{N}^{(e)} \underline{a}^{(e)}$$

, where $\underline{N}^{(e)}$ is the displacement interpolation or shape function matrix and $\underline{a}^{(e)}$ is the vector of nodal displacements. The strains within an element may be related to the displacements by

$$\underline{\underline{\varepsilon}}^{(e)} = \underline{\underline{B}}^{(e)} \underline{a}^{(e)}$$

, where $\underline{\underline{B}}$ is the strain-displacement matrix.

For linear elasticity, the stresses within the finite element are related to the strains using a relationship of the form

$$\underline{\underline{\sigma}}^{(e)} = \underline{\underline{D}}^{(e)} (\underline{\underline{\varepsilon}}^{(e)} - \underline{\underline{\varepsilon}}_0^{(e)}) + \underline{\underline{\sigma}}_0^{(e)}$$

, where $\underline{\underline{D}}$ is a matrix of elastic constants, and $\underline{\underline{\sigma}}_0$ and $\underline{\underline{\varepsilon}}_0$ are the initial stresses and strains respectively

The virtual work equation may be discretised (Finite Element Analysis Ltd, 2001) to give

$$\sum_{e=1}^n \delta \underline{a}^T \int_v \underline{B}^{(e)T} \underline{D}^{(e)} \underline{B}^{(e)} dv \underline{a} =$$

$$\delta \underline{a}^T \left[\begin{array}{l} \sum_{e=1}^n \int_v \underline{N}^{(e)T} \underline{f}^{(e)} dv + \sum_{e=1}^n \int_s \underline{N}_s^{(e)T} \underline{t}^{(e)} ds \\ - \sum_{e=1}^n \int_v \underline{B}^{(e)T} (\underline{\sigma}_0^{(e)} - \underline{D}^{(e)} \underline{\epsilon}_0^{(e)}) dv + \underline{E} \end{array} \right]$$

, where $N_s^{(e)}$ is the interpolation functions for the surfaces of the elements and n is the number of elements in the assemblage.

By using the virtual displacement theorem, the equilibrium equations of the element assemblage becomes

$$\underline{K} \underline{a} = \underline{R}$$

where \underline{K} is the structure stiffness matrix, defined as

$$\underline{K} = \sum_{e=1}^n \int_v \underline{B}^{(e)T} \underline{D}^{(e)} \underline{B}^{(e)} dv$$

and \underline{R} is the structure force vector, defined as

$$\underline{R} = \underline{R}_b + \underline{R}_s - \underline{R}_0 + \underline{R}_c$$

and \underline{R}_b is the force vector due to the element body loads

$$\underline{R}_b = \sum_{e=1}^n \int_v \underline{N}^{(e)T} \underline{f}^{(e)} dv$$

\underline{R}_s is the force vector due to the element surface tractions

$$\underline{R}_s = \sum_{e=1}^n \int_s \underline{N}_s^{(e)T} \underline{t}^{(e)} dv$$

\underline{R}_0 is the force vector due to the initial stresses and strains

$$\underline{R}_0 = \sum_{e=1}^n \int_v \underline{B}^{(e)T} (\underline{\sigma}_0^{(e)} - \underline{D}^{(e)} \underline{\epsilon}_0^{(e)}) dv$$

\underline{R}_c is the force vector due to concentrated loads

$$\underline{R}_c = \underline{E}$$

2.5.3 Formulation of Standard 2D Isoparametric Elements

One of the essential steps in analyzing a finite element model is selecting suitable finite elements type for the structures concerned. For both the transfer beam and shear wall, the concrete section is represented by plane stress (QPM8) surface elements. It is under the surface element category of 2D continuum. The 8 node rectangular element has 16 degree of freedoms, u_1 to u_8 and v_1 to v_8 at its eight nodes.

2D continuum elements are used to model solid structures whose behaviour may reasonably be assumed to be 2-dimensional. The plane stress elements are suitable for analysing structures which are thin in the out of plane direction, e.g. shear wall subject to in-plane loading (Figure 2.17).

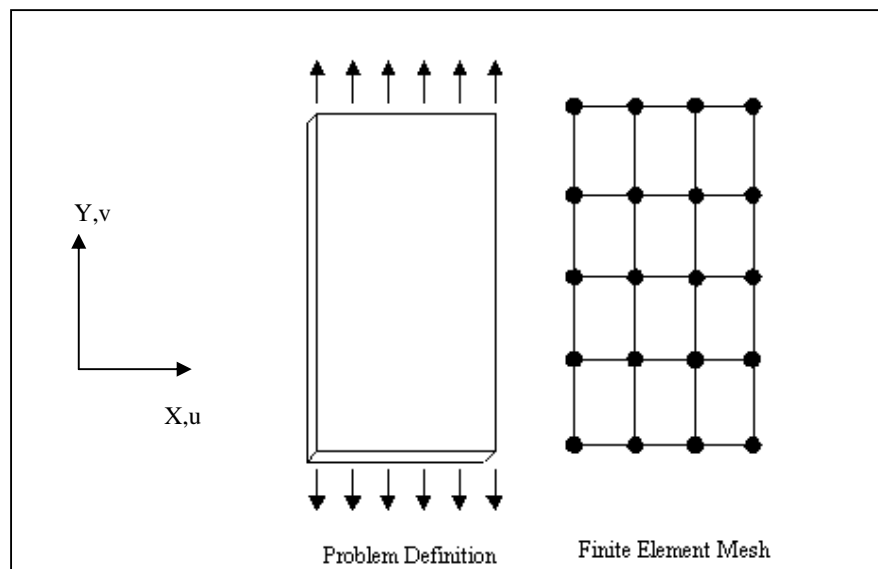


Figure 2.18 Example illustrating the use of plane stress elements subject to in plane loading

All the isoparametric elements described in this section must be defined using only X and Y coordinates. The plane stress elements are formulated by assuming that the variation of out of plane direct stress and shear stresses is zero, i.e.

$$\sigma_z = 0, \quad \sigma_{xz} = 0, \quad \sigma_{yz} = 0$$

Isoparametric finite elements utilize the following shape functions to interpolate the displacements and geometry (Finite Element Analysis Ltd, 2001), i.e.

$$\begin{aligned} \text{Displacement:} \quad U &= \sum_{i=1}^n N_i(\xi, \eta) U_i \\ \text{Geometry:} \quad X &= \sum_{i=1}^n N_i(\xi, \eta) X_i \end{aligned}$$

, where $N_i(\xi, \eta)$ is the element shape function for node i and n is the number of nodes.

For plane stress element (QPM8), the infinitesimal strain-displacement relationship (Finite Element Analysis Ltd, 2001) is defined as

$$\epsilon_X = \frac{\partial U}{\partial X} \quad , \quad \epsilon_Y = \frac{\partial V}{\partial Y} \quad , \quad \gamma_{XY} = \frac{\partial U}{\partial Y} + \frac{\partial V}{\partial X}$$

The isotropic elastic modulus matrices are (Finite Element Analysis Ltd, 2001)

$$\underline{D} = \frac{E}{(1-\nu^2)} \begin{bmatrix} 1 & \nu & 0 \\ \nu & 1 & 0 \\ 0 & 0 & \frac{(1-\nu)}{2} \end{bmatrix}$$

Thus, stress, $\sigma = \underline{D}\epsilon$

$$\begin{Bmatrix} \sigma_x \\ \sigma_y \\ \tau_{xy} \end{Bmatrix} = \frac{E}{(1-\nu^2)} \begin{bmatrix} 1 & \nu & 0 \\ \nu & 1 & 0 \\ 0 & 0 & \frac{(1-\nu)}{2} \end{bmatrix} \begin{Bmatrix} \epsilon_x \\ \epsilon_y \\ \gamma_{xy} \end{Bmatrix}$$

CHAPTER 3

METHODOLOGY

3.1 Introduction

In order to analyze the stress behaviour of the shear wall-transfer beam structure, the finite element method is employed throughout the research. Two dimensional analysis is carried out and plane stress element is used to represent both the shear wall and transfer beam element.

Linear-elastic concept is employed instead of the more ideal non-linear analysis for the purposes of achieving an adequate level of performance under ordinary serviceability condition. Linear elastic analysis simply means that the design is based on the uncracked concrete structure and that the material is assumed to be linearly elastic, homogeneous and isotropic. It is adequate in obtaining the stress distribution for preliminary study or design purpose.

A finite element model comprises shear wall and transfer beam from a case study will be created using LUSAS software. Throughout this project, the LUSAS Finite Element system is employed to carry out analysis on the vertical stress in wall, horizontal stress in wall, shear stress in wall, shear force in beam and bending moment in beam under both the vertical gravity load and lateral wind load. All these stress behaviour of the shear wall-transfer beam interaction zone obtained from the analysis are then compared with those yielded through analysis carried out by J.S Kuang and Shubin LI (2001) using finite element code SAP 2000 (Computers and

Structures, 1997). From the comparison, conclusion will be drawn for the various stress behaviour of the shear wall-transfer beam structure.

The finite element analysis in this project is carried out in two separate cases. The first case is as though carried out by J.S Kuang and Shubin Li, where the model is solely subjected to vertical loads. The dead load is factored with 1.4 while the live load is factored with 1.6. In the second case, the similar shear wall-transfer beam structure is subjected to both vertical loads and lateral wind load, all of which being factored with 1.2. This creates a platform for observing the changes in stress behaviour due to the wind load, which is not covered in the previous research.

3.2 LUSAS Finite Element System

A complete finite element analysis involves three stages: Pre-Processing, Finite Element Solve and Results-Processing.

Pre-processing involves creating a geometric representation of the structure, then assigning properties, then outputting the information as a formatted data file (.dat) suitable for processing by LUSAS. To create model for a structure, geometry (Points, Lines, Combined Lines, Surfaces and Volumes) has to be identified and drawn. After that attributes (Materials, Loading, Supports, Mesh, etc.) have to be defined and assigned. An attribute is first defined by creating an attribute dataset. The dataset is then assigned to chosen features.

Once a model has been created, the solution can be done by clicking on the solve button. LUSAS creates a data file from the model and solves the stiffness matrix, which finally yields the stresses sustained by the structure under loading in the form of contour plots, undeformed/deformed mesh plots etc.

3.2.1 Selecting Geometry of Shear Wall-Transfer Beam Finite Element Model

There are four geometric feature types in LUSAS, namely points, lines, surface and volume. In this analysis, both the shear wall and transfer beam are of surface feature type defined by lines and points.

3.2.2 Defining Attribute of Shear Wall-Transfer Beam Finite Element Model

A few attributes are needed to describe and characterize a finite element model. For a 2D model, the required attributes are mesh with selected element type, geometric properties such as thickness of a member, material properties, loading and support condition.

3.2.2.1 Mesh

Meshing is a process of subdividing a model into finite elements for solution. The number of division per line will determine how dense is the mesh and hence imply how accurate the structure analyzed will be. There are various mesh patterns which can be achieved using LUSAS. As for the analysis of the shear wall-transfer beam structure, regular mesh is selected.

3.2.2.2 Element Selection

For both the transfer beam and shear wall, the concrete section is represented by plane stress (QPM8) surface elements (Figure 3.2). The 2D continuum elements are used to model the structures as the normal stress and the shear stresses directed perpendicular to the plane are assumed to be zero.

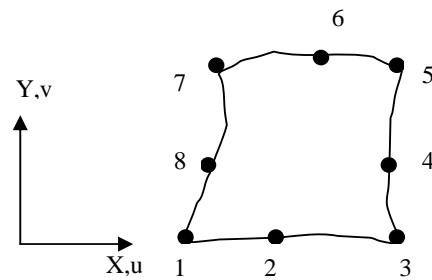


Figure 3.1 Plane stress (QPM8) surface elements

3.2.2.3 Defining the Geometric Properties

Geometric properties are used to describe geometric attributes which have not been defined by the feature geometry. The thickness of the beam, columns and shear wall need to be defined as geometric properties and assigned to the required surface. In this project, the thickness of wall is set as 225mm, the width of column is 1m and the breath of transfer beam is 0.8m.

3.2.2.4 Defining Material Properties

Every part of a finite element model must be assigned a material property dataset. In this project, the linear elastic behaviour is assumed for the shear wall-transfer beam structure and the concrete used are considered as isotropic. This indicates that the material properties are the same in all directions. This process includes the determination of the materials' elastic modulus and Poisson ratio. In this project, both the columns and transfer beam are assigned with the concrete grade C40 whereas the shear wall is assigned with grade C30.

3.2.2.5 Defining Support Condition

Support conditions describe the way in which the model is supported or restrained. A support dataset contains information about the restraints applied to each degree of freedom. In this project, fixed supports are provided at the base of the columns. In other words, they are restrained in x and y direction as well as restrained against moment.

3.2.2.6 Loading Assignment

Loading datasets describe the external influences to which the model is subjected. Feature based loads are assigned to the model geometry and are effective over the whole of the feature to which they are assigned. The defined loading value will be assigned as a constant value to all of the nodes/elements in the feature.

In this project, the main structural load of concern is the global distributed loads which emerge in the forms of distributed wind load acting laterally on the shear wall side face, and superimposed vertical loads acting on the slabs. The vertical loads consists of live loads and dead loads distributed from structural floor slabs to shear wall, thus subsequently to the supporting transfer beam. Selfweight of the concrete structure can be defined by body load which takes the unit weight of concrete and gravity acceleration into account.

3.2.3 Model Analysis and Results Processing

Results processing, also known as post-processing, is the manipulation and visualization of the results produced during an analysis. Results processing can involve the following steps, depending on the type of analysis (Figure 3.5):

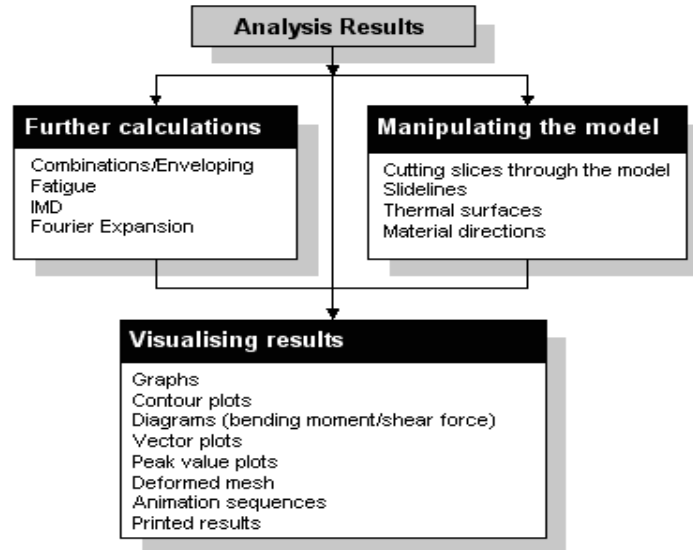


Figure 3.2 Results processing

3.3 Design Procedures of Transfer Beam Based on Ciria Guide 2 and CP 110

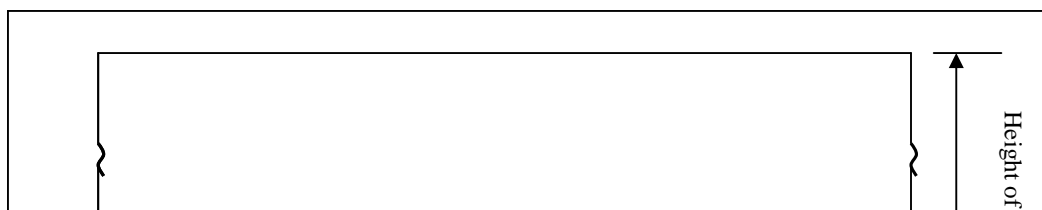
The Ciria guide has been prepared by a team of designers and approved as an authoritative practice in designing reinforced concrete deep beams. It is based on an exhaustive study of published literature and of research reports on the subject. The methods used in the guide conform to the limit state principals adopted in CP110 and the CEB-FIP recommendations.

3.3.1 Geometry

The first thing in designing the transfer beam is to determine its effective span and height. The effective span and height of a transfer beam (deep beam) is as shown in Figure 3.6 and the equation below:

Effective span, $l = l_o + (\text{the lesser of } c_1/2 \text{ or } 0.11l_o) + (\text{the lesser of } c_2/2 \text{ or } 0.11l_o)$

Active height, $h_a = h$ when $l > h$
 $= l$ when $h > l$



For practical construction purposes, the thickness of the beam, b , should not be less than the sum of 6 dimensions given below:

- II. Twice the minimum concrete cover to the outer layers of reinforcement
- III. A dimension allowing for four layers of web reinforcement, one vertical and one horizontal at each face of the beam, including bar deformation as appropriate.
- IV. Space for principal reinforcement bars if not accommodated in the web steel allowance.
- V. Space for the introduction and compaction of the concrete between the inner layer of the reinforcement – say, a minimum of 80mm.
- VI. Space for the vertical reinforcement from the supports, if not accommodated with other allowance.
- VII. Space for U-bar anchorage at the supports, if this is required. The diameter of U-bend depends on the force in the bars and the allowable bearing stress against the curve. As a first approximation the outside diameter of such a U-bar bend can be taken as 16 bar diameters. Thus the minimum thickness is rarely <200mm and is nearer to 300mm.

3.3.2 Force Computation

Vertical forces applied above a line $0.75 h_a$ above the beam soffit are considered applied at the top of the beam and may be represented in their original form or by their static equivalent, which may be uniformly or variably distributed along the span or part of the span. For loads applied below a line $0.75 h_a$ such as beam selfweight and floor load, they will be considered as hanging loads. To estimate bending moment, only forces applied over the clear span, l_o , need to be considered.

3.3.3 Ultimate Limit State

Ciria Guide 2 provides comprehensive procedures to design the transfer beam under ultimate limit state. In this project, the transfer beam is designed against the strength in bending, shear capacity and bearing capacity in order to obtain the required reinforcement to resist moment, and shear and bearing stress.

3.3.3.1 Strength in Bending

The area of reinforcement provided to resist positive and negative moment should satisfy the condition $A_s = M / 0.87 f_y z$, where

M = design moment at ultimate limit state

Z = lever arm at which the reinforcement acts

= $0.2l + 0.4h_a$ (single span, positive sagging moments, $l/h < 2$)

= $0.2l + 0.3h_a$ (multi span, mid span and support moments, $l/h < 2.5$)

Where adjacent span lengths differ, the lever arm over the support shall be related to the longer span, provided that the value for z does not exceed twice the shorter span.

The reinforcement over the support should be uniformly distributed in horizontal bands as illustrated in Figure 3.7. l_{\max} is the greater of the two spans adjoining the support under consideration. Where l_{\max} is greater than h , there are two bands. The upper band extends from the top of the beam to the depth of $0.2h$, and contains the fraction $0.5(l_{\max}/h - 1)$ of the total area of main support steel. The lower band extending from $0.2h$ to $0.8h$ contains the remainder of the reinforcement. Where l_{\max} is less than h , all the support bending reinforcement should be contained in a band extending from $0.2l_{\max}$ to $0.8l_{\max}$, measured from the soffit. Bar spacing is attached in **Appendix B**.

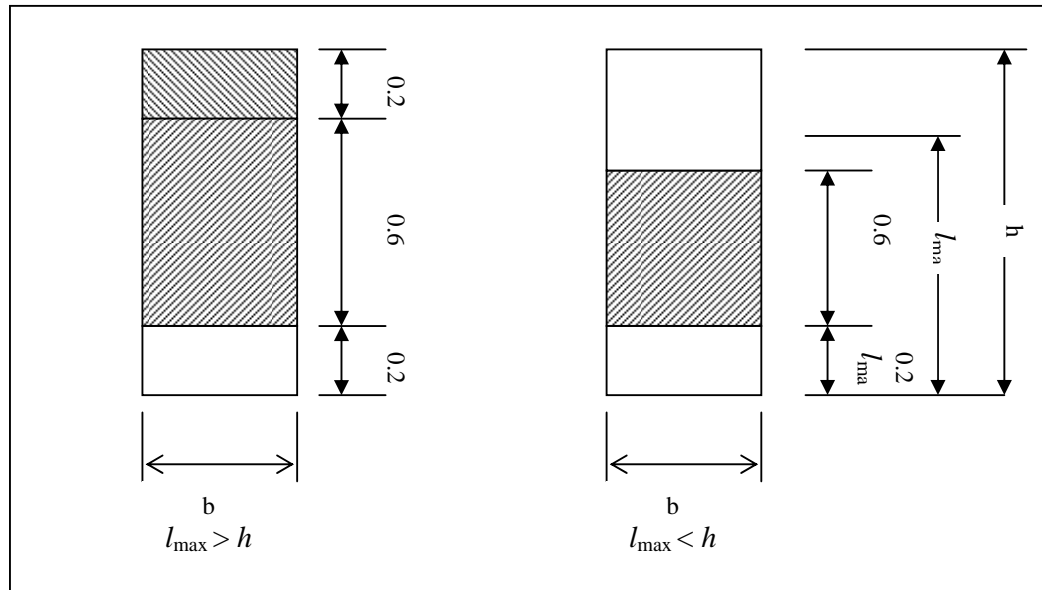


Figure 3.4 Bands of reinforcement for hogging moment

3.3.3.2 Shear Capacity

For loads applied to the bottom of the beam, $V < 0.75bh_a v_u$, where v_u is a maximum value for shear stress taken from CP 110, Table 6 and 26, for normal and light-weight aggregate concretes respectively. If this is not satisfied, the reinforcement or loading has to be revised. Uniformly distributed loads applied along the whole span to the bottom of the beam must be supported by vertical

reinforcement in both faces, at a design stress of $0.87f_y$. The area of the horizontal web reinforcement over the half of the beam depth, h_a , over a length of span $0.4h_a$ measured from the support face, should not be less than 0.8 of the uniformly distributed hanger steel per unit length. Bar spacing is attached in **Appendix B**.

For loads applied to the top of the beam, the shear capacity, V_{ct} is given by the lesser of $2bha^2 v_c k_s / x_e$, and $bh_a v_u$ where:

v_c = ultimate concrete shear stress (CP 110, Table 5 and 25)

$k_s = 1.0$ if $h_a/b < 4$

$= 0.6$ if $h_a/b > 4$

x_e = at least - the clear shear span for a load which contributes more than 50% of the total shear force at the support
 - $l/4$ for a UDL over the whole span
 - the weighted average of clear shear span where more than one load acts and none contributes more than 50% of the shear force at the support. The weighted average will be $\Sigma(v_r x_r) / \Sigma v_r$, where v_r is an individual shear force, and x_r is its corresponding shear span.

Under combined top and bottom loads, the following condition must be satisfied:

$V_{at} / V_{ct} + V_{ab} / V_{cb} < 1$, where V_{ct} = shear capacity assuming top loads only
 V_{cb} = shear capacity assuming bottom loads

V_{at} = applied shear from top loads

V_{ab} = applied shear from bottom loads

Or $V < V_{cb}$. If this is not satisfied, the reinforcement or loading has to be revised.

3.3.3.3 Bearing Capacity at Supports

To estimate the bearing stress, the reactions may be considered distributed uniformly on a thickness of wall, b , over the actual support length or a length of 0.2

l_o , if less. Where the effective lengths overlap on an internal support, the sum of the bearing stresses derived from adjacent spans should be checked against the limit. The stresses due to loads applied over supports should be included. Bearing stresses at supports should not exceed $0.4f_{cu}$.

3.3.4 Serviceability Limit State

In addition to the capability in terms of shear strength, bearing capacity and strength in bending, it is also important that the transfer beam is designed against the serviceability limit state through checking on its deflection and allowable crack width.

3.3.4.1 Deflection

Deformation in deep beams such as transfer beam is normally not significant. The centre span deflection of a simply supported deep beam may be assumed as $\text{span} / (2000 h_a / l)$ and $\text{span} / (2500 h_a / l)$ for uniformly distributed and centre-span point load respectively.

3.3.4.2 Crack Width

The minimum percentage of reinforcement in a deep beam should comply with the requirements of Cl 3.11 and 5.5, CP 110. Bar spacing should not exceed 250mm. In areas of a deep beam stressed in tension, the proportion of the total steel area, related to the local area of concrete in which it is embedded, should not be less than $0.52 \sqrt{f_{cu}} / 0.87 f_y$.

CHAPTER 4

ANALYSIS AND RESULTS

4.1 Introduction

In order to analyse the behaviour of shear wall and transfer beam due to the interaction between transfer beam and shear wall, a 2D finite element model, representing a 22-floors highrise shear wall structure, is created with the aid of LUSAS software. In this section, the stress behaviour of the transfer beam under superimposed loading and wind load will be obtained from the finite element analysis and presented in the graphical and tabular format. In order to verify these behaviours, the result as obtained through analysis carried out by J.S Kuang and Shubin LI (2001) using finite element program, SAP 2000, will be used as guidance for comparison. With the bending moment and shear stress thus obtained, it is possible to design the transfer beam using CIRIA Guide 2: 1977.

The elevation and side view of the structure is as shown in Figure 4.1. The figure shows part of the integral structure comprises shear wall panels being spaced at 4m and each of which is 225mm in thickness and 8m in length. Each shear wall panel is supported by 2m height transfer beam at its base. In addition to resisting lateral wind load, the shear walls are used to support floor slabs as well, as shown in Figure 4.1. In this project, only the particular shear wall panel at the edge of the structure alongside with the transfer beam and columns at its base will be modeled and analysed. The view of the structure's finite element model with meshing is shown in Figure 4.2.

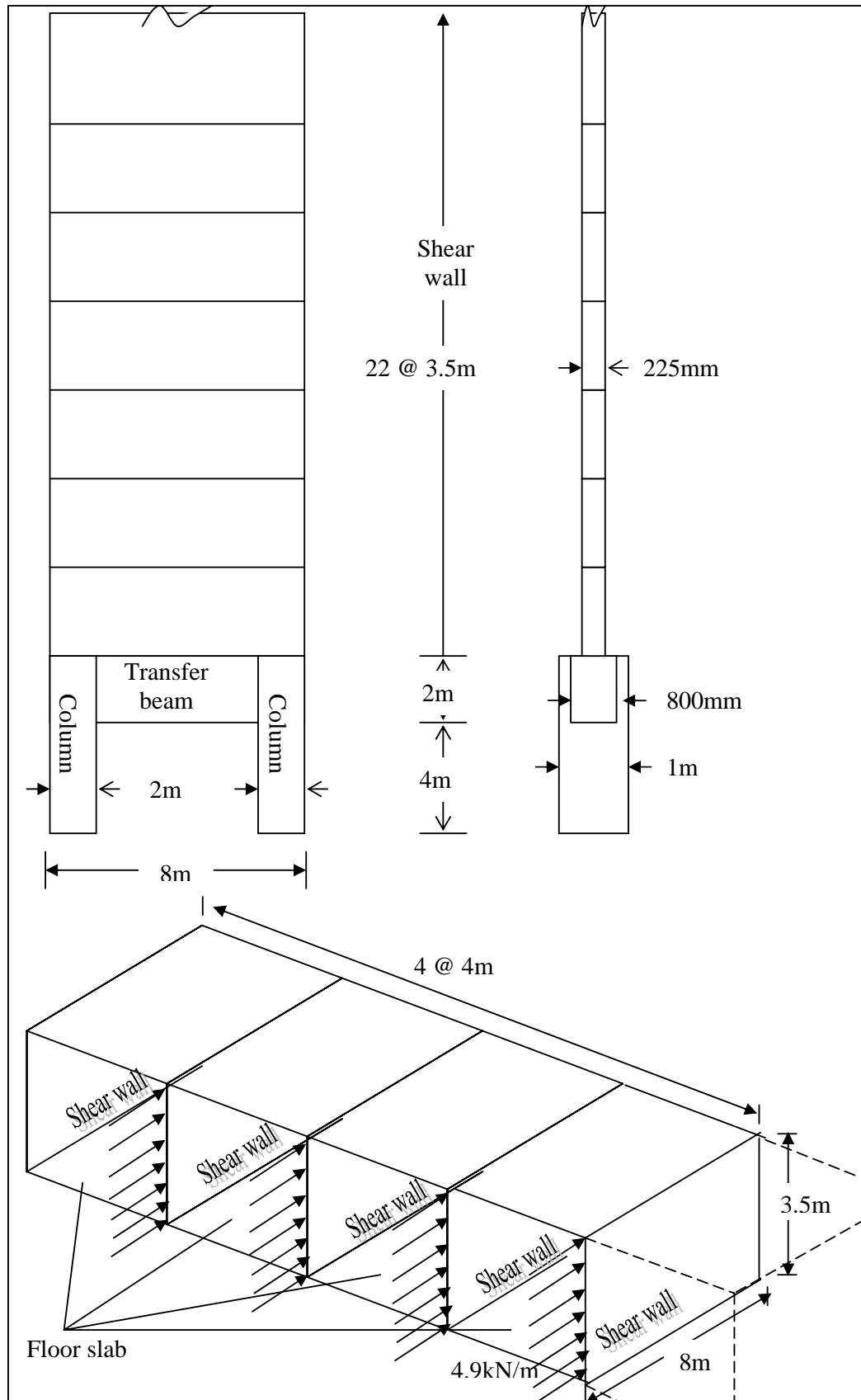


Figure 4.1 The views of the shear wall-transfer beam structure with dimension.

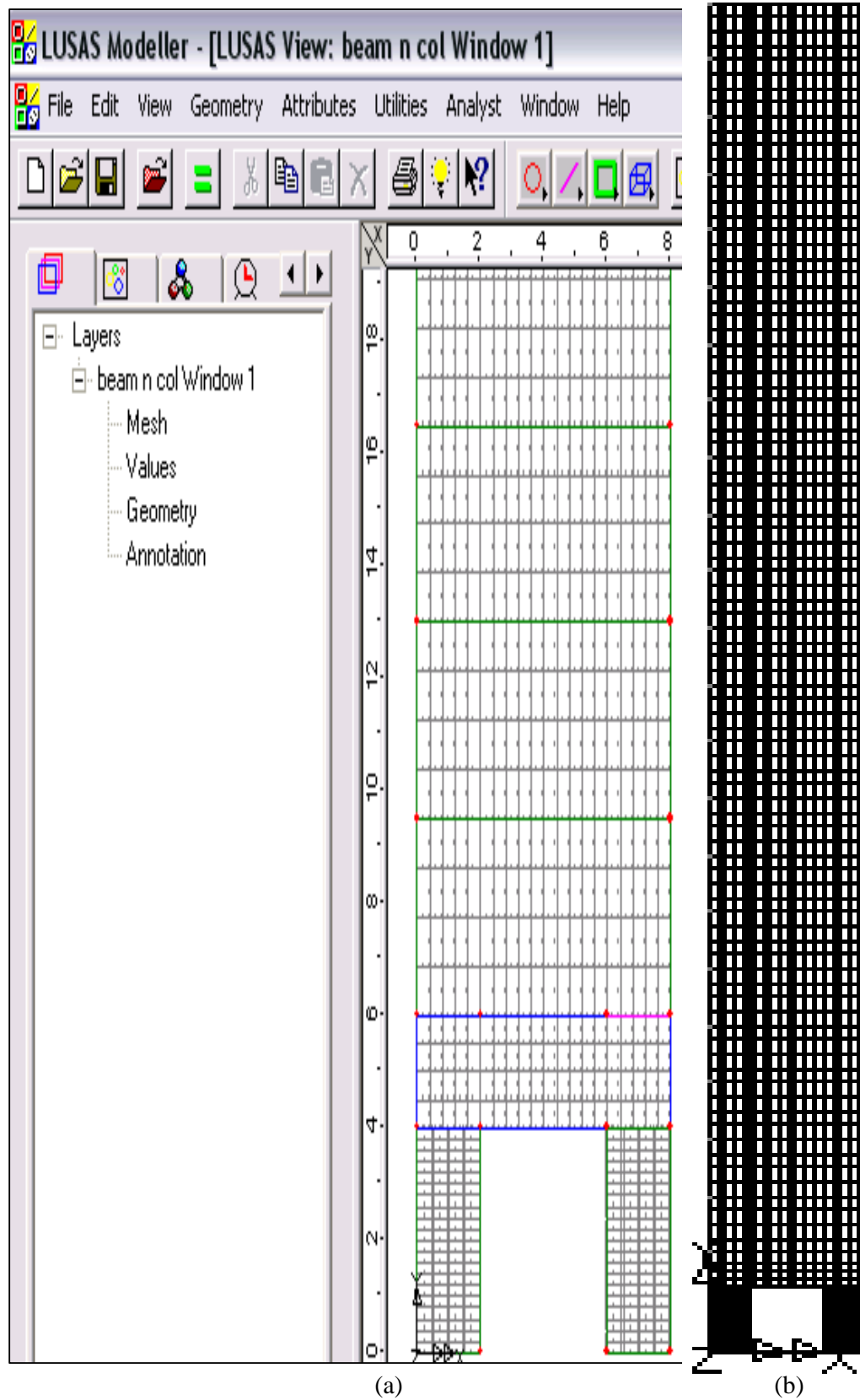


Figure 4.2 (a) Partial view and (b) full view of the shear wall-transfer beam structure's finite element model with meshing

The slabs are subjected to both dead loads and live loads. The design loads will then be transferred to the shear wall supporting the slabs and subsequently to the transfer beam at the base. For every floor level, the design (factored) load transferred to the shear wall from the slab is 21.85kN/m and 27.09kN/m for the case with and without the consideration of wind load respectively. The detailed calculation is displayed in Appendix D. In addition to the vertical loads, the shear wall is also subjected to lateral wind load. In this project, wind is assumed to be in one direction, with its basic speed being 24m/s. The wind pressure exerted laterally on the wall panel is assumed to be constant from top to bottom. The loading condition is as illustrated in Figure 4.1. The design wind load is calculated using the directional method as per Section 3 BS 6399: Part 2 (Wind Loads): 1997. The wind load thus obtained is 4.9kN/m and the details of computation are attached in Appendix C.

4.2 Geometry of Transfer Beam

The transfer beam in this project can be categorized as deep beam. Thus, it will be designed according to the CIRIA design guide for deep beams (CIRIA guide 2, January 1977). The guide provides comprehensive procedures for determining the geometry of deep beam such as its effective height and effective support width. With respect to this project, the procedures of determining the geometry of the transfer beam are displayed in Appendix E.

4.3 Analysis of Shear Wall-Transfer Beam Structure Using LUSAS 13.5

A similar finite element analysis on the stress behaviour due to interaction between shear wall and transfer beam had been carried out by J.S Kuang and Shubin Li in 2001 and their results of analysis are included in this project in Section 2.1. The similar analysis is conducted in this project with the LUSAS 13.5 software instead of the SAP 2000 software. The aim of using a different software package is to compare the results obtained from both approaches and thus verify the actual interaction effect.

In this project, the finite element model is created with designated geometry as shown in Figure 4.1. The concrete grade for transfer beam and columns is 40N/mm^2 and for shear wall is 30N/mm^2 . The concrete is designated to sustain moderate exposure and have fire resistance of 1.5 hour. The corresponding concrete cover of 30mm is thus selected.

The finite element analysis in this project is carried out in two separate cases. The first case is as though carried out by J.S Kuang and Shubin Li, where the model is solely subjected to vertical loads. In the second case, the similar shear wall-transfer beam structure is subjected to both vertical loads and lateral wind load. This creates a platform for observing the changes in stress behaviour due to the wind load, which is not covered in the previous research. Further on, the results obtained from analysis in second case, namely the bending moment and shear force, are utilized to design the transfer beam.

4.3.1 Case 1: Analysis of Shear Wall-Transfer Beam Structure Subjected to Vertical Loads Only

In this section, the vertical stress, horizontal stress and shear stress of the wall, and bending stress and shear stress in the transfer beam are obtained from the analysis and displayed in graphical and tabular format.

4.3.1.1 Deformation of Shear Wall – Transfer Beam Structure

The deformation of the shear wall-transfer beam structure under the vertical imposed loads is indicated by the deformed mesh as shown in Figure 4.3. From the deformed shape shown in the figure, it is evident that the deformation is focused at the interaction zone between the supporting columns and the transfer beam. The beam itself suffers from bending as expected, with compression along the top fiber

and tension along the bottom fiber. On the other hand, the columns at both sides which behave as compression members, suffer from buckling. As for the shear wall modeled on top of the transfer beam, the whole stretch of the shear wall settles as a result of the bending deformation of the transfer beam and vertical imposed load.

It is clear that without the effect of the lateral wind load, the structure only suffers from vertical displacement. The mode of failure can thus generally be predicted by the deformed mesh displayed in Figure 4.3.

4.3.1.2 Vertical Stress in Shear Wall

A few sections are cut across the shear wall-transfer beam structure along its elevation to study the vertical stress behaviour of the shear wall under the interaction between the two structures. The sections are made at the height of 6m, 9m, 14m and 45m and the results are displayed in the following tables (Table 4.1 – 4.4) and graphs (Figure 4.4).

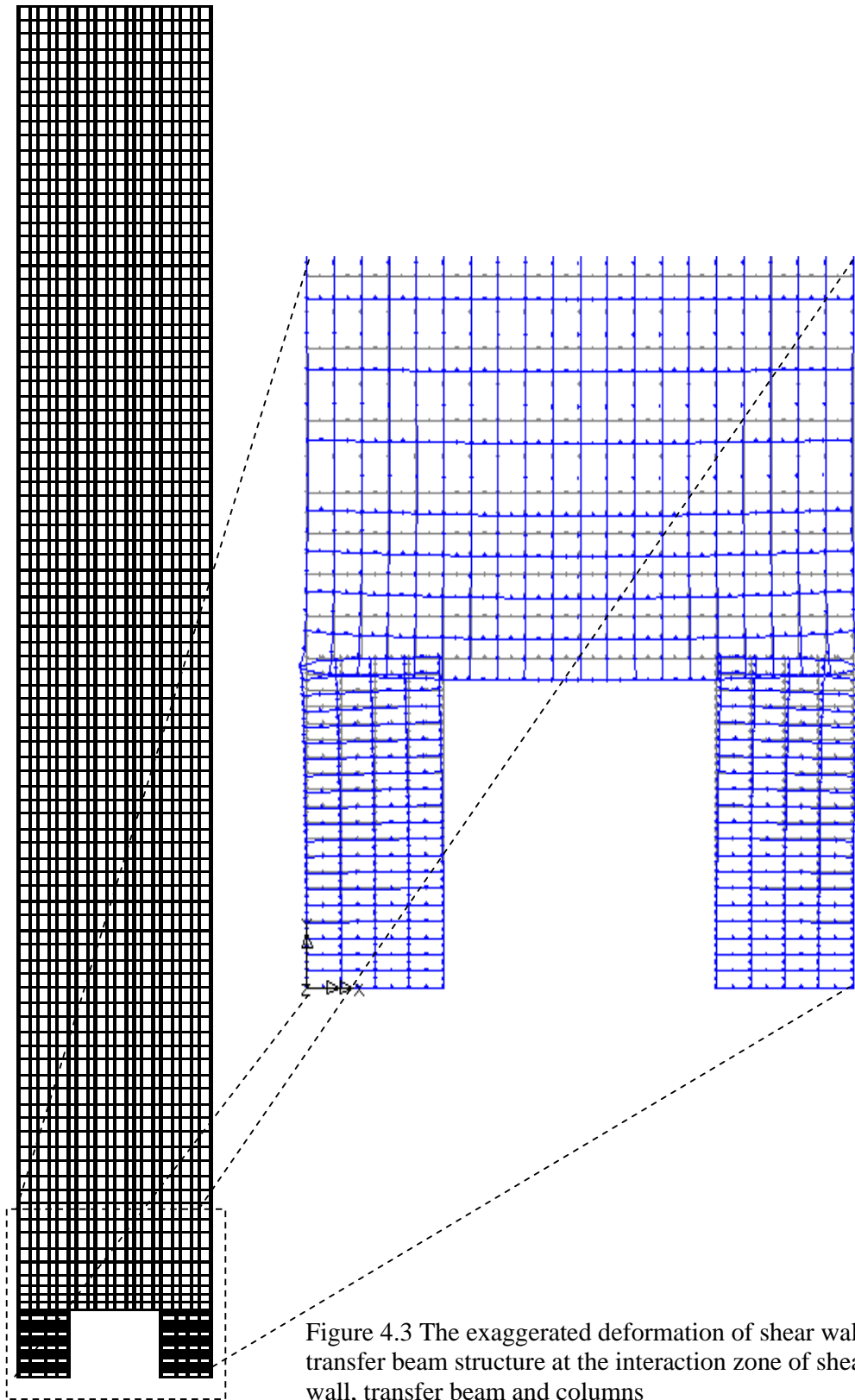


Figure 4.3 The exaggerated deformation of shear wall-transfer beam structure at the interaction zone of shear wall, transfer beam and columns

Span (m)	Vertical Stress (kPa)
0	-12043.8146144
0.4	-8030.816706009
0.8	-5589.932851111
1.2	-3581.443642261
1.6	-2187.26510737
2	-1280.463319037
2.4	-716.8030754873
2.8	-366.8506129922
3.2	-156.7822083825
3.6	-44.12166998736
4	-8.604500335897
4.4	-44.12166998767
4.8	-156.7822083823
5.2	-366.8506129916
5.6	-716.8030754866
6	-1280.463319036
6.4	-2187.265107368
6.8	-3581.443642259
7.2	-5589.932851109
7.6	-8030.816706006
8	-12043.81461439

Table 4.1 Vertical stress of shear wall at Section A-A (Y = 6m)

Span (m)	Vertical Stress (kPa)
0	-5327.377850819
0.4	-5397.906179177
0.8	-5259.007799742
1.2	-4977.616509235
1.6	-4617.199773013
2	-4234.388200044
2.4	-3874.509824951
2.8	-3569.417436718
3.2	-3339.828447903
3.6	-3197.969298936
4	-3150.055209704
4.4	-3197.969298935
4.8	-3339.828447902
5.2	-3569.417436716
5.6	-3874.509824948
6	-4234.388200041
6.4	-4617.19977301
6.8	-4977.616509231
7.2	-5259.007799738
7.6	-5397.906179173
8	-5327.377850814

Table 4.2 Vertical stress of shear wall at Section B-B (Y = 9m)

Span (m)	Vertical Stress (kPa)
0	-3818.543756934
0.4	-3847.237704145
0.8	-3874.422979988
1.2	-3898.095687769
1.6	-3916.398245816
2	-3929.412605701
2.4	-3937.89090206
2.8	-3942.898583975
3.2	-3945.526825439
3.6	-3946.696658425
4	-3947.0158564
4.4	-3946.696658424
4.8	-3945.526825438
5.2	-3942.898583973
5.6	-3937.890902058
6	-3929.412605698
6.4	-3916.398245813
6.8	-3898.095687765
7.2	-3874.422979984
7.6	-3847.23770414
8	-3818.543756928

Table 4.3 Vertical stress of shear wall at Section C-C (Y = 14m)

Span (m)	Vertical Stress (kPa)
0	-2225.891217654
0.4	-2218.520484711
0.8	-2217.917313507
1.2	-2218.057531401
1.6	-2218.384697231
2	-2218.689742857
2.4	-2218.930566492
2.8	-2219.105564498
3.2	-2219.222750967
3.6	-2219.289875364
4	-2219.311728219
4.4	-2219.289875364
4.8	-2219.222750968
5.2	-2219.105564499
5.6	-2218.930566494
6	-2218.68974286
6.4	-2218.384697234
6.8	-2218.057531405
7.2	-2217.917313511
7.6	-2218.520484716
8	-2225.891217659

Table 4.4 Vertical stress of shear wall at Section D-D (Y = 45m)

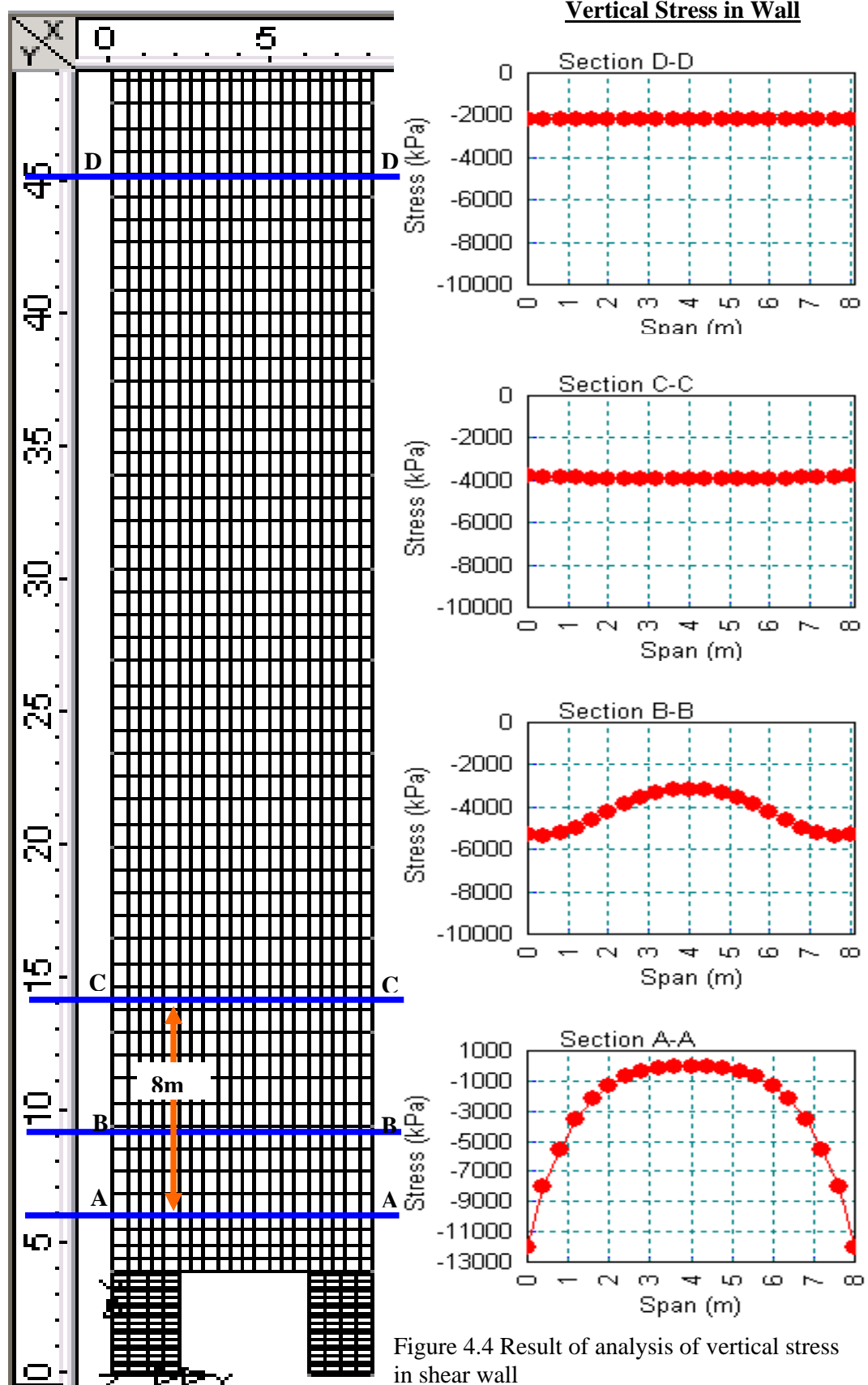


Figure 4.4 Result of analysis of vertical stress in shear wall

The vertical load exerted on the shear wall results in vertical stress along the elevation of the shear wall. Under normal situation, the stress behaves uniformly provided that the vertical loads are constant. However, this rule of thumb does not seem to apply in the case of the shear wall-transfer beam structure.

From the analysis result, it is observed that at $Y=6\text{m}$, which is the interaction surface, the vertical stress behaves as though a compression arch due to the interaction effect. This corresponds to the result obtained by J.S Kuang and Shubin Li, as shown in Figure 2.3. It can be seen that although the wall is subjected to uniformly distributed loading, the distribution of the vertical stress in the lower part of the shear wall becomes non-uniform. The vertical loading is transferred towards the support columns through the compression arch.

The redistribution of vertical stress in the arch form continues until the height of 8m from the shear wall-transfer beam interface, which equals the full span of the transfer beam (8m). Beyond the mark of the 8m distance from the interface, it is observed that the distribution of the compressive vertical stress in shear wall tends to behave uniformly. This simply implies that the interaction effect would lead to the redistribution of vertical stress in the lower part of the shear wall. It has no effect on the stretch of shear wall beyond the full span of the transfer beam as measured from the interaction surface. Since the wall is only subjected to gravity loads, the shear wall is only subjected to compression. The vertical stress is shown to decrease with the height of wall as the load increases from top to bottom.

4.3.1.3 Horizontal Stress in Shear Wall

A few sections are cut along the elevation of the shear wall-transfer beam structure to study the horizontal stress behaviour of the shear wall under the interaction between the two structures. The sections are made at the span of 2m, 4m and 5m and the results are displayed in the following tables (Table 4.5 – 4.7) and graphs (Figure 4.5).

Span (m)	Horizontal Stress (kPa)
0	6090.997162498
0	98.57201819275
0.5	3409.26891333
1	921.8368355378
1.5	-892.7784537575
2	-2568.234327738
2.875	-2323.031592331
3.75	-1641.134989279
4.625	-1092.470297817
5.5	-694.7557538116
6.375	-420.2697104656
7.25	-246.6488771798
8.125	-138.4051002817
9	-65.39258356798
9.875	-22.01844175969
10.75	-6.976895240387
11.625	-2.751143772558
12.5	5.457821219257
13.375	10.74891147998
14.25	4.933687035842
15.125	-1.215683533929
16	2.59665847479
16.875	6.636773202724

Table 4.5 Horizontal stress of shear wall at Section A-A (X = 2m)

Span (m)	Horizontal stress (kPa)
0	5502.069829593
0.5	3534.659592512
1	1562.49546363
1.5	-314.3844239937
2	-1975.909716348
2.875	-2526.597417681
3.75	-2316.772687087
4.625	-1794.083717159
5.5	-1241.942425043
6.375	-792.0175363966
7.25	-478.6943115112
8.125	-273.1083622931
9	-136.1912886244
9.875	-54.35184983932
10.75	-19.5471774783
11.625	-5.855218845748
12.5	7.853398972482
13.375	15.50167611557
14.25	8.601295021835
15.125	0.7931043395753
16	4.789438011287
16.875	9.108193672282

Table 4.6 Horizontal stress of shear wall at Section B-B (X = 4m)

0	5618.18740168
0.5	3526.961407013
1	1452.216757496
1.5	-464.9879592661
2	-2186.27789452
2.875	-2528.887811785
3.75	-2165.285707822
4.625	-1609.966749956
5.5	-1088.571551404
6.375	-684.2630296583
7.25	-410.2181818219
8.125	-232.9183466204
9	-114.6915426481
9.875	-44.1896290798
10.75	-15.4737438527
11.625	-4.814975621359
12.5	7.303226142161
13.375	14.31517793934
14.25	7.571525887765
15.125	0.1051025424432
16	4.154438859277
16.875	8.505119158752

Table 4.7 Horizontal stress of shear wall at Section C-C (X = 5m)

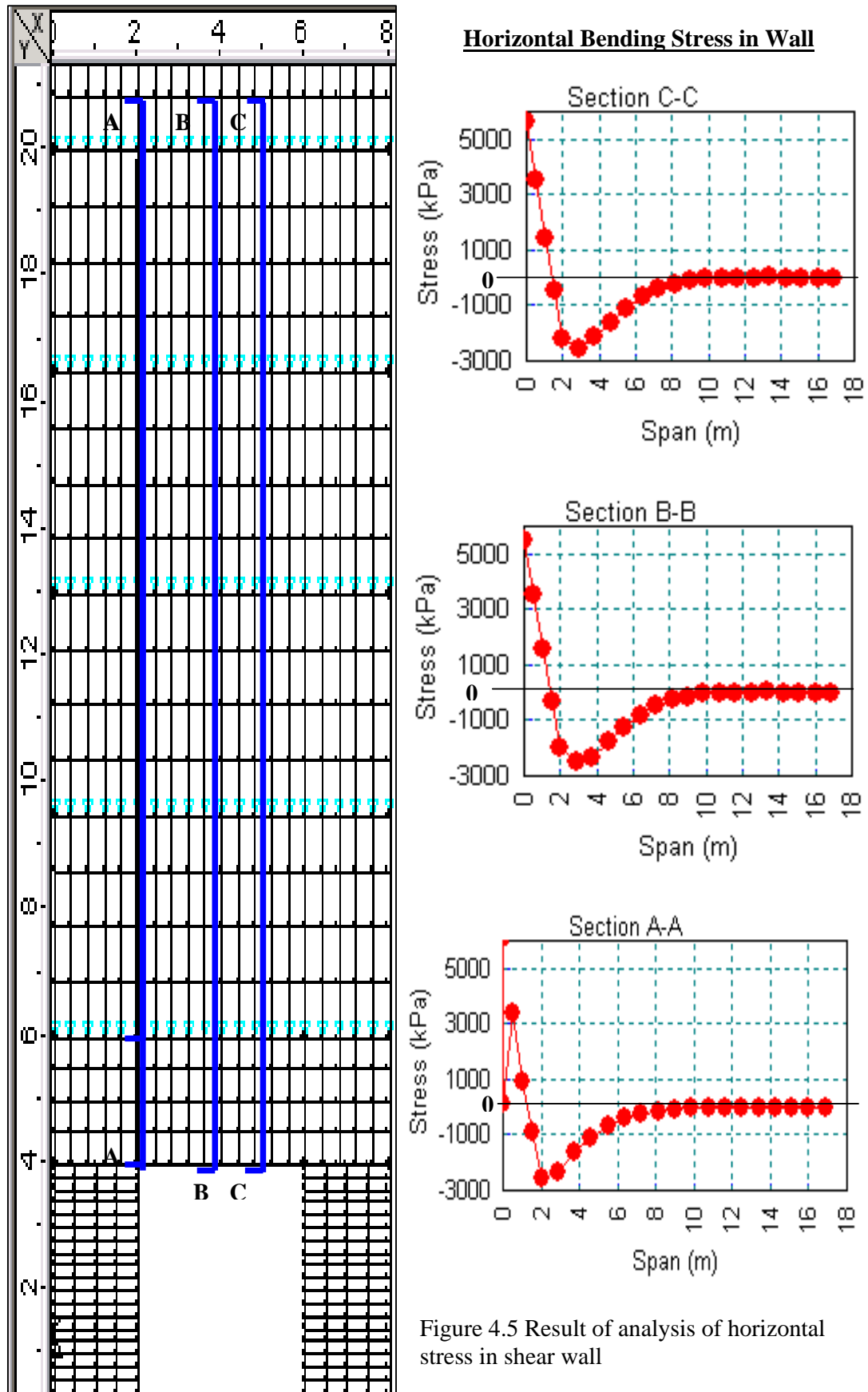


Figure 4.5 Result of analysis of horizontal stress in shear wall

The distribution of the horizontal stress is shown in Figure 4.5. In the graphs, the transfer beam portion is represented by the span of 0m to 2m in elevation while the shear wall portion is represented by the span beyond 2m.

From the graphs shown in Figure 4.5, it is observed that the horizontal stress of the shear wall-transfer beam structure, regardless of the section's distance from the column supports, follows a general pattern. The intensity of the horizontal stress is seen varied along the vertical direction. It is observed that a small portion of shear wall adjacent to the wall-beam interaction surface suffers from compression due to the interaction between the interaction effects. This portion of shear wall could suffer from concrete crushing failure if the compressive strength is exceeded.

As for the transfer beam, the horizontal stress behaviour varies in two distinct patterns. It is observed that the lower half of the beam suffers from tensile stress while the upper half suffers from compressive stress. The compressive horizontal stress is developed at the half height of the beam (1m from beam soffit) and increasing up to the wall-beam interaction surface. It is learnt from the graph that the compressive stress starts to decrease beyond the interaction surface. It is observed that beyond the height equals the full span of transfer beam (8m beyond top surface of transfer beam), the stress distribution becomes insignificant and neither the compressive stress nor tensile stress is prevalent in that stretch of shear wall. In other words, the horizontal bending stress in the shear wall beyond the interaction zone is not critical under the pure vertical loading.

4.3.1.4 Shear Stress in Shear Wall and Transfer Beam

A few sections are cut across the shear wall-transfer beam structure along its elevation to study the shear stress behaviour of the structure under the interaction between the two structures. Sections are made at the height of 4m (at the interface between transfer beam and supporting columns), 6m, 14m and 45m and the results are displayed in the following tables (Table 4.8 – 4.11) and graphs (Figure 4.6).

Span (m)	Actual Shear Stress(kPa)
0	1007.41848683
0.4	7307.819288511
0.5	-3225.534557778
0.8	1226.217683546
1	-3603.877392178
1.2	256.8620775178
1.5	-214.5053034952
1.6	111.4950812042
2	-892.9245420144
2	49.21222774882
2.4	24.55784121732
2.8	13.57804678801
3.2	7.700275978744
3.6	3.617346003398
4	-1.10143005827e-011
4.4	-3.617346003275
4.8	-7.700275978575
5.2	-13.57804678822
5.6	-24.55784121732
6	892.9245420141
6	-49.21222774856
6.4	-111.4950812041
6.5	214.5053034951
6.8	-256.8620775177
7	3603.877392176
7.2	-1226.217683546
7.5	3225.534557777
7.6	-7307.819288508
8	-1007.418486831

Table 4.8 Shear stress of transfer beam at Section A-A (Y = 4m)

Span (m)	Actual Shear Stress(kPa)
0	0.1559028622773
0.4	5.829789871517
0.8	8.241092558
1.2	6.529146059328
1.6	2.934299592194
2	-0.8317416192594
2.4	-3.617354472537
2.8	-4.83343592529
3.2	-4.379495266118
3.6	-2.567404131314
4	9.658242459766e-011
4.4	2.567404131701
4.8	4.379495266474
5.2	4.833435925644
5.6	3.617354472544
6	0.8317416194425
6.4	-2.934299592086
6.8	-6.529146059184
7.2	-8.241092557975
7.6	-5.829789871477
8	-0.1559028621086

Table 4.10 Shear stress of shear wall at wall at Section C-C (Y = 14m)

Span (m)	Actual Shear Stress(kPa)
0	-780.6827134571
0.4	-2266.579411968
0.8	-2803.899739394
1.2	-2654.937883622
1.6	-2201.7384038
2	-1690.016185809
2.4	-1240.558940393
2.8	-863.8911689407
3.2	-545.2949486357
3.6	-263.8178589675
4	4.778439866016e-010
4.4	263.817858968
4.8	545.294948636
5.2	863.8911689408
5.6	1240.558940393
6	1690.01618581
6.4	2201.7384038
6.8	2654.937883622
7.2	2803.899739394
7.6	2266.579411967
8	-780.6827134571

Table 4.9 Shear stress of shear wall at Section B-B (Y=6m)

Span (m)	Actual Shear Stress(kPa)
0	-0.3786759172064
0.4	1.443485664813
0.8	1.544499546897
1.2	1.252080707036
1.6	0.9191512872187
2	0.6584532246608
2.4	0.4679261446888
2.8	0.324092696183
3.2	0.2061905802376
3.6	0.1007257037119
4	-2.984791326549e-010
4.4	-0.1007257042298
4.8	-0.2061905807574
5.2	-0.3240926968227
5.6	-0.4679261455547
6	-0.6584532248897
6.4	-0.9191512876701
6.8	-1.252080707272
7.2	-1.5444995474
7.6	-1.443485664844
8	0.3786759174276

Table 4.11 Shear stress of shear Section D-D (Y = 45m)

Shear Stress in Wall and Transfer Beam

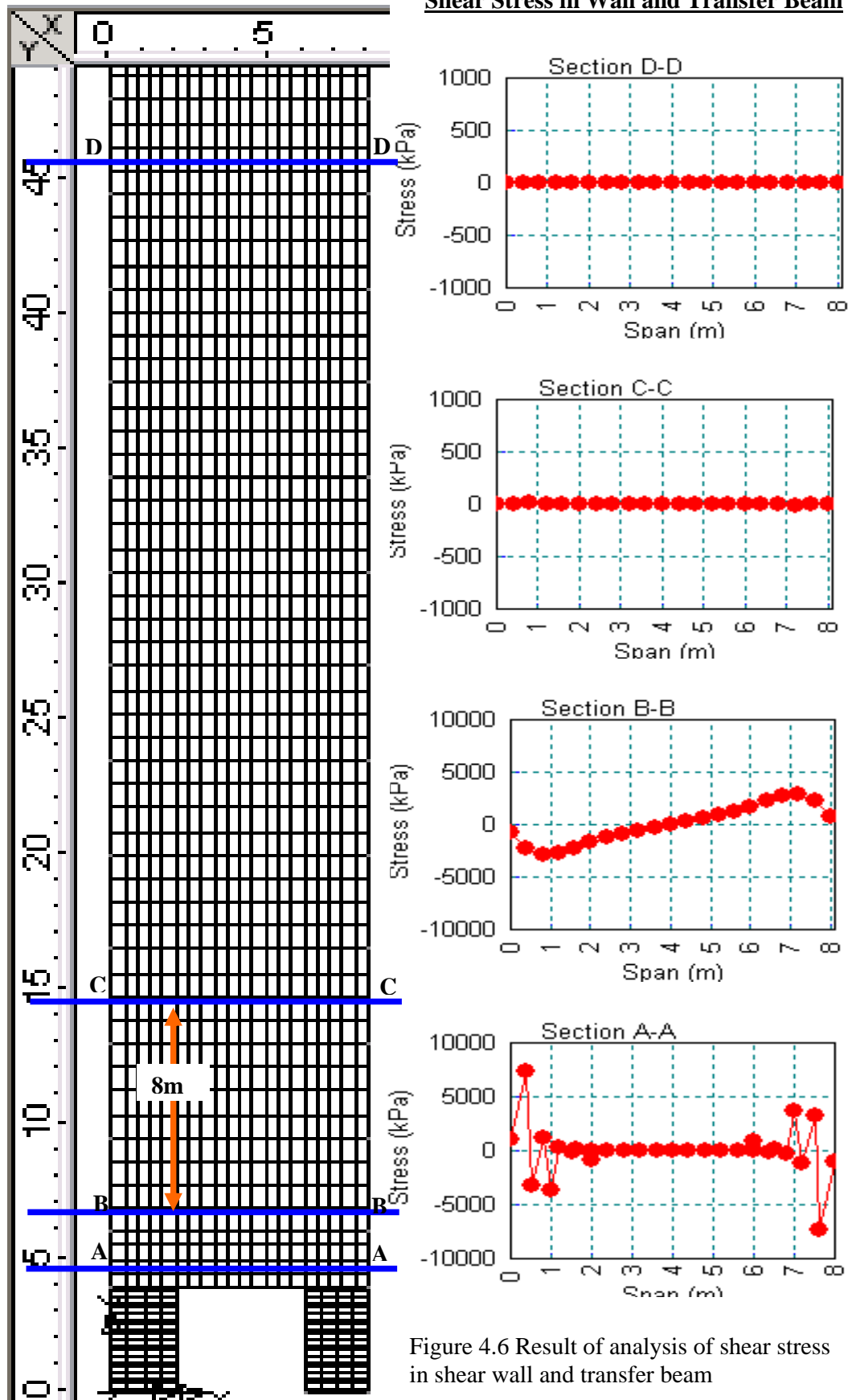


Figure 4.6 Result of analysis of shear stress in shear wall and transfer beam

The distribution of shear stress in the wall-beam system is shown in Figure 4.6. It is seen that the shear stress is dominated in the lower part of the shear wall, and the maximum intensity of shear stress is reached at the beam-column interface. This stress pattern suits the result obtained by J.S Kuang and Shubin Li through their previous analysis as shown in Figure 2.5. It is noticed from the analysis that the columns sustain most of the shear stress transferred from the shear wall to the single-span transfer beam, with the maximum shear stress being 7307.82kPa at the support.

From the results displayed in Table 11 and 12, it is also observed that the intensity of the shear stress approximates zero beyond a height equal to L (span of transfer beam = 8m) above the wall-beam interface, as indicated by shear stress along the Section C-C and D-D. It implies that in the higher parts of the shear wall, the interaction effect does not affect the shear stress distribution in the wall. Hence, it can be concluded that only the transfer beam and lower part of shear wall (within the height of L from wall-beam interface) serve as the recipient to the shear stress contributed by the superimposed structural loads and that the majority part of the shear wall does not sustain vertical shear stress.

4.3.1.5 Mean Shear Stress along Transfer Beam

The mean shear stress along the transfer beam is necessary information used in determining the maximum shear force throughout the beam section and also the location of maximum bending moment. Via LUSAS 13.5 this parameter is yielded by making several cross sectional cuts along the beam and the results obtained are displayed in Table 4.12. The distance X as mentioned in the table is measured from the outer face of column. The shear force of the cross section concerned is obtained by simply multiplying the shear stress with the cross sectional area.

From the result obtained, it is found that the maximum shear force 4028.976kN occurs at the supports.

Distance of Cross Section, X (m)	Mean Shear Stress (kPa)	Shear Force (kN)
0	613.23	981.168
0.5	2518.11	4028.976
1.0	1486.26	2378.016
1.5	568.35	909.36
2.0	451.84	722.944
2.5	186.13	297.808
3.0	99.26	158.816
3.5	41.68	66.688
4.0	-3.44	-5.504
4.5	-41.68	-66.688
5.0	-99.26	-158.816
5.5	-186.13	-297.808
6.0	-451.84	-722.944
6.5	-568.35	-909.36
7.0	-1486.26	-2378.02
7.5	-2518.11	-4028.98
8.0	-613.23	-981.168

Table 4.12 Shear stress and shear force along transfer beam

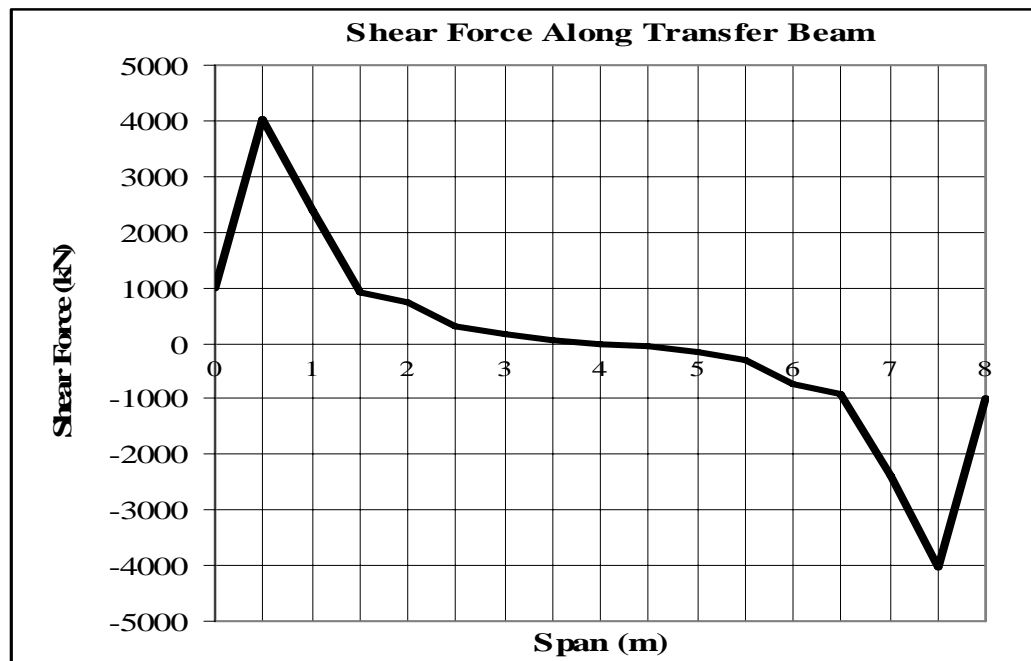


Figure 4.7 Shear force distribution along the transfer beam.

4.3.1.6 Bending Moment along Transfer Beam

As mentioned by Ove Arup and partners in the CIRIA Guide 2:1977, only the forces applied over the clear span of the transfer beam needs to be considered in estimating the bending moment. For the case in this project, the same rule applies. The bending moment cannot be directly yielded from the finite element analysis on plane stress element like transfer beam in this project. Hence, the bending moment has to be derived from bending stress, which is an available stress parameter in plane stress element analysis, using the flexure formula, $\sigma = -My/I$, where

σ = Bending stress obtained from FEM analysis

M = the resultant bending moment computed about the neutral axis of the cross section

I = moment of inertia of the cross sectional area computed about the neutral axis
 $= (1/12) (0.8) (2)^3 = 0.5333\text{m}^4$

y = perpendicular distance from the neutral axis to the farthest point away from it = 1m

The bending moment thus obtained from the flexure formula is displayed in Table 4.13 and Figure 4.8. In this case, X is measured from inner face of the columns. From the results obtained, it is noticed that the distribution of bending moment assembles that of the previous research as elaborated in Section 2.1.4. The positive bending moment occurs at the mid-span of the beam and decreases towards the support columns. Two contraflexural points are observed in the Figure 4.8, which indicate that negative moments occur close to the ends of the beam. The difference is that there is no one distinct maximum moment in the mid-span and the maximum bending moment, 2206.06kNm, occurs at section $x = 0.5\text{m}$ and 3.5m .

In order to verify the bending moment obtained from the finite element analysis, the interaction-based design formulas for transfer beams based on box foundation analogy initiated by Kuang and Li in 2005, as explained in Section 2.1.6, is employed to provide a comparison on the value. This is shown as below.

$$M_b = M_o \frac{E_b I_b}{E_w I_w + E_b I_b}$$

$$\frac{E_b I_b}{E_c I_c} = \frac{0.8(2^3)}{1(2^3)} = 0.8 > 0.1, < 10$$

$$\therefore L_e = (0.9 + 0.1 \log 0.8)4 = 3.56\text{m}$$

$$H_e = (0.47 + 0.08 \log 0.8)L = 0.46L < 0.54L$$

$$= 0.46(8) = 3.7\text{m}$$

$$\text{Load from slab / floor} = (6.38 + 5)\text{kN/m}$$

$$= 11.38\text{kN/m (Unfactored loading)}$$

$$\text{Total applied load, W} = 23(11.38) + \text{dead load of wall and transfer beam}$$

$$= 23(11.38) + (24)[22(0.225)(3.5) + 0.8(2)]$$

$$= 715.94\text{kN/m}$$

$$M_o = 1/8(715.94)(8^2) = 5727.52\text{kNm}$$

$\therefore M_b =$ Mid-span moment of transfer beam

$$= 5727.52 \left[\frac{0.8(2^3)}{0.8(2^3) + 0.175(3.7^3)} \right] = 2060\text{kNm}$$

The value M_b as obtained above is found to be approximate to the mid-span moment obtained from the finite element analysis, 2023.75kNm (at X=2m) as shown in Table 4.13. This assures that the result obtained using finite element analysis is valid.

Distance of Cross Section, X (m)	Max Bending Stress (kPa)	Bending Moment (kNm)
0	4638.71	-2473.9787
0.5	-4136.36	2206.0587
1.0	-3943.71	2103.312
1.5	-3833.86	2044.7253
2.0	-3794.53	2023.7493
2.5	-3833.86	2044.7253
3.0	-3928.59	2095.248
3.5	-4136.36	2206.0587
4.0	4638.71	-2473.9787

Table 4.13 Bending stress and bending moment along clear span of transfer beam

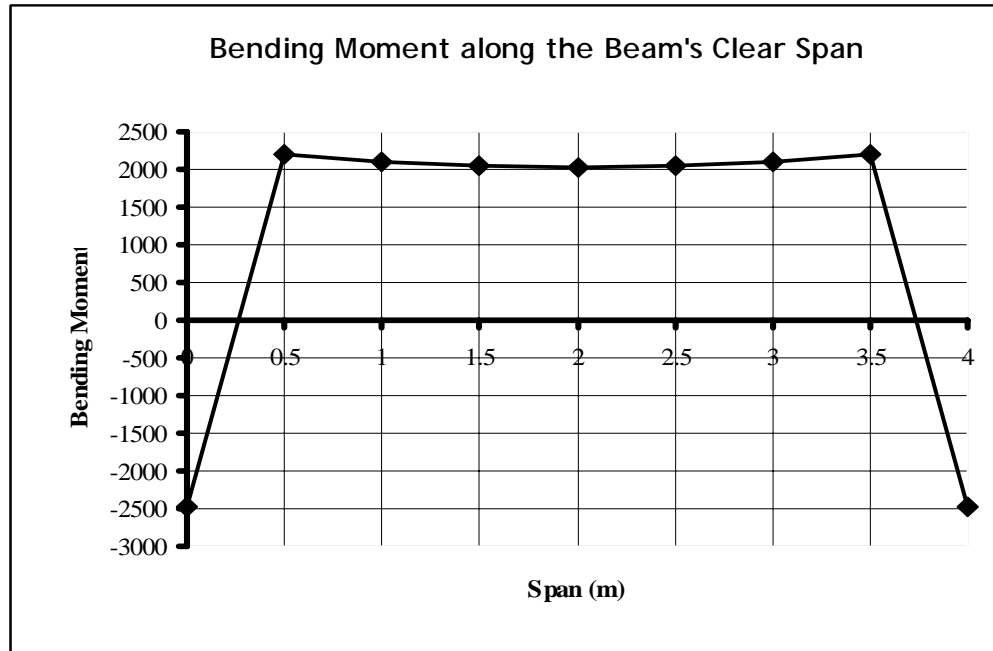


Figure 4.8 Bending moment distribution along the clear span of transfer beam.

4.3.2 Case 2: Analysis of Shear Wall-Transfer Beam Structure Subjected to Vertical Loads and Wind Load

In this section, the vertical stress, horizontal stress and shear stress of the wall, and bending stress and shear stress in the transfer beam are obtained from the analysis. The stress behaviour obtained in this section will be compared with those from section 4.3.1.

4.3.2.1 Deformation of Shear Wall – Transfer Beam Structure

The deformation of the shear wall-transfer beam structure, under both the lateral wind load and vertical imposed is indicated by the deformed mesh as shown in Figure 4.9. The mode of failure can thus generally be predicted by the deformed mesh displayed in the figure.

From the deformed shape shown in the figure, it is observed that the structure behaves like a cantilever as expected. The top part of the shear wall suffers from lateral drifting when in-plane wind load is imposed on the shear wall, with the maximum displacement being 0.2961m at node 6810 (top level). This behaviour simply means that tension dominates the windward shear wall face whereas compression dominates the leeward face.

From the deformed shape of the transfer beam, it is noticed the transfer beam does not bend as if what is observed in the deformed shape of transfer beam in case 1. It is observed that the bending pattern is no longer symmetrical and increasing towards the right-side column. As for the columns, the windward column appears to be intact to the lateral wind load as the lateral force exerted by the wind is entirely taken up by the shear wall mass on top. Meanwhile, the leeward column is seen to suffer from local buckling as the shear wall transferred the compressive stress generated by wind load to the column.

4.3.2.2 Vertical Stress in Shear Wall

A few sections are cut across the shear wall-transfer beam structure along its elevation to study the vertical stress behaviour of the shear wall under the interaction between the two structures. The sections are made at the height of 6m, 9m, 14m and 45m and the results are displayed in the following tables (Table 4.14 – 4.17) and graph (Figure 4.10).

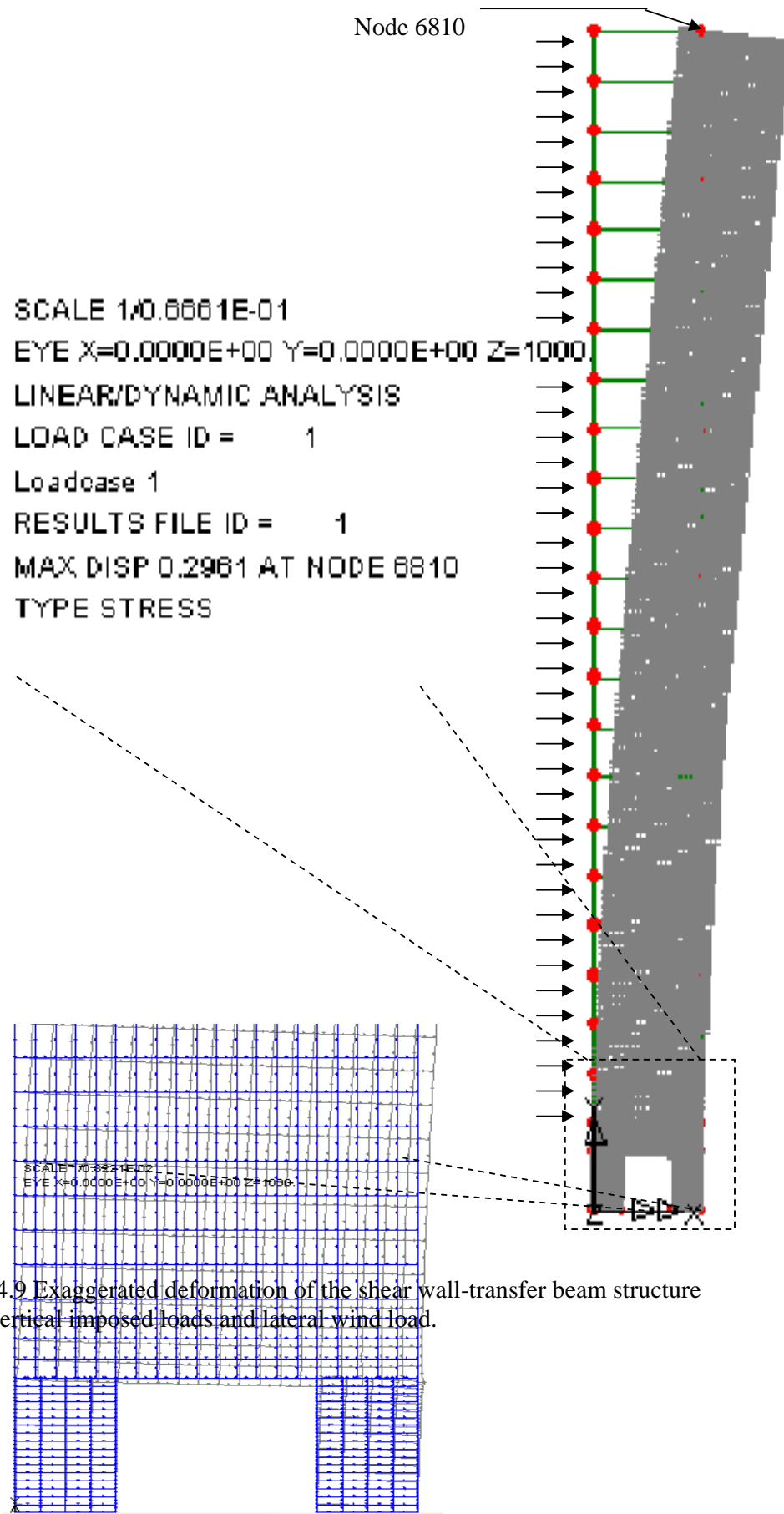


Figure 4.9 Exaggerated deformation of the shear wall-transfer beam structure under vertical imposed loads and lateral wind load.

Span (m)	Vertical Stress (kPa)
0	-4256.198504243
0.4	-2262.817132721
0.8	-1210.484837035
1.2	-430.2117282475
1.6	37.46093167203
2	277.06820096
2.4	364.1860043867
2.8	358.9746007945
3.2	290.1318983851
3.6	169.364250483
4	-4.762595930182
4.4	-243.6002332269
4.8	-569.6196225109
5.2	-1021.138499611
5.6	-1663.748481249
6	-2603.083561092
6.4	-4014.448035247
6.8	-6084.595304586
7.2	-8959.604173079
7.6	-12348.82009312
8	-17652.19856268

Table 4.14 Vertical stress of shear wall at Section A-A (Y = 6m)

Span (m)	Vertical Stress
0	1854.105317267
0.4	1158.802704726
0.8	624.3247473547
1.2	196.04392212
1.6	-172.662227832
2	-521.8712221911
2.4	-883.5675922931
2.8	-1281.889295771
3.2	-1734.992004271
3.6	-2256.722507508
4	-2857.788365029
4.4	-3546.112330974
4.8	-4326.192133101
5.2	-5197.430763665
5.6	-6151.436004958
6	-7168.677686936
6.4	-8215.34770259
6.8	-9240.967208647
7.2	-10182.58277954
7.6	-10971.37112423
8	-11541.24394423

Table 4.15 Vertical stress of shear wall at Section B-B (Y = 9m)

Span (m)	Vertical Stress (kPa)
0	2344.898679774
0.4	1738.055572214
0.8	1132.356470857
1.2	529.496524297
1.6	-69.03290003142
2	-663.3388332549
2.4	-1254.082497647
2.8	-1842.163706473
3.2	-2428.478144973
3.6	-3013.745345766
4	-3598.388324366
4.4	-4182.464133709
4.8	-4765.643385347
5.2	-5347.242465485
5.6	-5926.30371826
6	-6501.734413366
6.4	-7072.48640461
6.8	-7637.822818572
7.2	-8197.623893074
7.6	-8753.440234575
8	-9307.06226425

Table 4.16 Vertical stress of shear wall at Section D-D (Y = 14m)

Span (m)	Vertical Stress
0	-204.8223984872
0.4	-373.0169688243
0.8	-547.3474191713
1.2	-722.8824643074
1.6	-899.103907538
2	-1075.773264589
2.4	-1252.785759422
2.8	-1430.068121979
3.2	-1607.55347128
3.6	-1785.173297421
4	-1962.855247189
4.4	-2140.522911746
4.8	-2318.095899931
5.2	-2495.489764957
5.6	-2672.616216727
6	-2849.385336219
6.4	-3025.713593495
6.8	-3201.548964593
7.2	-3376.973133784
7.6	-3552.347497766
8	-3732.440008414

Table 4.17 Vertical stress of shear wall at Section D-D (Y = 45m)

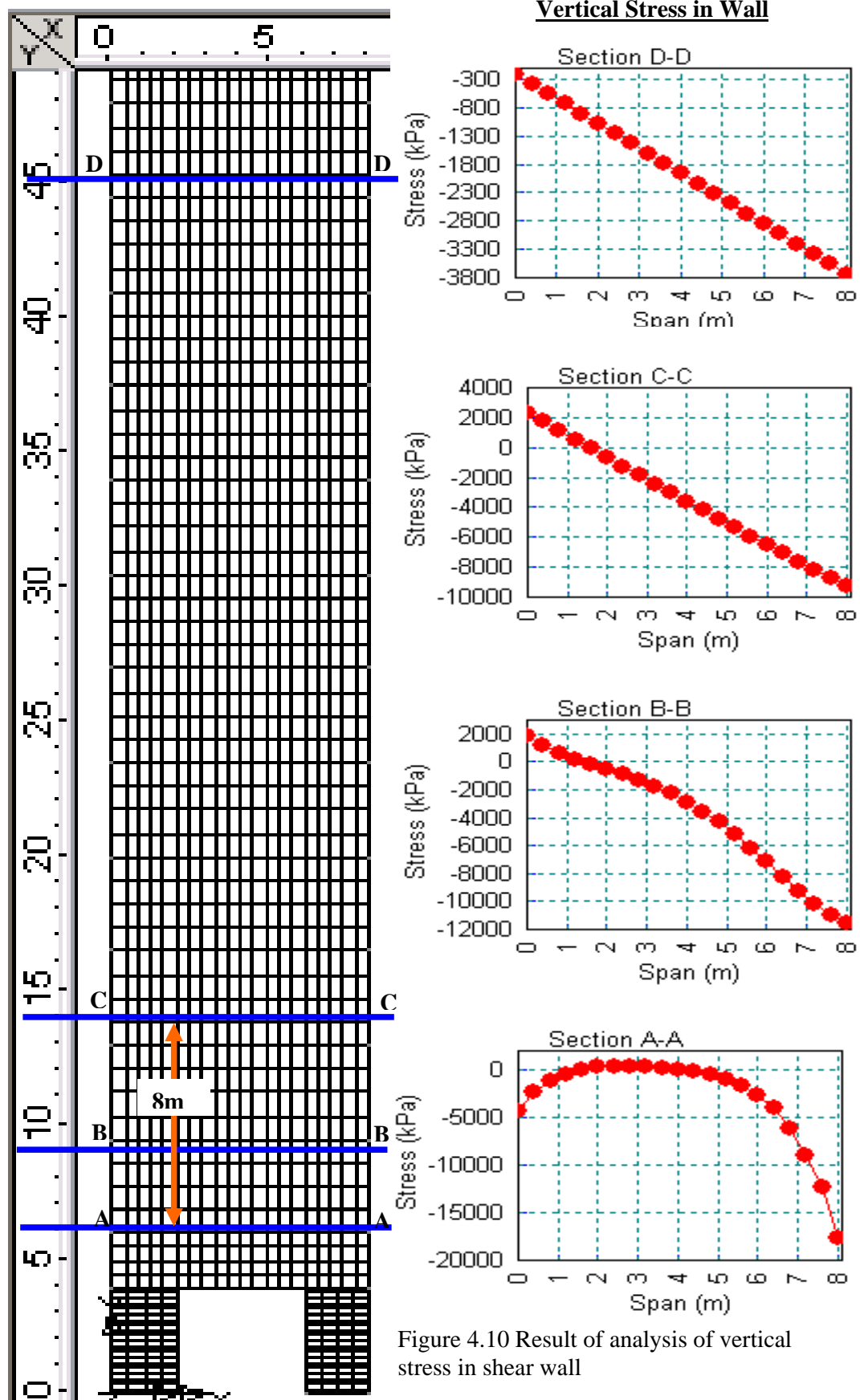


Figure 4.10 Result of analysis of vertical stress in shear wall

The vertical load and lateral wind load exerted on the shear wall results in vertical stress along the vertical stretch of the shear wall. However, the results of analysis obtained when the structure is subjected to both wind load and vertical loads are entirely different from when it is subjected to vertical loads only.

From Figure 4.10, it is observed that the compression curve still exists at the interaction surface like what is observed in Figure 4.4 (when the structure is subjected to vertical loads only). The difference is that the compression curve is no longer symmetrical, which means that the vertical stress is no longer distributed evenly to both the columns. In this case, it is noticed that the vertical stress is more focused on the right-side column. The lateral wind load creates an additional clockwise overturning moment on the wall which needs to be countered. This countering moment is rendered by the increased reaction on the right-hand-side column. With the increased reaction force, more vertical stress is transferred to that column to achieve equilibrium in vertical force (support of greater reaction force always sustains greater load in order to achieve equilibrium in force).

At the interface, the structure suffers from compressive stress at the area near the supports and suffers from tensile stress at midspan. It is noticed that the distribution of vertical stress on the shear wall does not approach constant distribution pattern with the increase of height as illustrated in Figure 4.4. This is due to the existence of lateral wind load which leads to the concentration of compressive stress on the right-hand- side column. Because of the relatively small gravity loads, the wind load induces tension along the edge of the shear wall as observed in Section B-B and C-C in Figure 4.10, which could lead to tension cracks if not catered for.

4.3.2.3 Horizontal Stress in Shear Wall

A few sections are cut along the elevation of the shear wall-transfer beam structure to study the horizontal stress behaviour of the shear wall under the interaction between the two structures. The sections are made at the span of 2m, 4m

and 5m and the results are displayed in the tables (4.18 – 4.20) and graphs (Figure 4.11).

Span (m)	Horizontal Stress (kPa)
0	3641.404196811
0	65.79308754631
0.5	2284.183533684
1	880.7574072405
1.5	-238.0582188316
2	-1130.107344724
2.875	-1366.610607546
3.75	-1170.24198502
4.625	-877.9896860399
5.5	-605.2787388295
6.375	-390.4382800327
7.25	-243.77327374
8.125	-148.0540485719
9	-82.59179826059
9.875	-43.37827737336
10.75	-28.86864370825
11.625	-24.29601890928
12.5	-17.21330311233
13.375	-12.84620776021
14.25	-17.59707393494
15.125	-22.66888263305
16	-19.70571819142
16.875	16.53866743287

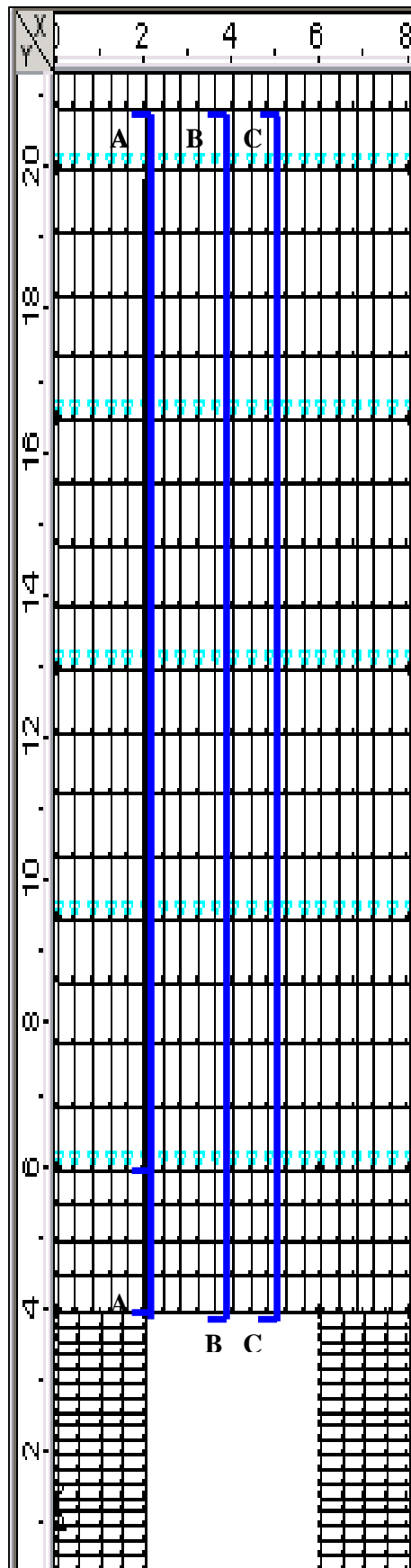
Table 4.18 Horizontal stress of shear wall at Section A-A (X = 2m)

Span (m)	Horizontal Stress (kPa)
0	5002.455746687
0.5	3211.121620232
1	1415.54992107
1.5	-293.2999877275
2	-1806.142774711
2.875	-2308.988637254
3.75	-2119.381707397
4.625	-1644.385836513
5.5	-1143.222506058
6.375	-734.685434942
7.25	-449.016342202
8.125	-261.2887252897
9	-137.239914834
9.875	-63.30989997725
10.75	-30.96858220296
11.625	-17.85431305566
12.5	-5.962310575553
13.375	0.4043546865632
14.25	-5.251563629051
15.125	-11.73862289441
16	-8.710908945725
16.875	-5.391539564568

Table 4.19 Horizontal stress of shear wall at Section B-B (X = 4m)

0	6095.895370434
0.5	3694.164588689
1	1379.47903452
1.5	-723.5165009249
2	-2680.648945101
2.875	-2807.016555762
3.75	-2239.753236711
4.625	-1588.710705796
5.5	-1043.804146174
6.375	-646.5061098663
7.25	-385.445936712
8.125	-220.0426889934
9	-112.274990191
9.875	-48.71748368948
10.75	-22.13432992939
11.625	-11.95271782428
12.5	-1.58322791186
13.375	4.173602758382
14.25	-1.379418052899
15.125	-7.58238868927
16	-4.49315336702
16.875	-1.1289511244650

Table 4.20 Horizontal stress of shear wall at Section C-C (X = 5m)



Horizontal Bending Stress in Wall

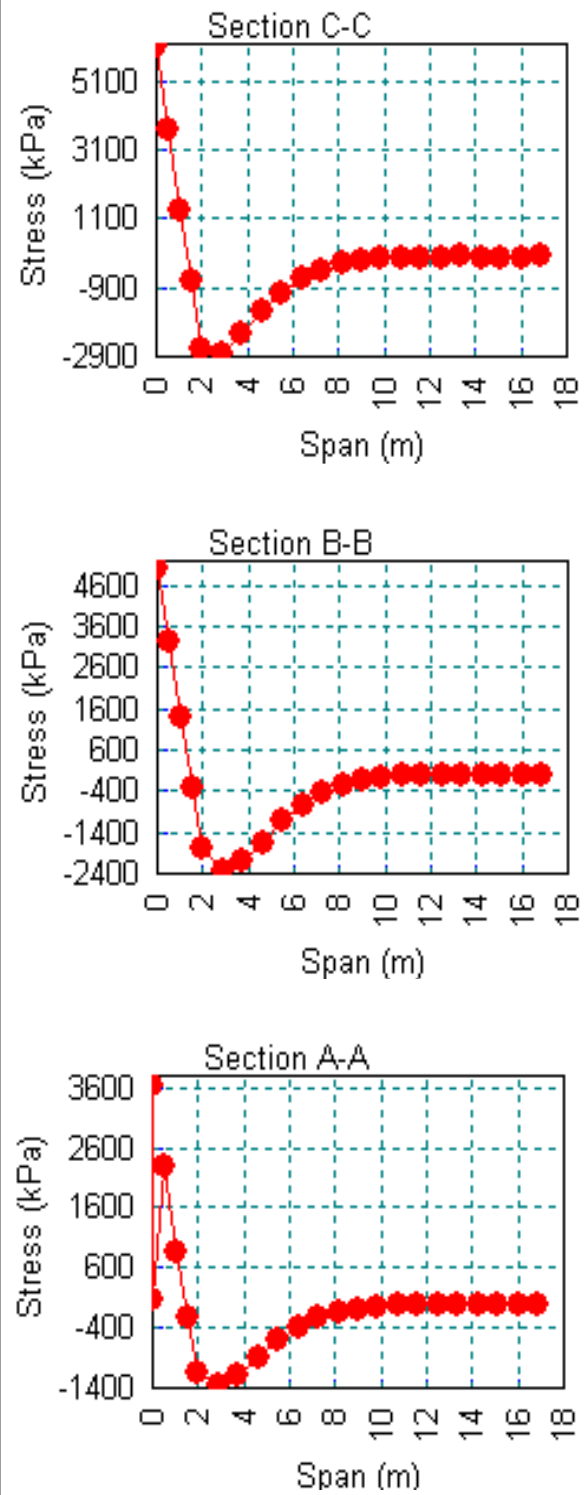


Figure 4.11 Result of analysis of horizontal stress in shear wall

The distribution of the horizontal stress is shown in Figure 4.11. Like what is observed in the case where the shear wall-transfer beam structure is subjected to vertical loads only as shown in Figure 4.5, the horizontal stress distribution for the case where both vertical and lateral loads are applied generally follows the similar pattern.

For the transfer beam, the horizontal stress behaviour resembles the results displayed in section 4.3.1.3 where the stress varies in two distinct patterns. It is observed that the lower half of the beam suffers from tensile stress while the upper half suffers from compressive stress.

When subjected to both vertical and lateral wind loads, it is found that the shear wall is subjected to compressive stress (negative X direction) throughout the stretch. This is understandable as this horizontal stress is developed to counter the lateral wind load from positive X direction. It is learnt from the graph that the compressive stress starts to decrease beyond the interaction surface but the stress distribution does not appear to approach a constant value even after the interaction zone (height from interface equals full span of transfer beam = 8m) has been exceeded. Instead, the compressive stress only starts to become constant after the height of 11.625m as shown in Table 4.18-4.20. This is mainly because the lateral wind load induces additional horizontal stress on the shear wall, which disrupts the stress equilibrium of the upper part shear wall.

4.3.2.4 Shear Stress in Shear Wall and Transfer Beam

A few sections are cut across the shear wall-transfer beam structure along its elevation to study the shear stress behaviour of the structure under the interaction between the two structures. Sections are made at the height of 4m (at the interface between transfer beam and supporting columns), 6m, 14m and 45m and the results are displayed in the following tables (Table 4.21 – 4.24) and graphs (Figure 4.12).

Span (m)	Actual Shear Stress(kPa)
0	2511.97397603
0.4	3049.348829001
0.5	-1643.190907553
0.8	621.465586364
1	-930.7148559367
1.2	100.3034747239
1.5	-119.4223021589
1.6	49.26776236369
2	-262.9837465825
2	11.53793986296
2.4	-1.284843728555
2.8	-8.958688893936
3.2	-13.64127931543
3.6	-17.38932182616
4	-20.71750864972
4.4	-23.96974473128
4.8	-27.64813954051
5.2	-33.65670799965
5.6	-45.94838486394
6	1363.341319862
6	-77.98141542625
6.4	-153.4783306069
6.5	270.6307203544
6.8	-367.1182261459
7	5634.587029545
7.2	-1608.84679583
7.5	4223.76281282
7.6	-10250.50790444
8	702.0834398332

Table 4.21 Shear stress of shear wall at Section A-A (Y = 4m)

Span (m)	Actual Shear Stress(kPa)
0	0.7354971195885
0.4	69.90753798803
0.8	129.2355629288
1.2	178.2967697199
1.6	219.0719578622
2	253.064389687
2.4	281.2539494941
2.8	304.1203664572
3.2	321.7038883665
3.6	333.6838576217
4	339.487772826
4.4	338.4184904418
4.8	329.792547508
5.2	313.0794002634
5.6	288.0262947294
6	254.7698559032
6.4	213.8950480483
6.8	166.5039619593
7.2	114.1776565733
7.6	58.96104790556
8	0.3637899085176

Table 4.23 Shear stress of shear wall at Section C-C (Y = 14m)

Span (m)	Actual Shear Stress(kPa)
0	-339.3386104357
0.4	-1216.26546237
0.8	-1616.13405881
1.2	-1659.995415539
1.6	-1550.103499904
2	-1395.96529809
2.4	-1247.4481281
2.8	-1102.119894415
3.2	-948.4144473917
3.6	-771.7517734316
4	-557.8330174244
4.4	-291.7375506466
4.8	43.73305567805
5.2	469.6693929263
5.6	1009.580934181
6	1678.627142626
6.4	2455.121711075
6.8	3169.027451024
7.2	3482.621683843
7.6	2902.796941547
8	1078.060743257

Table 4.22 Shear stress of shear wall at Section B-B (Y = 6m)

Span (m)	Actual Shear Stress(kPa)
0	0.00401845331808
0.4	36.77781915173
0.8	68.45266693843
1.2	96.10392002835
1.6	120.0183738401
2	140.2871110142
2.4	156.9071803269
2.8	169.8571227374
3.2	179.1168191601
3.6	184.6714066756
4	186.5103333455
4.4	184.6252600162
4.8	179.0078475313
5.2	169.6475439522
5.6	156.5294863617
6	139.6335556732
6.4	118.9382928438
6.8	94.44074665478
7.2	66.23199974072
7.6	34.59884752224
8	0.6166481789298

Table 4.24 Shear stress of shear wall at Section D-D (Y = 45m)

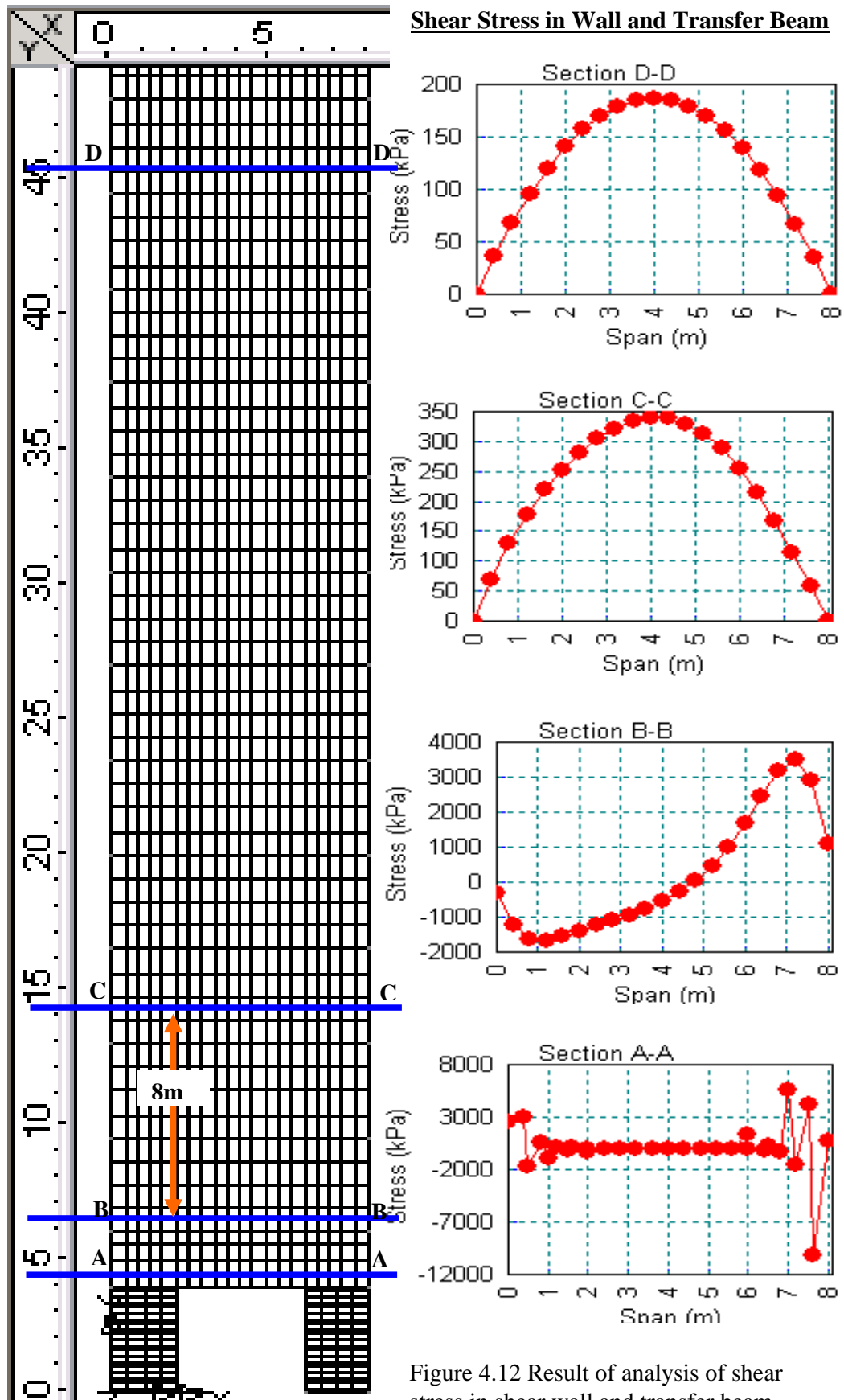


Figure 4.12 Result of analysis of shear stress in shear wall and transfer beam

The distribution of shear stress in the wall-beam system is shown in Figure 4.12. It is seen that the maximum intensity of shear stress is reached at the beam-column interface. The right-hand-side column sustains most of the shear stress transferred from the shear wall to the single-span transfer beam, with the maximum shear stress being 10250.51kPa. The existence of wind load causes the concentration of compression stress on the right-hand-side column. This concentrated stress disrupts the inherent uniform vertical stress distribution and leads to high shear stress in the shear wall as shown in section C-C and D-D in Figure 4.12.

However, it is learnt from the analysis that the shear stress is no longer only dominated in the lower part of the shear wall, as observed in section 4.3.1.4 where only vertical loads are applied. Symmetrical shear stress distribution observed along the shear wall is seen increasing from zero at the extreme edges to the maximum exactly at the mid-span as the vertical stress redistribution occurs in the wall

The shear stress in shear wall is seen decreasing with the height due to the reduction in vertical loads and thus vertical stress. The result, again, stresses the difference in stress distribution on the shear wall-transfer beam structure when lateral load exists. It is crystal clear that in the case where both lateral wind loads and vertical loads are applied simultaneously on the transfer beam-shear wall structure, shear stress exists in both the beam and wall.

4.3.2.5 Mean Shear Stress along Transfer Beam

In this section, the mean shear stress along the transfer beam, which is part and parcel of the shear wall-transfer beam structure subjected to both lateral wind load and vertical loads, is studied. The yielded shear stress distribution is used to identify the critical sections subjected to high shear force. Several cross sectional cuts are made along the beam and the shear force obtained is displayed in Table 4.25. The shear force of the cross section concerned is obtained by simply multiplying the shear stress with the cross sectional area. X is measured from the outer face of column.

The shear force distribution as illustrated in Figure 4.13 is significantly varied from that of Figure 4.7. It is noticed that the effect of wind load contributes to an asymmetrical shear force distribution curve along the beam, where a relatively high concentration of shear force occurs at the right-hand-side column. From the result obtained, the maximum shear force is 5670.83kN at the right-side supports.

Distance of Cross Section, X (m)	Mean Shear Stress (kPa)	Shear Force (kN)
0	184.51	295.216
0.5	1039.67	1663.472
1.0	459.49	735.184
1.5	423.60	677.76
2.0	463.08	740.928
2.5	447.91	716.656
3.0	460.71	737.136
3.5	462.09	739.344
4.0	442.95	708.72
4.5	386.16	617.856
5.0	281.43	450.288
5.5	108.82	174.112
6.0	-359.96	-575.936
6.5	-611.52	-978.432
7.0	-2163.73	-3461.97
7.5	-3544.27	-5670.83
8.0	-932.21	-1491.54

Table 4.25 Shear stress and shear force along transfer beam

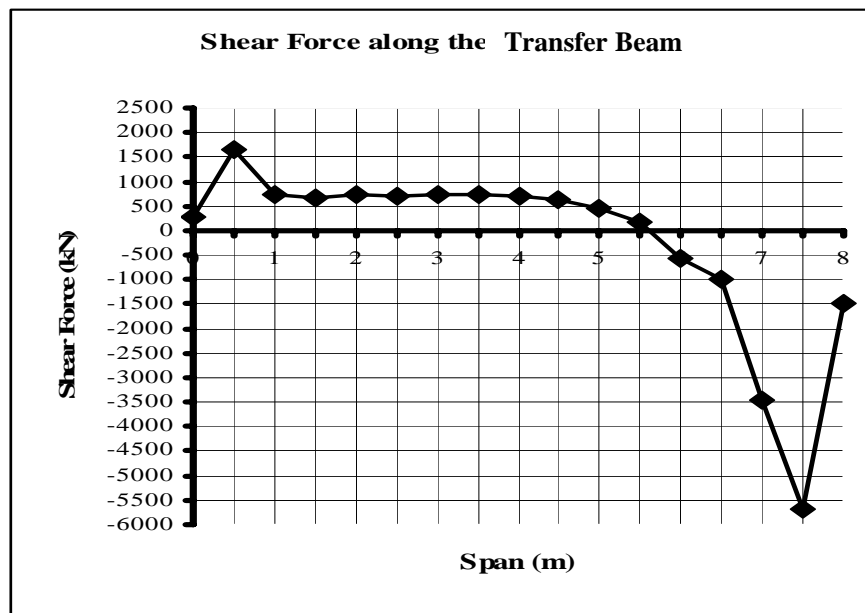


Figure 4.13 Shear force distribution along the transfer beam.

4.3.2.6 Bending Moment along Transfer Beam

As mentioned in section 4.3.1.6, only the forces applied over the clear span of the transfer beam needs to be considered in estimating the bending moment. With the aid of the flexure formula, the bending moment along the transfer beam is derived from the available bending stress and displayed in Table 4.26 and Figure 4.14.

In this case, X is measured from inner face of the columns. From the results obtained, it is noticed that the distribution of bending moment varies tremendously for the case where only vertical loads are applied and where both wind loads and vertical loads are applied. The positive bending moment occurs along the clear span of the beam and increases from left to right. This phenomenon can actually be understood by referring to section A-A of Figure 4.8 where it is observed that there is a high concentration of vertical stress at the area near the right-hand-side column due to the wind load effect. The pure sagging (positive) moment along the clear span of the transfer beam suggests that the transfer beam is in full tension as the high vertical stress concentrates at the right-side column.

The maximum bending moment, 3132.14kNm, does not occur at the mid-span of the beam, but culminates at section $x = 4\text{m}$, which is just adjacent to the column face. The bending reinforcement should thus be spanned over the full span of the transfer beam in view of the high sagging moment near the supports.

Distance of Cross Section, X (m)	Max Bending Stress (kPa)	Bending Moment (kNm)
0	-2481.22	1323.3173
0.5	-2510.27	1338.8107
1.0	-2758.30	1471.0933
1.5	-3070.67	1637.6907
2.0	-3454.68	1842.496
2.5	-3910.17	2085.424
3.0	-4394.75	2343.8667
3.5	-5036.57	2686.1707
4.0	-5872.76	3132.1387

Table 4.26 Bending stress and bending moment along clear span of transfer beam

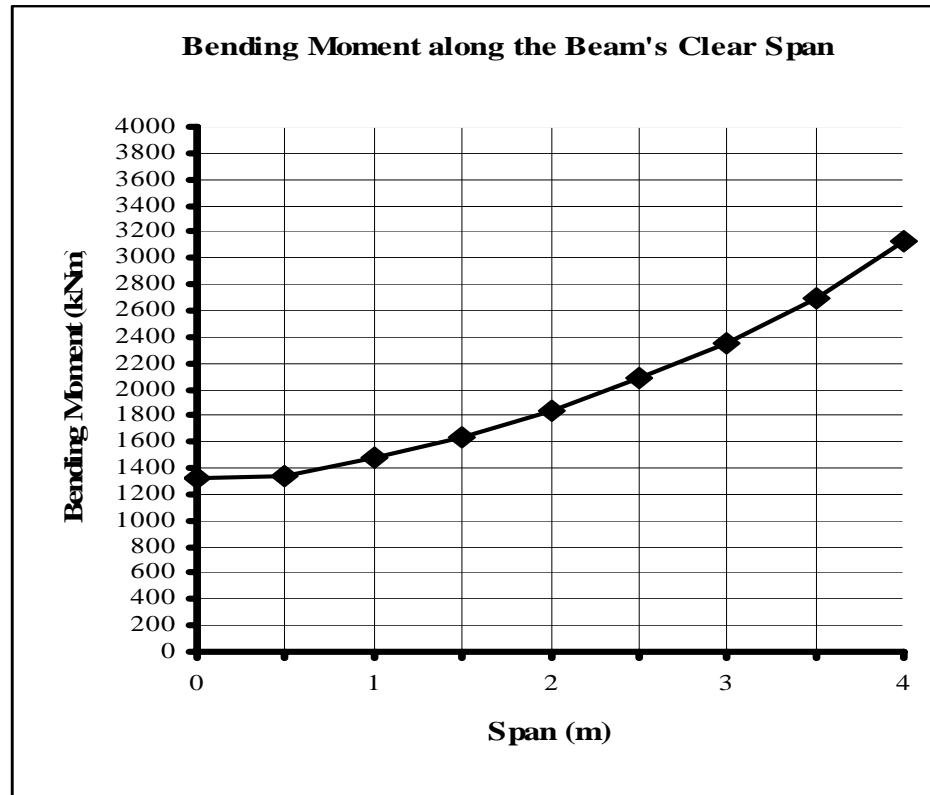


Figure 4.14 Bending moment distribution along the clear span of transfer beam.

4.4 Design of Transfer Beam Using Analysis Result of Case 2

In case 2, the shear wall-transfer beam structure is subjected to both the vertical superimposed loads and lateral wind load and the whole structure is analysed using the LUSAS 13.5 software. The bending moment and shear force thus yielded from the analysis, as displayed in Table 4.26 and Table 4.25 respectively, are used as the major parameters in designing the transfer beam. The design procedure is as per CIRIA Guide 2 1977 (Section 2 – Simple Rules for the Analysis of Deep Beams).

The entire design procedures and checking have been elaborated in Section 3.3 whereas the detail of design is displayed in Appendix E. The ultimate output of the transfer beam design is given by the bending steel reinforcement, web reinforcement and vertical shear reinforcement. The required bending (sagging) reinforcement is 10T25 being spaced at 140mm side by side in 2 layers with each

layer consists of 5T25. It is not to be curtailed and is distributed over a depth of $0.2h_a$. For the depth of $0.2h_a$ to top of the beam, web reinforcement of 12T25 @ 140mm is provided. 6T25 is introduced on the top of the transfer beam as a minimum top reinforcement. In order to cater for the shear force along the beam, shear links of T10-200 along the beam's clear span. At the support, the shear force is catered for by the main bending steel which extends into the columns, and the columns' starter bars. The detailing of the transfer beam is shown in Figure 4.15.

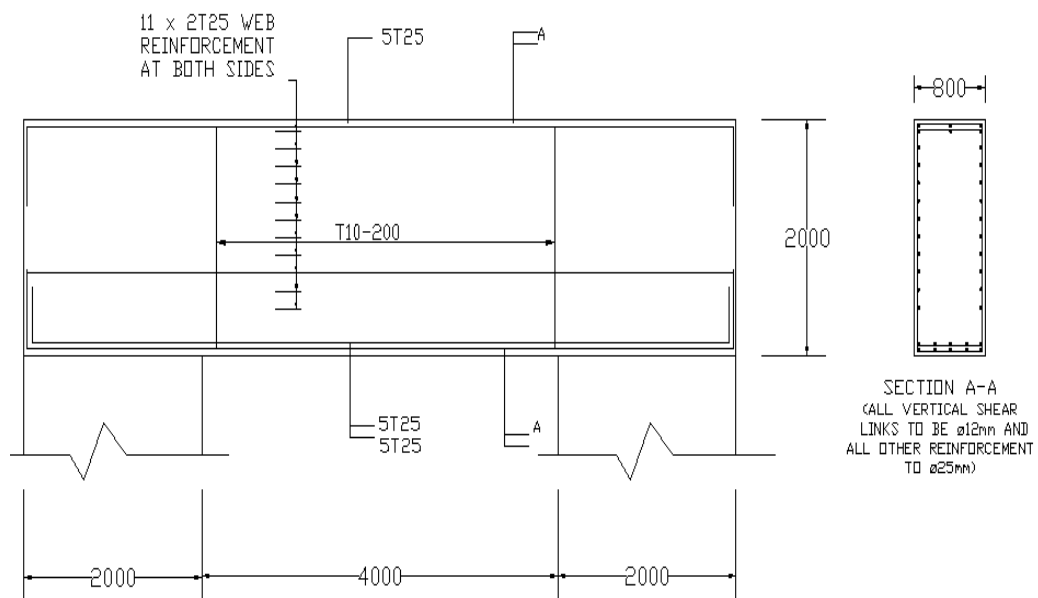


Figure 4.15. Detailing of transfer beam in longitudinal and cross section view (not to scale).

CHAPTER 5

CONCLUSION AND RECOMMENDATION

5.1 Conclusion

A few conclusions can be drawn on the results of analysis obtained from the two case studies carried out. The two cases concerned are: Case 1: Analysis of Shear Wall-Transfer Beam Structure Subjected to Vertical Loads Only, and Case 2: Analysis of Shear Wall-Transfer Beam Structure Subjected to Vertical Loads and Wind Load.

5.1.1 Case 1: Analysis of Shear Wall-Transfer Beam Structure Subjected to Vertical Loads Only

From the finite element analysis carried out on the shear wall-transfer beam structure, which is subjected to vertical superimposed loads only, a few conclusion can be drawn on the behaviour of the structure due to the interaction effect. Generally, the stress behaviour of the transfer beam and shear wall corresponds to the result obtained by J.S Kuang and Shubin Li in their previous research. The interaction effect has been shown to cause significant stress redistributions both in the beam and in the shear wall within an interactive zone, which is considered as the region in the shear wall above a height equal to the span of the transfer beam from the wall-beam interface.

- a) Due to the interaction effect between the shear wall and transfer beam, the vertical stress behaves as though a compression arch at the interaction surface. The vertical loading is transferred towards the support columns through the compression arch. The redistribution of vertical stress in the arch form continues until the height equals the full span of the transfer beam. The vertical stress distribution becomes uniform beyond this mark.
- b) Shear wall at the interaction zone suffers from compressive horizontal stress due to the interaction effects. As for the transfer beam, the lower half of the beam suffers from tensile stress while the upper half suffers from compressive stress.
- c) The shear stress is dominated in the lower part of the shear wall. The maximum intensity of shear stress is reached at the beam-column interface; with the columns zone suffer the greatest shear stress. The intensity of the shear stress approximates zero beyond a height equal to L (span of transfer beam) above the wall-beam interface.
- d) Maximum shear force of the beam occurs at the column zones whereas maximum bending moment of the beam occurs at the midspan.

5.1.2 Case 2: Analysis of Shear Wall-Transfer Beam Structure Subjected to Vertical Loads and Wind Load.

For the case where both the vertical superimposed loads and wind load are applied, the stress behaviour of the shear wall-transfer beam structure no longer follows the pattern as displayed by case 1. No evident interaction zone is defined from the stress distribution. A few conclusions can be drawn on the behaviour of the structure due to the interaction effect.

- a) The vertical stress is no longer distributed evenly to both the columns, but more focused on the right-hand-side column. At the interface, the structure suffers from compressive stress at the area near the supports and suffers from tensile stress at midspan. The distribution of vertical stress on the shear wall

does not approach constant distribution pattern with the increase of height due to the existence of lateral wind load.

- b) The shear wall is subjected to compressive horizontal stress (negative X direction) throughout the stretch to counter the lateral wind load from positive X direction. As for the transfer beam, the lower half of the beam suffers from tensile stress while the upper half suffers from compressive stress.
- c) The maximum intensity of shear stress is reached at the beam-column interface with the right-hand-side column sustains most of the shear stress transferred from the shear wall to the single-span transfer beam. The shear stress is no longer only dominated in the lower part of the shear wall. The upper part of the shear wall suffers from shear stress as well in a decreasing manner with height. The symmetrical shear stress distribution in the wall increases from zero at the extreme edges to the maximum point exactly at the mid-span.
- d) The maximum shear force in the transfer beam occurs at the column zones. The effect of wind load contributes to an asymmetrical shear force distribution curve along the beam, where a relatively high concentration of shear force occurs at the right-hand-side column.
- e) The positive bending moment occurs along the clear span of the beam and increases from left to right. The maximum bending moment does not occur at the mid-span of the beam, but culminates at a section just adjacent to the column face, which is the end of the transfer beam's clear span.

5.1.3 Design of Reinforcement for Transfer Beam

Based on the bending moment and shear force values obtained from analysis in Case 2, conclusion can be made on the types and amount of reinforcement required to cater for the bending moment capacity, shear capacity and bearing capacity of the beam. The details of reinforcement are as follow:

- a) Bending reinforcement - 10T25
 - Not to be curtailed and distributed over a depth of $0.2 h_a (=400\text{mm})$ from beam's soffit.

- b) Beam's top reinforcement – 6T25
- c) Shear reinforcement - T10-200 throughout the beam's span
- d) Web reinforcement - 22T25@150 (11T25-200 at each face of transfer beam)
- distributed from the level of 0.4m from soffit to top

5.2 Recommendation

In this project, the entire finite element model comprising the shear wall and transfer beam structure is analysed with the linear-elastic behaviour, which could still provide satisfactory approximation for the design purpose of this project. To take account of the reserve of in-plane moment capacity beyond the elastic analysis, permissible concrete and reinforcement of $0.45f_{cu}$ and $0.87f_y$ are used in elastic analysis at ultimate load with an enhanced value of modular ratio.

However, in the actual situation, the shear wall-transfer beam structure could behave non-linearly if the structure starts to crack. After cracking, the structure would result in a major redistribution of stresses and undergo deformation due to yielding of steel reinforcement and cracking of concrete. The shear wall may exhibit a sudden loss in lateral load capacity due to web crushing. This behaviour implies that the elasticity of the structure could not be recovered and that inelastic analysis should be conducted instead.

In view of the significance of the non-linear behaviour on the reinforced concrete structure, a few recommendations are proposed here to improve on the finite element model in order to generate more precise view on the stress behaviour of the shear wall and transfer beam due to their interaction. The recommendations are:

- a) Depending on how large the deflections were, serious errors could be introduced if the effects of nonlinear geometry were neglected. To take account of the possible cracks and deformation in the transfer beam and shear wall, which could disrupt the elastic behaviour of the shear wall-transfer

beam structure, it is recommended that nonlinear finite element analysis should be carried out on the structure. It also helps identify the failure mode of the structure and the critical stress components when failure occurs.

- b) Experimental work should be carried out to test the validity of the analytical results obtained through finite element analysis. In order to test the structure, a shear wall-transfer beam model of compatible scaled-down size and similar material properties should be tested under ultimate limit state.
- c) The behaviour of shear wall with openings loaded on transfer beam could be a research orientation of interest as most of the shear wall structures contain openings along its face. The presence of openings on the shear walls could significantly weaken the strength of the shear wall and could have completely different stress behaviour.
- d) Other possible orientations in research involve the consideration of multiple-span instead of single-span transfer beam in the analyse to observe the change in stress distribution, consideration of transfer beam being loaded with coupling shear wall, consideration of the effect of different loadings in different spans, and so forth.
- e) In future studies, it is recommended that steel reinforcement being embedded into the transfer beam and shear wall. The embedment of reinforcement ensures that the stresses behaviour obtained from the finite element analysis resembles the actual behaviour of the structure.

REFERENCES

1. Kuang, J.S and Atanda, A.I (1998). Interaction based analysis of continuous transfer girder system supporting in-plane loaded coupled shear walls. *The Structural Design of Tall Buildings*. 7: 285–293.
2. Kuang, J.S and Li, S.B (2001). Interaction based Design Table for Transfer Beams Supporting In-plane Loaded Shear Walls. *The Structural Design of Tall Buildings*. 10: 121-133
3. Kuang, J.S and Li, S.B (May 2005). Interaction based Design Table for Transfer Beams: Box Foundation Analogy. *Practice Periodical on Structural Design and Construction*. ASCE. 132pp
4. Schaich, J and Weischede, D (March 1982). Detailing of Concrete Structures (in German). *Bulletin d' Information 150, Comite Euro-International du Beton*. Paris. 163pp.
5. Schaich, J, Schafer, K and Jennewein, M (March 1991). Towards a Consistent Design of Structural Concrete Using Strut-and-Tie Models. *The Structural Engineer*. Vol.69, No.6: 13pp
6. Rogowsky, D.M and Marti, P (1991). Detailing of Post-Tensioning. *VSL Report Series*. No.3, VSL International Ltd., Bern. 49pp.
7. Rogowsky, D.M and MacGregor, J (August 1986). Design of Deep Reinforced Concrete Continuous Beams, *Concrete International: Design and Construction*. Vol.8, No.8: 49-58.
8. Adebar, P and Zhou, Z.Y (1993). Bearing Strength of Compressive Struts Confined by Plain Concrete. *ACI Structural Journal*. Vol.90, No.5, September-October. 534-541.

9. Doran, B. (2003). Elastic-plastic analysis of R/C coupled shear walls: The equivalent stiffness ratio of the tie elements. *J. Indian Inst. Sci.* Indian Institute of Science. May - Aug. 83. 87–94.
10. Cardenas, Russell and Corly (1980). Strength of Low Rise Structural Wall. *Reinforced Concrete Structures Subjected to Wind and Earthquake Forces*. SP-63, American Concrete Institute, Detroit. 25-34
11. Kotsovos and Pavlovic (1995). Two Dimensional Analysis: Structural Walls. *Structural Concrete Finite Element Analysis for Limit State Design*. Thomas Telford Publications, London. 284-293
12. Zienkiewicz, O.C (1977). *The Finite Element Method (Third Edition)*, McGraw-Hill, London.
13. Inoue, N, Yang, K.J and Shibata, A. Dynamic Non-linear Analysis of Reinforcement Concrete Shear Wall by Finite Element Method with Explicit Analytical Procedure. *Earthquake Engng. Struct. Dyn.* John Wiley & Sons Ltd. 26. 967–986,
14. Bathe, K.J (1982). Formulation of Continuum elements. *Finite Element Procedures in Engineering Analysis*. Prentice Hall Inc. 197.
15. Leonhardt, F. and Walther, R. (1970). Deep Beams. *Deutscher Ausschuss für Stahlbeton Bulletin*. Wilhelm Ernst and Sohn. January. 178.
16. Kong, F.K and Robins, P.J. (1972). Shear Strength of Reinforced Concrete Deep Beams *Concrete*. March. 6 (No.3):34-36.
17. Ove Arup and Partners (1977). Behaviour of Deep Beams: an Explanation of the Rules. *The Design of Deep Beams in Reinforced Concrete*. Ciria Publication. January. 8-48.
18. Cheung, Y.K. and Chan, H.C. (1990). Finite Element Analysis. *Reinforced Concrete Deep Beams*. Blackie and Son Ltd. 205.
19. Schueller, W. (1977). *High-rise Building Structures*. John Wiley and Sons. 84

Appendix A

Internal forces of the transfer beam-shear wall system (Figure 11) subjected to a uniformly distributed load are determined as follows.

Table AI. Vertical stress coefficient k_{σ_y}

Beam width	Span/depth ratio L/h_b	Column flexural stiffness h_c/L					
		0-06	0-08	0-10	0-12	0-14	0-16
$b = 2t$	3-0	2-328	2-206	2-003	1-942	1-880	1-721
	4-0	3-002	2-766	2-449	2-323	2-206	2-020
	5-0	3-571	3-224	2-796	2-603	2-430	2-176
	6-0	4-033	3-569	3-024	2-772	2-553	2-262
	7-0	4-408	3-832	3-176	2-873	2-616	2-311
	8-0	4-716	4-037	3-279	2-933	2-645	2-341
	9-0	4-971	4-201	3-351	2-968	2-654	2-360
	10-0	5-187	4-335	3-402	2-987	2-658	2-371
$b = 3t$	3-0	2-245	2-180	2-035	1-906	1-869	1-751
	4-0	2-923	2-745	2-489	2-294	2-201	2-027
	5-0	3-497	3-212	2-847	2-586	2-435	2-204
	6-0	3-966	3-566	3-087	2-767	2-568	2-288
	7-0	4-347	3-837	3-248	2-877	2-638	2-319
	8-0	4-660	4-049	3-359	2-944	2-673	2-322
	9-0	4-920	4-219	3-438	2-985	2-688	2-310
	10-0	5-140	4-357	3-495	3-010	2-691	2-291

Table AII. Axial force coefficient $k_T (\times 10^{-1})$

Beam width	Span/depth ratio L/h_b	Column flexural stiffness h_c/L					
		0-06	0-08	0-10	0-12	0-14	0-16
$b = 2t$	3-0	1-635	1-371	1-107	0-934	0-781	0-628
	4-0	1-915	1-633	1-350	1-168	1-007	0-845
	5-0	2-001	1-723	1-446	1-265	1-106	0-946
	6-0	1-987	1-720	1-453	1-282	1-131	0-980
	7-0	1-930	1-676	1-421	1-262	1-122	0-983
	8-0	1-858	1-615	1-372	1-225	1-097	0-970
	9-0	1-783	1-550	1-317	1-181	1-066	0-950
	10-0	1-709	1-485	1-262	1-137	1-032	0-928
$b = 3t$	3-0	1-595	1-349	1-103	0-937	0-788	0-640
	4-0	1-946	1-664	1-383	1-195	1-026	0-857
	5-0	2-106	1-813	1-519	1-325	1-151	0-977
	6-0	2-145	1-854	1-563	1-373	1-203	1-033
	7-0	2-125	1-843	1-561	1-378	1-216	1-054
	8-0	2-079	1-808	1-536	1-363	1-210	1-057
	9-0	2-021	1-762	1-502	1-338	1-194	1-051
	10-0	1-960	1-712	1-465	1-310	1-175	1-039

A.1. Maximum vertical compression stress in shear wall σ_y

$$\sigma_y = k_{\sigma_y}(w/t) \quad (A1)$$

where the coefficient k_{σ_y} is given in Table AI.

Table AIII. Span moment coefficient k_{M_1} ($\times 10^{-2}$)

Beam width	Span/depth ratio L/h_b	Column flexural stiffness h_c/L					
		0.06	0.08	0.10	0.12	0.14	0.16
$b = 2t$	3.0	2.687	2.448	2.209	2.053	1.914	1.775
	4.0	1.485	1.375	1.264	1.193	1.129	1.066
	5.0	0.866	0.814	0.762	0.729	0.699	0.670
	6.0	0.531	0.507	0.483	0.467	0.453	0.440
	7.0	0.341	0.330	0.319	0.312	0.306	0.300
	8.0	0.229	0.224	0.219	0.216	0.213	0.210
	9.0	0.163	0.160	0.157	0.155	0.153	0.151
	10.0	0.123	0.120	0.117	0.115	0.113	0.111
$b = 3t$	3.0	3.376	3.085	2.793	2.596	2.418	2.240
	4.0	2.009	1.859	1.709	1.607	1.516	1.425
	5.0	1.220	1.145	1.071	1.021	0.976	0.931
	6.0	0.768	0.732	0.696	0.672	0.651	0.630
	7.0	0.499	0.483	0.467	0.457	0.448	0.439
	8.0	0.336	0.329	0.322	0.318	0.315	0.312
	9.0	0.234	0.231	0.228	0.227	0.226	0.224
	10.0	0.170	0.167	0.165	0.164	0.163	0.163

Table AIV. Support moment coefficient k_{M_2} ($\times 10^{-2}$)

Beam width	Span/depth ratio L/h_b	Column flexural stiffness h_c/L					
		0.06	0.08	0.10	0.12	0.14	0.16
$b = 2t$	3.0	0.400	0.166	-0.069	-0.206	-0.321	-0.334
	4.0	0.251	0.038	-0.174	-0.279	-0.361	-0.446
	5.0	0.145	-0.039	-0.223	-0.309	-0.375	-0.443
	6.0	0.076	-0.080	-0.235	-0.305	-0.356	-0.404
	7.0	0.030	-0.099	-0.229	-0.283	-0.321	-0.354
	8.0	-0.002	-0.108	-0.214	-0.254	-0.280	-0.305
	9.0	-0.024	-0.110	-0.196	-0.224	-0.238	-0.258
	10.0	-0.041	-0.109	-0.177	-0.193	-0.198	-0.215
$b = 3t$	3.0	0.531	0.301	0.071	-0.060	-0.170	-0.280
	4.0	0.392	0.160	-0.072	-0.199	-0.303	-0.408
	5.0	0.263	0.048	-0.167	-0.273	-0.356	-0.440
	6.0	0.173	-0.018	-0.209	-0.295	-0.359	-0.423
	7.0	0.110	-0.055	-0.220	-0.289	-0.338	-0.388
	8.0	0.067	-0.074	-0.214	-0.270	-0.308	-0.346
	9.0	0.035	-0.082	-0.200	-0.245	-0.274	-0.303
	10.0	0.012	-0.085	-0.182	-0.218	-0.240	-0.262

Positive = sagging moments; negative = hogging moments.

A.2. Tensile axial force in transfer beam T

$$T = k_T(w/t) \quad (\text{A2})$$

where the coefficient k_T is given in Table AII.

Table AV. Support moment coefficient k_{M_3} ($\times 10^{-2}$)

Beam width	Span/depth ratio L/h_b	Column flexural stiffness h_c/L					
		0-06	0-08	0-10	0-12	0-14	0-16
$b = 2t$	3-0	0-177	0-390	0-599	0-766	0-924	1-082
	4-0	0-190	0-409	0-628	0-803	0-969	1-135
	5-0	0-194	0-423	0-651	0-833	1-004	1-176
	6-0	0-198	0-433	0-668	0-853	1-028	1-202
	7-0	0-203	0-440	0-681	0-868	1-043	1-218
	8-0	0-208	0-446	0-691	0-878	1-053	1-227
	9-0	0-213	0-450	0-699	0-886	1-059	1-233
	10-0	0-218	0-453	0-705	0-892	1-064	1-237
$b = 3t$	3-0	0-132	0-330	0-528	0-695	0-856	1-017
	4-0	0-142	0-359	0-576	0-759	0-935	1-111
	5-0	0-150	0-382	0-614	0-809	0-995	1-181
	6-0	0-158	0-400	0-642	0-842	1-034	1-225
	7-0	0-166	0-414	0-663	0-866	1-058	1-251
	8-0	0-173	0-426	0-678	0-882	1-075	1-268
	9-0	0-179	0-435	0-690	0-894	1-086	1-278
	10-0	0-185	0-442	0-700	0-902	1-093	1-284

Table AVI. Support moment coefficient k_{M_4} ($\times 10^{-2}$)

Beam width	Span/depth ratio L/h_b	Column flexural stiffness h_c/L						
		0-06	0-08	0-10	0-12	0-14	0-16	
$b = 2t$	3-0	0-111	0-272	0-432	0-554	0-668	0-823	
	4-0	0-118	0-285	0-452	0-591	0-723	0-852	
	5-0	0-121	0-294	0-466	0-602	0-729	0-871	
	6-0	0-124	0-300	0-476	0-617	0-750	0-883	
	7-0	0-128	0-306	0-483	0-635	0-782	0-890	
	8-0	0-132	0-310	0-488	0-655	0-820	0-894	
	9-0	0-135	0-313	0-491	0-674	0-858	0-897	
	10-0	0-138	0-316	0-494	0-692	0-895	0-899	
	$b = 3t$	3-0	0-082	0-223	0-364	0-484	0-599	0-713
		4-0	0-089	0-242	0-395	0-523	0-645	0-768
5-0		0-094	0-256	0-418	0-549	0-674	0-798	
6-0		0-099	0-266	0-433	0-565	0-690	0-815	
7-0		0-105	0-274	0-442	0-575	0-699	0-824	
8-0		0-110	0-279	0-448	0-580	0-705	0-829	
9-0		0-116	0-284	0-452	0-584	0-708	0-832	
10-0		0-121	0-288	0-455	0-586	0-710	0-833	

A.3. Mid-span moment in transfer beam M_1

$$M_1 = k_{M_1}(wL^2) \quad (\text{A3})$$

where the coefficient k_{M_1} is given in Table AIII.

A.4. Support moment in transfer beam M_2

$$M_2 = k_{M_2}(wL^2) \quad (\text{A4})$$

where the coefficient k_{M_2} is given in Table AIV.

A.5. Column moment M_3

$$M_3 = k_{M_3}(wL^2) \quad (\text{A5})$$

where the coefficient k_{M_3} is given in Table AV.

A.6. Column moment M_4

$$M_4 = k_{M_4}(wL^2) \quad (\text{A6})$$

where the coefficient k_{M_4} is given in Table AVI.

Appendix B

Minimum Reinforcement in Deep Beam and Maximum Bar Spacing

Crack width

The minimum percentage of reinforcement in a deep beam should comply with the requirements of Clauses 3.11 and 5.5 of CP 110. Bar spacings should not exceed 250 mm.

In areas of a deep beam stressed in tension, the proportion of the total steel area, relative to the local area of concrete in which it is embedded, shall not be less than $0.52\sqrt{f_{cu}}/0.8f_y$. This amount of reinforcement, expressed as a percentage of the area of concrete in which embedded, is given on Table 1 for concrete and steel strengths, f_{cu} and f_y , respectively.

TABLE 1 Minimum steel percentages

f_y (N/mm ²)	f_{cu} (N/mm ²)				
	15	20	25	30	40
250	0.93	1.07	1.20	1.31	1.51
410	0.56	0.65	0.73	0.80	0.92
425	0.54	0.63	0.70	0.77	0.89
460	0.50	0.58	0.65	0.71	0.82
485	0.48	0.55	0.62	0.67	0.78
500	0.46	0.53	0.60	0.65	0.76

For maximum crack widths of 0.3 and 0.1 mm, bar spacings should not exceed those given in Tables 2 and 3, respectively. The bar spacings given in Table 2 should not be exceeded in a normal environment in zones stressed in tension, to assure adequate stiffness. The bar spacing given by Table 3 may be adopted when the environment requires a higher standard of protection for the reinforcement (see Clause 2.2.3.2 of CP 110). Bar spacing less than 100 mm, depending on the bar diameter, is not usually considered to be a practicable arrangement.

TABLE 2 Maximum bar spacings (mm) for a maximum crack width of 0.3 mm

f_y (N/mm ²)	Width of beam, b (mm)					
	200	300	500	750	1000	1500
250	260	280	305	330	340	360
410	170	185	200	215	220	230
425	165	180	195	205	215	225
460	155	165	180	195	200	210
485	150	160	175	185	190	200
500	145	155	170	180	185	195

TABLE 3 Maximum bar spacing (mm) for a maximum crack width of 0.1 mm

f_y (N/mm ²)	Width of beam, b (mm)					
	200	300	500	750	1000	1500
250	105	110	120	125	130	135
420	70	70	75	80	80	85
425	65	70	75	75	80	80
460	60	65	70	70	75	75
485	60	60	65	70	70	70
500	55	60	65	65	70	70

Appendix C
Calculation of Lateral Wind Load on Shear Wall as per BS 6399 Loading
for Buildings): Part 2 (Wind Loads): 1997

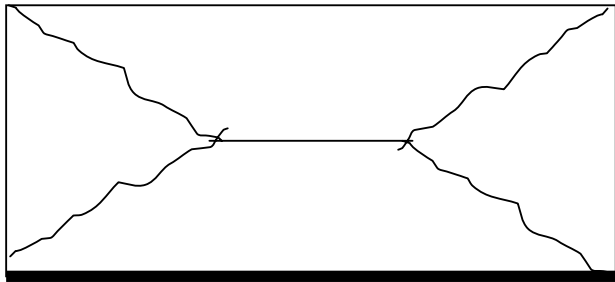
Wind Speed Calculations using Section 3: Directional method				
Basic wind speed	V _b	24	m/s	From map (Fig 6)
Annual risk of exceedance	Q	0.02		Use 0.02 for standard annual risk
Probability Factor	Sp	1.00		See annex D (UK Only)
Topographic increment	Sh	0		See section 3.2.3.4, figures 7-9 and Table 25
Altitude		0	m	Altitude at site
Altitude factor	S _a	1.00		= 1+0.001 x Altitude (See section 3.2.2)
Wind direction	° E of N (or All)	All		
Direction factor	S _d	1.00		From Table 3 (UK only)
Seasonal factor < 1.00 for sub annual exposure	S _s	1		From Table D.1 (UK Only)
				V _s = V _b S _a S _d S _s S _p (Sect. 2.2.2.1)
Site wind speed	V _s	24.0	m/s	Mean hourly speed at 10m height above open level country
Reference height	H _r	83	m	From 1.7.3.1 or use height AGL of building.
Height of obstructions	H _o	0	m	Average upwind of building. (Sect. 1.7.3.3)
Distance of obstructions	X	0	m	from face of building
Effective Height	H _e	83.0	m	for X > 6 H _o , H _e = H _r for X < 2H _o , H _e > H _r - 0.8H _o & > 0.4 H _r else H _e > H _r - 1.2H _o + 0.2X & > 0.4 H _r
Upwind distance to sea		100	km	See section 1.7.2 A lake is 1 km or more wide
Fetch factor	S _c	1.395		From table 22
Turbulence factor	S _t	0.137		Basic Values for Open Country
Upwind distance to edge of town		0	km	for sites in towns and cities. (See 1.7.2) 0 km upwind is country exposure
Fetch adjustment factor	T _c	1.000		From table 23
Turbulence adjustment factor	T _t	1.000		Adjustment factors for town terrain
Mean wind speed	V _m	33.5		V _s x S _c x T _c
Intensity of turbulence	I _u	0.137		S _t x T _t
Diag. size of loaded area	a	77.4	m	See figure 5 and sect. 2.1.3.4 for definitions
Gust duration	t	10.40	s	4.5 a/(V _s S _c T _c) > 1s (Equation F.1)
Gust peak factor	G _t	2.46		= 0.42 Ln(3600/ t) < 3.44 (Annex F)
Design Gust Wind Speed	V_e	44.7	m/s	V _m (1 + G _t I _u) = V _s S _b (from sect. 3.2.3)
Design Gust Pressure	Q	1225	Pa	0.613 V _e ² (Equation 16)

Design wind load = Design gust pressure x length of the shear wall bay

$$= 1.225\text{kPa} \times 4\text{m} = 4.9\text{kN/m}$$

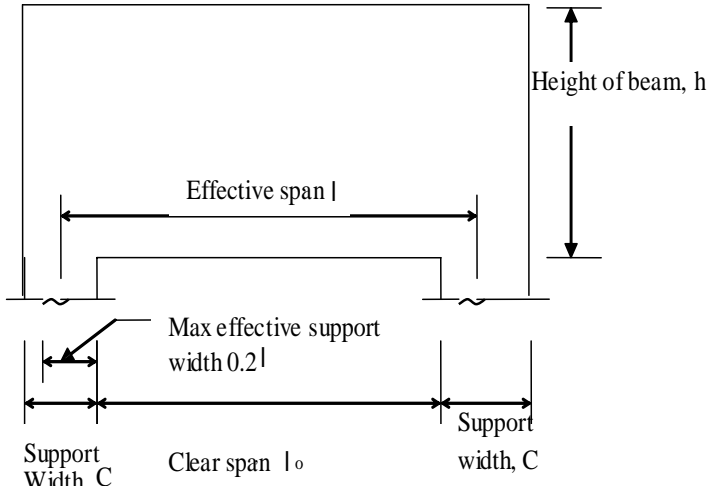
Appendix D

Calculation of Vertical Load Transferred from Slab to Shear Wall

	<p>For residence unit:</p> <p>Live load = 5kN/m^2</p> <p>Dead load: Cement render = 0.5 kN/m^2 Services = 0.5 kN/m^2 Ceramic tiles = 0.58kN/m^2 Slab selfweight = $\frac{24 \times 0.2}{1000} = 4.8\text{kN/m}^2$ <u>6.38kN/m^2</u></p> <p>Design load = $1.2G_k + 1.2Q_k$ (with wind load) = $1.2 (6.38 + 5)$ = 13.656kN/m^2</p> <p>Design load = $1.4G_k + 1.6Q_k$ (without wind load) = $1.4 (6.38) + 1.6(5)$ = 16.932kN/m^2</p> <div style="text-align: center;">  </div>	
<p>Table 3.15 BS8110: Part 1 1997</p>	<p>Shear force coefficient for the discontinuous edge AB connected to shear wall = 0.40</p> <p>Hence, UDL transferred to shear wall from slab = $0.4(4)(13.656) = 21.85\text{kN/m}$ (with wind load) = $0.4(4)(16.932) = 27.09\text{kN/m}$ (without wind load)</p>	

Appendix E

Design of Transfer Beam as per CIRIA Guide 2 1977 (Section 2 – Simple Rules for the Analysis of Deep Beams)

	<p><u>Geometry</u></p>  <p>The diagram illustrates the geometry of a beam. It shows a rectangular cross-section with a height h. The effective span is l. The clear span is l_o. The support width is C. The maximum effective support width is $0.2l$. The diagram also shows the relationship between the effective span l and the clear span l_o and support width C.</p>	
<p>CIRIA Guide 2 2.2.1</p>	<p>Clear span, l_o = 4m Support width, C = 2m Effective support width is lesser of $0.2 l_o$ (=800mm) or C</p> <p>Effective span = $4000 + 2(400) = 4800\text{mm}$ Thickness = 800mm Effective depth = $h - \text{concrete cover} - \phi_{\text{hanger bar}} - \phi_{\text{hanger bar}}$ $= 2000 - 30 - 25 - 25$ $= 1280\text{mm}$</p>	<p>$C=0.8\text{m}$ $l=4.8\text{m}$</p>
<p>2.6.2</p>	<p><u>General</u></p> <p>Max. bar spacing = 196mm Min. % steel = $0.82\% = 0.0082(800)(1000) = 6560\text{mm}^2/\text{m}$</p>	

<p>CIRIA Guide 2 2.4.1</p>	<p><u>Strength in Bending</u></p> <p>From the analysis, maximum bending moment is 3132.14kNm</p> <p>$l/h = 4800/2000 > 1.5$</p> <p>$M = 3132.14\text{kNm} < 0.12f_{cu}bh_a^2 = 0.12(40)(800)(2000^2)$ $= 15360 \text{ kNm}$</p> <p>\therefore Lever arm, $z = 0.2l + 0.4 h_a$ $= 0.2(4.8) + 0.4(2) = 1.76\text{m}$</p> <p>At midspan, $A_s = M/0.87f_yz$ $= 4450\text{mm}^2 = 4450 / 0.4 = 11125\text{mm}^2/\text{m}$ $> 6560\text{mm}^2/\text{m}$ (minimum reinforcement)</p> <p>This bending (sagging) reinforcement is not to be curtailed and may be distributed over a depth of $0.2 h_a (=400\text{mm})$.</p>	<p>=>ok!</p> <p>Use 10T25</p> <p>=>ok!</p>
<p>BS 8110 3.4.5.2</p>	<p><u>Shear Capacity at Supports</u></p> <p>$100A_s / bd = 100(4450) / (800)(1280) = 0.435$</p> <p>$400 / d = 400 / 1280 = 0.3125$</p> <p>$v_c = 0.79(100A_s / bd)^{1/3} (400/d)^{1/4} (f_{cu}/25)^{1/3} / 1.25$ $= 0.419\text{N/mm}^2$</p> <p>For nominal shear links, $A_{sv} = 0.4b_v s_v / 0.95f_{yv}$ Using bar T10, $s_v = 157(0.95)(460) / 0.4(800)$ $= 214\text{mm}$</p> <p>Capacity of T10-200, $v = v_c + (A_{sv} / s_v)(0.95f_{yv}) / b$ $= 0.848 \text{ N/mm}^2$</p> <p>>shear stress at midspan of transfer beam (Section 4.3.2.4 Table 4.25)</p> <p>From the analysis, shear force at the supports are 1064.622kN and 3629.33kN, whereas at the midspan of beam is less than capacity of nominal links (T10-200). Hence use nominal links throughout the beam.</p>	<p>400/d = 1</p> <p>use $s_v = 200$</p> <p>use T10-200</p>

	<p><u>Bearing Stress</u></p> <p>CIRIA Shear force at support = 3629.33kN</p> <p>Guide 2 Average stress = Shear force / col. thickness (col. width + 0.2 h_a)</p> <p>2.4.3 $= 3629330 / 1000[2000+0.2(4000)]$ $= 1.3 \text{ Nmm}^{-2}$ $< 0.4f_{cu} = 16 \text{ Nmm}^{-2}$</p>	=>ok!
	<p><u>Bursting Tension caused by Columns on Transfer Beam</u></p> <p>CIRIA Since $l/h_a = 4800/2000 > 1$,</p> <p>Guide 2 The compressive stress due to bending will exceed the bursting</p> <p>4.1.1 tension caused by the concentrated support reaction => no tension is developed</p>	
	<p><u>Reinforcement</u></p> <p>CIRIA Reinforcement designated to cater for the positive bending</p> <p>Guide 2 moment is not to be curtailed in the span and may be</p> <p>2.4.2 distributed over a depth of $0.2h_a (=0.4\text{m})$</p> <p>For top bars, since there is no negative bending moment, minimum reinforcement is distributed over a depth of $0.2h_a$ from top of beam.</p> <p>Hence, top reinforcement = $6560 \text{ mm}^2/\text{m}$ $= 2624 \text{ mm}^2$</p> <p>Web reinforcement (required at the level 0.4m from soffit to top) = Min. % steel = $6560\text{mm}^2/\text{m} (1.6\text{m})$ = 10496 mm^2 = 22T25 @ 150mm</p>	use 6T25

Check on Bearing Stress and Anchorage

For full tension lap on a T25 bar, Force = $0.87f_yA_s$

$$= 0.87(460)(491)$$

$$= 196.5\text{kN}$$

BS8110 For deformed bar in tension, concrete grade C40,

3.12.8.3 Ultimate anchorage bond stress = 2.6N/mm^2

Tension lap = Anchorage force / (Bond stress)($\pi\phi$)

$$= 196500 / 2.6\pi(25) = 962\text{mm}$$

For main bending steel,

Force to be anchored = $0.87(460)(4450)/1000 = 1780.89\text{kN}$

The horizontal bending steel at the lower zone of beam (within $0.2h_a = 0.4\text{m}$) consists of 10T25 bars spaced at 140mm

\therefore Force / bar = $1780.89\text{kN} / 10 = 178.089\text{kN}$

At supports,

Length required to anchor 80% of force in bar

$$= 178.089\text{kN} (0.8) / (2.6)(\pi)(25) = 697.7\text{mm}$$

20% of force in bar is used to check bearing stress in U bar.

F_{bt} = tensile force in the bar

$$= 178.089\text{kN}(0.2) = 35.62\text{kN}$$

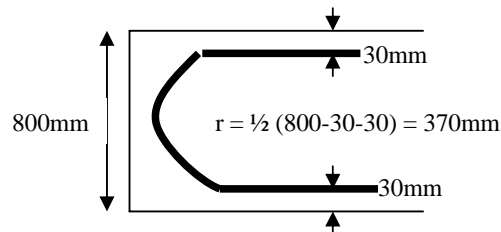
Bearing stress = $F_{bt} / r\phi$

$$= 35620\text{kN} / (370) (25) = 3.85\text{Nmm}^{-2}$$

$$< 1.5f_{cu} / [1+2\phi/a_b]$$

$$= \frac{1.5(40)}{[1+2(25)/(25+25)]} = 30\text{Nmm}^{-2}$$

=>ok!



\therefore The internal bearing stress is satisfactory and the U-bar anchorage meets the 80% anchorage condition.